2016

Citrate Coated Silver Nanoparticles With Modulatory Effects On Aflatoxin Biosynthesis In Aspergillus Parasiticus

Chandrani Mitra
University of South Carolina

CITRATE COATED SILVER NANOPARTICLES WITH MODULATORY EFFECTS ON AFLATOXIN BIOSYNTHESIS IN *ASPERGILLUS PARASITICUS*

By

Chandrani Mitra

Bachelor of Pharmacy
Rajiv Gandhi University of Health Sciences, 2004

Master of Technology in Pharmaceutical Chemistry
Vellore Institute of Technology University, 2007

Submitted in Partial Fulfillment of the Requirements

For the Degree of Doctor of Philosophy in

Environmental Health Sciences

The Norman J. Arnold School of Public Health

University of South Carolina

2016

Accepted by:

Anindya Chanda, Major Professor

Alan Decho, Committee Member

Jamie Lead, Committee Member

Mohammed Baalousha, Committee Member

John Ferry, Committee member

Cheryl L. Addy, Vice Provost and Dean of the Graduate School

DEDICATION

This work is dedicated to my Guruji and my parents, Indra Gopal and Jharna Mitra who always believed in me and taught me not to give up no matter how difficult it could be. To my husband, Suman Kada for his love, constant support and patience helped me to complete this journey. To my mentor, Dr. Anindya Chanda for his continuous support and encouragement.

ACKNOWLEDGEMENTS

I express my deep sense of gratitude to my major advisor and committee chair, Dr. Anindya Chanda for his continuous support & encouragement throughout the Ph.D. study and research. He has spent his valuable time despite his busy schedule. I would like to thank all my Ph.D. committee members: Dr. A. Decho, Dr. J. Lead, Dr. M. Baalousha, and Dr. J. Ferry without whose help this project would not have been completed. My sincere thanks to Dr. Chandler, Dr. Scott, and Dr. Porter for their motivation, enthusiasm and immense knowledge which guided me in the right direction. In addition to my committee, I would like to thank the Department of Environmental Health Sciences for their support and generosity. I also thank Dr. Soumitra Ghoshroy for his insightful comments towards my research work. I thank my fellow colleagues Phani Gummadidala, Virginia Hopkins, Allison Shaffer, Gabriel Kenne, Kamalia Afshinnia, Sahar Pourhoseini, Chuan Hong, and Kamaljeet Kaur for the stimulating group discussion, and for all the fun we have had. Words fall short for an acknowledging my husband, my parents, my in-laws, who have always been the source of encouragement, inspiration, and moral support.

ABSTRACT

The manufacture and usage of silver nanoparticles has drastically increased in recent years (Fabrega et al. 2011a). Hence, the levels of nanoparticles released into the environment through various routes have measurably increased and therefore are concern to the environment and to public health (Panyala, Peña-Méndez and Havel 2008). Previous studies have shown that silver nanoparticles are toxic to various organisms such as bacteria (Kim et al. 2007), fungi (Kim et al. 2008), aquatic plants (He, Dorantes-Aranda and Waite 2012a), arthropods (Khan et al. 2015), and mammalian cells (Asharani, Hande and Valiyaveettil 2009) etc. Most of the toxicity studies are carried out using higher concentrations or lethal doses of silver nanoparticles. However, there is no information available on how the fungal community reacts to the silver nanoparticles at nontoxic concentrations. In this study, we have investigated the effect of citrate coated silver nanoparticles (AgNp-cit) at a size of 20nm on *Aspergillus parasiticus*, a popular plant pathogen and well-studied model for secondary metabolism (natural product synthesis). *A. parasiticus* produces 4 major types of aflatoxins. Among other aflatoxins, aflatoxin B_1 is considered to be one of most potent naturally occurring liver carcinogen, and is associated with an estimated 155,000 liver cancer cases globally (Liu and Wu 2010); therefore, contaminated food and feed are a significant risk factor for liver cancer in humans and animals (CAST 2003; Liu and Wu 2010).

In this study, we have demonstrated the uptake of AgNp-cit (20nm) by *A. parasiticus* cells from the growth medium using a time course ICP-OES experiment. It was observed that the uptake of AgNp-cit had no effect on fungal growth and significantly decreased intracellular oxidative stress. It also down-regulated aflatoxin biosynthesis at the level of gene expression of aflatoxin pathway genes and the global regulatory genes of secondary metabolism. We also observed that the fungus successfully reverts its aflatoxin biosynthesis to normal levels once the level of AgNp-cit decreased significantly in the growth medium. A stability study of AgNp-cit in the fungal growth medium, along with mycelia, was conducted using UV-vis spectroscopy. The result showed that the distinctive peak (at 395nm wavelength) of silver nanoparticles, size of 20nm, shifted to a higher wavelength (400nm-500nm), broadened, and decreased over time. At 30-hour post inoculation the UV-vis peak at 395 nm wavelength was not observed at all. The peak shifts may occur due to organic molecules from the medium replacing the citrate surface coating. Another possible explanation for the peak shift are the interactions between the surface coating and other inorganic components in the medium. Peak broadening may suggest possible aggregation or formation of corona on the surface of AgNp due to particle-protein interactions (leading to AgNp aggregation in the growth medium). Reduction of peak height may suggest nanoparticle uptake by the mycelia, dissolution of nanoparticles into charged ions as well as possible interaction with other ions in the growth medium or the formation of precipitate of silver salt.

We have investigated effects of different sizes (15 nm, 20 nm, and 30 nm) of AgNp-cit and pvp coated silver nanoparticles (AgNp-pvp (20 nm)) on growth and aflatoxin B_1 biosynthesis in *A. parasiticus*. AgNp-cit size of 15nm showed maximum

aflatoxin inhibition at 25ng/mL. For 20nm and 30nm AgNp-cit the strongest aflatoxin inhibition was observed at 50ng/mL concentration. The aflatoxin inhibitory effect was also found to be AgNp coating dependent. For 20nm AgNp-cit the strongest aflatoxin inhibition was seen at 50ng/mL (calculated) while for 20nm AgNp-pvp, the maximum aflatoxin inhibition was observed at 60ng/mL (calculated) concentration. Acute toxicity of silver nanoparticles on various organisms are well-studied but large knowledge gap still exist on the assessment of its chronic toxicity at low concentrations. Our study suggested that at low concentrations (ng/mL) AgNp still can produce biological effects on fungal cells. Further understanding of AgNp induced biological effects at low concentrations/environmentally relevant concentrations is necessary in investigating the environmental health effects.

TABLE OF CONTENTS

DEDICATION iii

ACKNOWLEDGEMENTS iv

ABSTRACT v

LIST OF TABLES x

LIST OF FIGURES xi

CHAPTER 1: LITERATURE REVIEW 1

1.1 AFLATOXINS: DISCOVERY, EXPOSURE, TOXICITY, RISK ASSESSMENT AND ECONOMIC IMPACT 1

1.2 AFLATOXIN BIOSYNTHESIS 8

1.3 REGULATORY FACTORS AFFECTING AFLATOXIN GENE EXPRESSION 12

1.4 FACTORS AFFECTING AFLATOXIN BIOSYNTHESIS 13

1.5 EFFECT OF AFLATOXIN & OTHER MYCOTOXIN & THEIR PRODUCRES ON MICROBIAL INTERACTIONS IN THE ENVIRONMENT 15

1.6 NANOPARTICLES: BACKGROUND, ANTIMICROBIAL ACTIVITY, EXPOSURE, AND RISK ASSESSMENT 17

1.7 GOAL OF MY STUDY 32

CHAPTER 2: SYNTHESIS AND CHARACTERIZATION OF CITRATE-COATED SILVER NANOPARTICLES 34

2.1 INTRODUCTION 35

2.2 MATERIALS AND METHODS 38

2.3 RESULT & DISCUSSION 41

2.4 CONCLUSION 44

CHAPTER 3: EFFECT OF CITRATE COATED SILVER NANOPARTICLES ON THE GROWTH AND AFLATOXIN BIOSYNTHESIS IN *ASPERGILLUS PARASITICUS* . 46

3.1 INTRODUCTION 47

3.2 MATERIALS AND METHODS 49

3.3 RESULTS AND DISCUSSION 53

3.4 CONCLUSION 68

CHAPTER 4: EFFECT OF SILVER NANOPARTICLE COATING AND SIZE ON AFLATOXIN BIOSYNTHESIS IN *A. PARASITICUS* 81

4.1 INTRODUCTION 83

4.2 MATERIALS & METHODS 85

4.3 RESULT AND DISCUSSION 87

4.4 CONCLUSION 94

CHAPTER 5: OVERALL DISCUSSION 101

FUTURE STUDIES 107

REFERENCES 109

LIST OF TABLES

Table 2.1 A comparison of UV-vis spectrophotometer absorbance, DLS z-average size, PDI, TEM average size, and ICPOES values for different AgNp particles 43

Table 3.1 List of primers used for RT-PCR..... 74

LIST OF FIGURES

Figure 1.1 Molecular structure of major types of aflatoxins 2

Figure 1.2 Biotransformation of aflatoxin B1 in the liver 6

Figure 1.3 Aflatoxin biosynthesis pathway 10

Figure 1.4 Aflatoxin gene cluster (80kb) in *A. parasiticus*, arrowhead represents the direction of transcription 11

Figure 1.5 Exposure of nanomaterial in the environment 28

Figure 2.1 Schematic diagram of synthesis of citrate coated silver nanoparticles of different sizes 39

Figure 2.2 Characterization of AgNp-cit of size 15nm 44

Figure 2.3 Characterization of AgNp-cit of size 20nm 44

Figure 2.4 Characterization of AgNp-cit of size 30nm 45

Figure 2.5 Characterization of AgNp-pvp of size 20nm 45

Figure 3.1 Possible mechanisms of nanoparticle uptake by eukaryotic cell 62

Figure 3.2 Effect of AgNp-cit on growth & aflatoxin biosynthesis in *A. parasiticus* 70

Figure 3.3 Interaction of AgNp-cit with the fungal growth medium with or without mycelia 71

Figure 3.3 Interaction of AgNp-cit (at higher concentration (100ng/mL) with the growth medium with or without mycelia 72

Figure 3.4 Uptake of AgNp-cit by *A. parasiticus* 73

Figure 3.5 Effect of AgNp-cit on transcript accumulation of aflatoxin regulatory genes 75

Figure 3.6 Effect of AgNp-cit on transcriptional inhibition of global regulators of secondary metabolism 75

Figure 3.7 Effect of AgNp-cit on ROS generation 76

Figure 3.8 Effect of AgNp-cit and $AgNO_3$ on transcriptional inhibition of SOD genes .. 77

Figure 3.9 Effect of AgNp-cit on *A. parasiticus* growth and aflatoxin biosynthesis upon completion of AgNp-cit uptake 78

Figure 3.10 Effect of AgNp-cit on transcriptional activation of aflatoxin regulatory genes on aflatoxin biosynthesis at 40 hours' post inoculation 79

Figure 3.11 Effect of AgNp-cit and $AgNO_3$ on ROS generation at 40 hours' post inoculation 80

Figure 4.1 Effect of AgNp-cit size of 15nm on aflatoxin production by *A. parasiticus* at 40-hour time point 94

Figure 4.2 Effect of AgNp-cit size of 20nm on aflatoxin production by *A. parasiticus* at 40-hour time point 95

Figure 4.3 Effect of AgNp-cit size of 30nm on aflatoxin production by *A. parasiticus* at 40-hour time point 95

Figure 4.4 Effect of AgNp-pvp size of 20nm on aflatoxin production by *A. parasiticus* at 40-hour time point 96

Figure 4.5 Effect of $AgNO_3$ on aflatoxin production by *A. parasiticus* at 40-hour time point. 96

Figure 4.6 Effect of AgNp-cit (15nm size) on the growth of *A. parasiticus* 97

Figure 4.7 Effect of AgNp-cit (20nm size) on the growth of *A. parasiticus* 97

Figure 4.8 Effect of AgNp-cit (30nm size) on the growth of *A. parasiticus* 98

Figure 4.9 Effect of AgNp-pvp (20nm size) on the growth of *A. parasiticus* 98

Figure 4.10 Effect of $AgNO_3$ on the growth of *A. parasiticus* 99

Figure 4.11 Effect of $AgNO_3$ on transcriptional accumulation of SOD genes 99

Figure 4.12 Effect of AgNp-cit on transcriptional accumulation of SOD genes 100

Figure 5.1 Working model to elucidate the effect of AgNp-cit on growth and aflatoxin biosynthesis in *A. parasiticus* 105

CHAPTER 1

LITERATURE REVIEW

1.1 AFLATOXINS: DISCOVERY, EXPOSURE, TOXICITY, RISK ASSESSMENT AND ECONOMIC IMPACT

Discovery:

Aflatoxin was discovered around 1960, specifically after the outbreak of a disease called turkey 'X' disease (NESBITT et al. 1962). This disease killed hundreds of turkeys on a poultry farm in England. The source of the outbreak of the disease was then traced and found to be associated with the animal feed, which came from Brazil. After an intensive investigation in 1961, the toxin was identified as a fungal metabolite and was named aflatoxin after *Aspergillus flavus*. Aflatoxin is one of the most widely studied mycotoxins, and is a naturally occurring, low molecular weight secondary metabolite produced by multiple fungal strains, mainly species in the *Aspergillus* genus (SPENSLEY 1963, Shapira et al. 1997). Chemically, aflatoxins are a bifurano-coumarin derivatives group with four major products: B_1, B_2, G_1, and G_2 (structures are shown in Figure 1.1). When separated by their R_f value (coefficient named "retention value"; which is the ratio between the migration distance of a substance and the migration distance of the solvent front) with the help of Thin layer chromatograph (TLC), they emit

blue or green fluorescence under ultraviolet light (Nesheim 1971, Pons, Cucullu and Franz 1972). The other significant members of the aflatoxin family are M_1, M_2, D_1, B_3, and Q_1. Aflatoxin M_1 is an oxidized form of aflatoxin B_1. It is modified in the gastrointestinal tract and can be excreted in the urine, feces and in milk (Nabney et al. 1967).

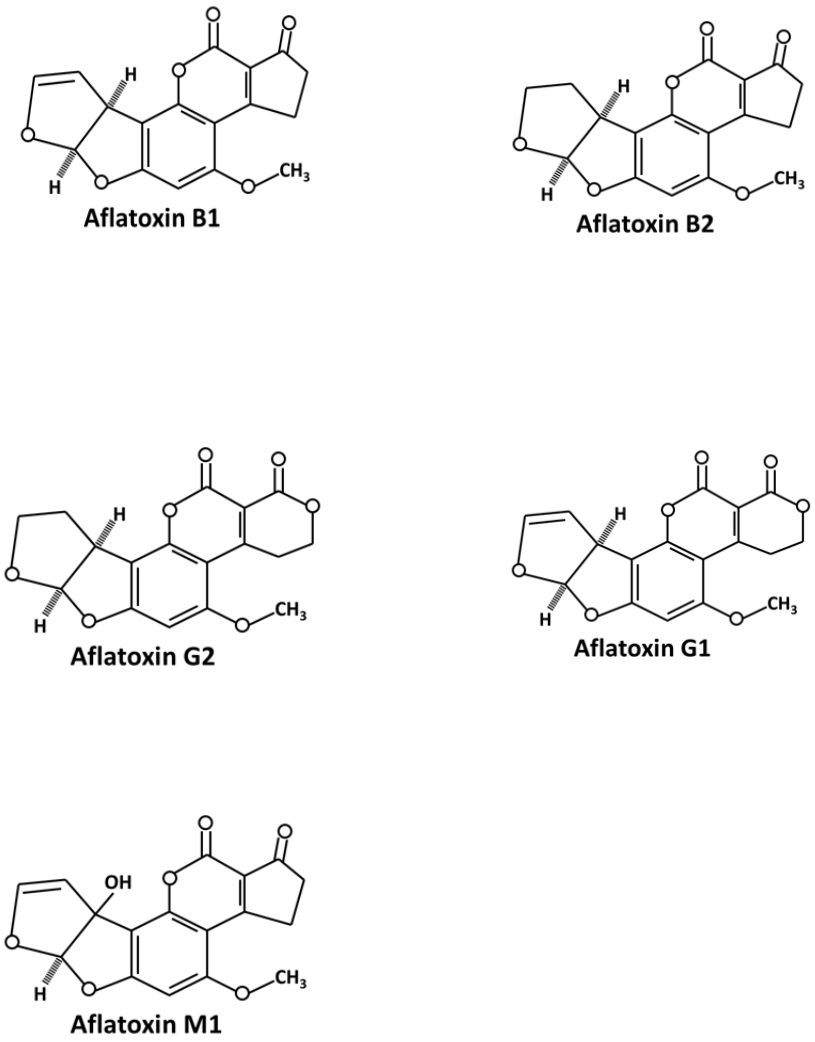

Figure 1.1: Molecular structure of major types of aflatoxins

Exposure: aflatoxin in food commodities

Aflatoxins are present in a wide range of food commodities such as peanuts, tree nuts, spices, cotton seeds, dry fruits, maize. They may also be found in milk, and cheese, but maize and peanuts are the main sources of human exposure to aflatoxin because they are highly consumed throughout the world and are susceptible crops to aflatoxin contamination (Kamika and Takoy 2011). Aflatoxins often occur in crops in the fields prior to harvest, postharvest, or during storage (Wu and Khlangwiset 2010). Farmers and other agricultural workers may be exposed to aflatoxin by inhaling the dust generated during the handling of contaminated crops (Burg, Shotwell and Saltzman 1981). The highest levels of aflatoxins are detected in commodities from warmer regions (tropical and subtropical countries) of the world (Cotty and Jaime-Garcia 2007). Insect or rodent infestation may also facilitate mold growth. Acute exposure to aflatoxins may result in gastrointestinal disorders and immune dysfunction, resulting in increased susceptibility to bacterial, fungal, and viral diseases (Gong et al. 2004). The disease associated with chronic aflatoxin ingestion is hepatocellular carcinoma (HCC or liver cancer) which is the third-leading cause of cancer death globally according to a World Health Organization report (2008), with about 550,000– 600,000 new cases emerging each year. About 83% of these deaths occur in East Asia and sub-Saharan Africa (Parkin et al. 2005) and aflatoxin consumption is also associated with growth stunting in children (Wu and Khlangwiset 2010, Pitt , Semple, Frio and Hicks 1989). In the United States, the maximum quantity of aflatoxin permitted in food in the U.S. is 20µg/kg. However, it is estimated that children in the rural areas of the southern US ingest approximately 40 µg

aflatoxin through contaminated food every day, which could lead to a significant rise in aflatoxin-induced liver cancer cases (Semple et al. 1989).

Toxicity:

The diseases caused by aflatoxin consumption are collectively called 'aflatoxicosis'. Aflatoxins showed mutagenic, teratogenic, hepatocarcinogenic, and immunosuppressive effects in experimental animals (Yu, Bhatnagar and Ehrlich 2002). An extremely high level of aflatoxin exposure is characterized by hemorrhage, acute liver damage, edema, and death in humans. Chronic and low levels of aflatoxin exposure in animals can result in jaundice, anemia, impaired growth, and an enhanced mortality rate (Wu and Khlangwiset 2010). Among all the other aflatoxins, aflatoxin B_1 is one of the most potent, naturally occurring carcinogens (Chanda, Roze and Linz 2010). The primary disease associated with aflatoxin B_1 is hepatocellular carcinoma (Liu and Wu 2010). The toxic effect of aflatoxin B_1 was found to be species, gender, and age specific (Cole and Schweikert 2003). Some species are more susceptible to aflatoxicosis like rats, pigs and ducklings, but other species are more tolerant, such as sheep and cattle.

Aflatoxins are lipophilic in nature; they generally get absorbed from the site of exposure into the blood stream (Agag 2004). It has been reported that aflatoxins can be absorbed from the respiratory system in workers at feed mills (Autrup, Schmidt and Autrup 1993). In animals, ingested aflatoxin readily gets absorbed in the gastrointestinal tract and gets metabolized in the liver. In the liver cells aflatoxin B_1 gets converted into different metabolites that might get transmitted to edible animal products. It can also be excreted in the milk of lactating animals as one of its metabolites, aflatoxin M_1 (Shreeve,

Patterson and Roberts 1979, Veldman et al. 1992). The maximum (80%) amount of aflatoxin gets excreted from the body via urine within 48-72 hours of ingestion and only 5% of the aflatoxin is traceable in the liver bound protein (Nabney et al. 1967). Aflatoxin B_1 can induce liver lesions, liver carcinoma, and the proliferation of bile ducts in experimental animals (NEWBERNE et al. 1964).

In general aflatoxin B_1 metabolism is divided into 2 phases (Diaz and Murcia 2011). Phase I consists of enzyme mediated oxidation, hydrolysis, reduction reactions. Phase II metabolism consists of conjugation reaction of the compounds modified from the phase I metabolism. Most of the phase I reactions are oxidation or hydroxylation reactions which are mostly catalyzed by cytochrome P450 enzymes. Cytochrome P450, 1A2 and 3A4 enzymes in the liver metabolize aflatoxin into aflatoxin-8,9-epoxide, which then binds to a protein or to DNA and initiates liver carcinoma (HCC) (Wu and Khlangwiset 2010, Eaton and Gallagher 1994). It is evident that Aflatoxin B1-8,9-epoxide can induce activating mutations in the ras (small GTPase family protein) oncogene in experimental animals. In the presence of water, the epoxide gets hydrolyzed and becomes available to be linked to serum proteins (Groopman et al. 1985). The conjugation step is mostly the detoxification step where aflatoxin undergoes phase II biotransformation (Neal et al. 1998). The resulting aflatoxin conjugates get extracted in the bile. In the deconjugation stage, the bio-transformed aflatoxin gets reabsorbed in the body.

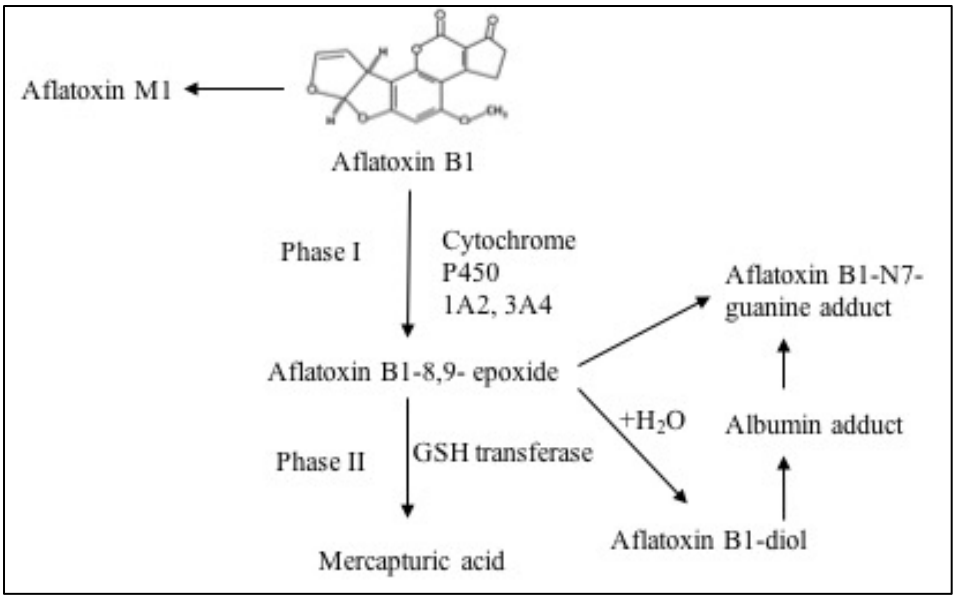

Figure 1.2: Biotransformation of aflatoxin B1 in the liver

Risk Assessment:

Aflatoxin contaminations in crops are a major concern in developing countries, where a large portion of the population is suffering from starvation or where levels of aflatoxin in food is not regulated strictly (Liu and Wu 2010). On the contrary, developed countries tend to have diverse food supplies along with strict regulations that monitor aflatoxin levels in food. It is reported that liver cancer rates in developing countries are 2-10 times higher than those of developed countries (Henry et al. 1999). It was reported jointly by the Food and Agricultural Organization / World Health Organization / United Environment Program Conference that "in developing countries, where food supplies are already limited, drastic legal measures may lead to lack of food and excessive prices. It must be remembered that people living in these countries cannot exercise the option of starving to death today in order to live a better life tomorrow" (Henry et al. 1999). There have been several reported cases of acute aflatoxicosis in Africa associated with home

grown contaminated maize consumption. For example, including in 1982, in Kenya, 12 people died, and in 2004, 125 people died as well as 317 people became ill (Lewis et al. 2005). In 1974, in the western part of India more than 100 people died and 397 people became ill ((CDC) 2004, Krishnamachari et al. 1975).

In 1998, the Food Agricultural Organization/ World Health Organization expert committee jointly conducted a quantitative risk assessment study on aflatoxin-induced liver cancer, using the existing epidemiological data, obtained from China. The study determined that HCC (Hepatocellular Carcinoma) incidence would decrease by 300 cases/billion people/year if the aflatoxin standard of 10µg/kg-20µg/kg was followed in nations with HBV (hepatitis B virus) prevalence of 25% (Yeh et al. 1989, Wu et al. 2011). A quantitative cancer risk assessment study was conducted to estimate number of cancer cases worldwide that could be directly linked to aflatoxin. Based on the aflatoxin potency factors and exposure data, it was determined that approximately 4.8% - 28.2% of liver cancer cases are attributed to aflatoxin (Liu and Wu 2010). However, all the epidemiological studies were conducted in countries where liver cancer cases (HBV, HCV) are high, which might magnify the risk of liver cancer from aflatoxin exposure (Cardwell and Henry 2004).

Economic impact of aflatoxin

It is estimated that economic damage due to crop (especially corn) wastage resulting from aflatoxin contamination could range from US$52.1 million to US$1.68 billion (Mitchell et al. 2016); the annual costs associated with loss of aflatoxin contaminated corn and peanuts alone are US$225 million and US$25.8 million,

respectively (Schmale and Munkvold 2009). It is predicted that with the change in global climate, aflatoxin contamination in crops and aflatoxin-related liver diseases would increase drastically over the years.

1.2 AFLATOXIN BIOSYNTHESIS

Aflatoxin biosynthesis is a very complex process. It has been proposed that, approximately 27 enzymatic steps and at least 30 genes are involved in aflatoxin biosynthesis. In *A. flavus*, and *A. parasiticus* aflatoxin pathway genes are clustered within the 75-kb DNA region in the fungal genome (Yu et al. 2004, Ehrlich 2009, Chang et al. 1995, Yabe and Nakajima 2004). Aflatoxin gene expression is regulated by different regulatory factors like nutrient source, pH, temperature, light and many others. The *aflR* gene, encoding a 47kDa sequence-specific DNA-binding protein, initiates the transcriptional activation process by binding to the promoter region in the DNA and starts a cascade of biosynthetic reaction processes towards aflatoxin synthesis (Roze et al. 2007, Georgianna and Payne 2009, Chang et al. 1995). Aflatoxins are polyketide derived secondary metabolites, and the pathway starts with a simple molecule, like acetate, which converts to polyketide. Polyketide changes to anthraquinones, to xanthones and finally to aflatoxin (Yu et al. 2004, Bennett and Christensen 1983).

Acetate → Polyketide → Anthraquinone → Xanthone → Aflatoxin

Initially, acetate and malonyl-CoA are converted to a hexanoyl unit by a specialized fatty acid synthase. This is then extended by a polyketide synthase to norsolorinic acid (NOR), which is the first stable intermediate in the aflatoxin biosynthetic pathway and *Nor-1* gene was the first to be cloned in *A. parasiticus* (Chang, Skory and Linz 1992, Payne and

Brown 1998). *aflA*, *aflB*, and *aflC* genes are involved in the conversion of acetate to NOR. The gene *Nor-1* was named according to its substrate norsolorinic acid and it is considered the early gene in the biosynthetic pathway. The polyketide then undergoes multiple enzymatic conversions in the pathway. In the middle of the of the pathway, intermediate versicolorin B synthase catalyzes an important step which is responsible for the bisfuran ring required to bind aflatoxin to DNA (Payne and Brown 1998). Versicolorin B is situated at the branching step of the pathway where it branches two different ways. The conversion of Versicolorin B to Sterigmatocystin (ST) leads to the production of aflatoxin B_1 and the conversion of versicolorin B to dihydrodemethylsterigmatocystin leads to the production of aflatoxin B_2. Aflatoxin B_1 and aflatoxin G_1 contain the dihydrobisfuran ring produced from demethylsterigmatocystin, and aflatoxin B_2 and aflatoxin G_2 contain the tetrabisfuran ring produced from dihydrodemethylsterigmatocystin. Sterigmatocystin is a potent mycotoxin and produced by more than 20 *Aspergillus* species as their final product.

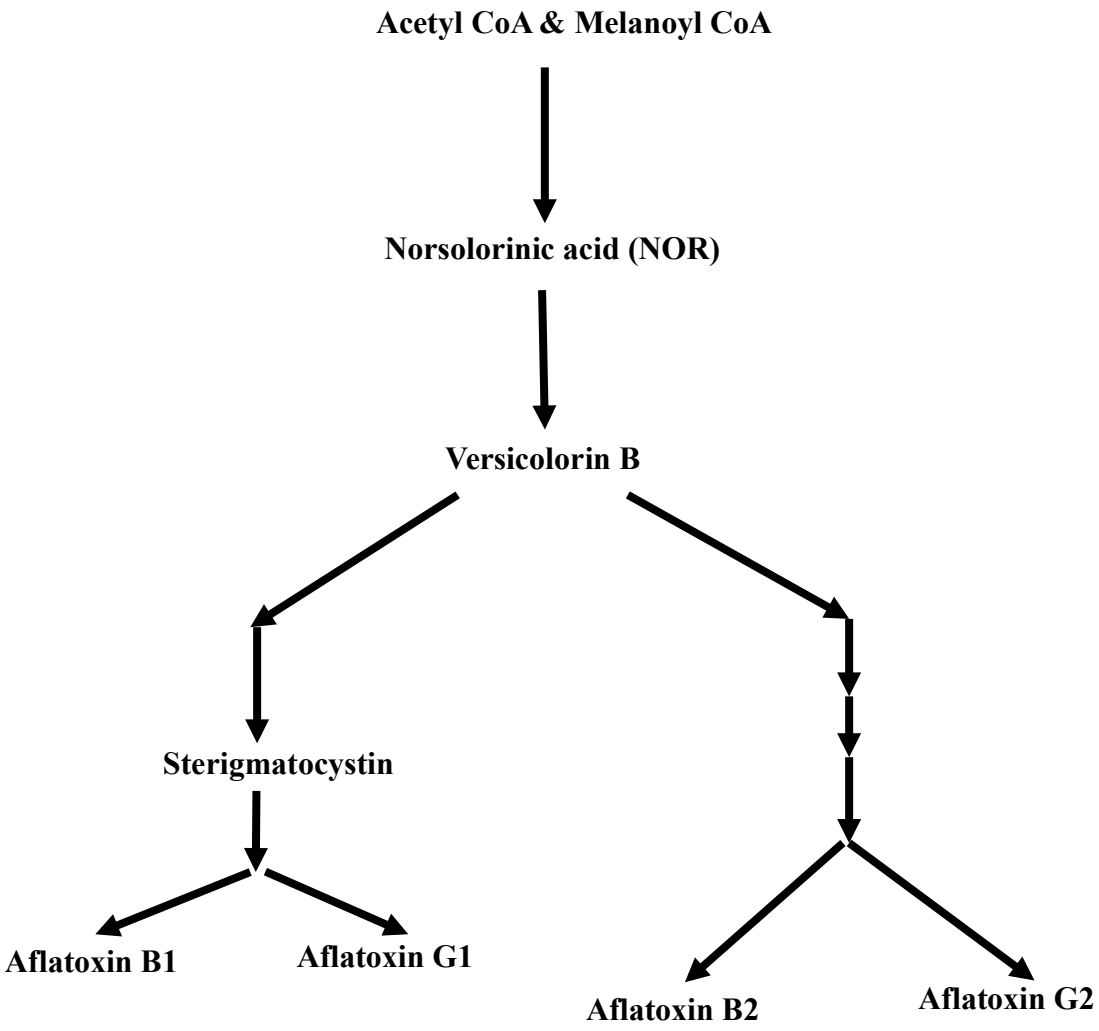

Figure 1.3: Aflatoxin biosynthesis pathway (Singh and Hsieh 1977).

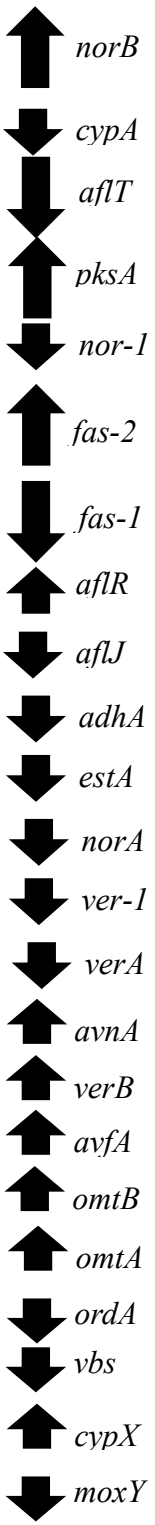

Figure 1.4: Aflatoxin gene cluster (80kb) in *A. parasiticus*, arrowhead represents the direction of transcription (Chang et al. 2007).

1.3 REGULATORY FACTORS AFFECTING AFLATOXIN GENE EXPRESSION

The gene *aflR* is the key regulator of the aflatoxin biosynthetic pathway. It encodes the protein AflR (a zinc binuclear DNA-binding protein) that positively regulates the expression of most of the genes involved in aflatoxin or sterigmatocystin biosynthesis. Disruption of *aflR* completely blocks the expression of the genes in this biosynthetic pathway and aflatoxin/sterigmatocystin production gets inhibited (Prieto, Yousibova and Woloshuk 1996). It was found that in wild type *A. parasiticus*, upregulation of *aflR* transcription leads to excess production of aflatoxin and increased accumulation of *nor-1*, *ver-1*, and *omtA* transcripts (Chang et al. 1995) and it can regulate multiple parts in the aflatoxin biosynthesis pathway. It was also suggested that along with *aflR*, other transcription factors such as NorLbp and CRE1bp, TATA binding protein and their associated cis-acting binding sites also participate in the regulation of aflatoxin biosynthesis (Miller et al. 2005).

It is also reported that G-protein receptors have a role in regulating the aflatoxin biosynthetic pathway (de Souza et al. 2013). *A. parasiticus* produces aflatoxin in yeast extract sucrose (YES) growth medium, but it does not synthesize any aflatoxin in yeast extract peptone (YEP) growth medium (Cary, Montalbano and Ehrlich 2000). The possible explanation is that glucose/sucrose activates a signal transduction pathway that is transduced into aflatoxin gene expression. The involvement of G protein, cAMP, and PKA in the regulation of aflatoxin biosynthesis is well documented (Shimizu and Keller 2001). It has been reported that two global regulators of secondary metabolism, *laeA* and *veA* genes regulate the activation of the aflatoxin gene cluster (Sarikaya-Bayram et al.

2015, Bayram et al. 2008). The LaeA (nuclear protein) contains S-adenosylmethionine binding motif which can activate transcription of a gene cluster in aflatoxin secondary metabolism (Brakhage 2013). LaeA methylates histone proteins are associated with cluster for secondary metabolism and make the region accessible to gene transcription. The *veA* gene was reported to be essential for the light dependent growth condition. VeA migrates from cytoplasm towards the nucleus in the absence of light to form a complex with LaeA, which is necessary is for both development and secondary metabolism (Yin and Keller 2011). When the *veA* gene was deleted from *A. parasiticus* strains, it resulted in a blockage in the production of aflatoxin intermediates (Calvo et al. 2004).

1.4 FACTORS AFFECTING AFLATOXIN BIOSYNTHESIS

Aflatoxin gene expression can be affected by many environmental factors like carbon source, nitrogen source, trace elements, pH, and temperature (Wilkinson et al. 2007, Klich 2007).

Effect of pH: Many studies have suggested that secondary metabolism is influenced by the pH of growth medium. It was shown that at pH 4.0 or below, the sclerotia formation was reduced by 50% but aflatoxin production was maximum (Cotty 1988). In another study it was observed that aflatoxin biosynthesis reduces with an increase in the pH of the growth medium (Keller et al. 1997).

Effect of carbon and nitrogen source: Glucose, sucrose, and sorbitol are sources of carbon and are essential for fungal growth, sporulation, and aflatoxin biosynthesis (Abdollahi and Buchanan 1981). On the contrary, peptone (Abdollahi and Buchanan 1981) and complex sugars like galactose, xylose, mannitol, and lactose do not support

aflatoxin production well (Kachholz and Demain 1983). Some studies have shown that nitrate as a source of nitrogen suppresses production of aflatoxin intermediates in *A. parasiticus* (Kachholz and Demain 1983). Other studies have indicated that, aflatoxin production increases in ammonium-based media and decreases in nitrate-based media (Keller et al. 1997).

Effect of trace metals: Certain metals were found to influence aflatoxin biosynthesis. A very small amount of aflatoxin was produced when zinc, iron, or magnesium were removed from the growth medium. On the contrary manganese, copper, mercury, cadmium, and silver were able to reduce aflatoxin biosynthesis (Marsh, Simpson and Trucksess 1975, Davis, Diener and Agnihotri 1967).

Effect of temperature: It has been reported that temperature is one of the most important factors which can alter metabolic activities in fungi (Schindler, Palmer and Eisenberg 1967). Maximum aflatoxin production was observed at 24^0C and maximum fungal growth occurred at 29^0-35^0C. No significant amount of aflatoxin was produced below 10^0C or above 41^0C.

Effect of growth medium composition: Composition of the growth medium and pH regulates aflatoxin biosynthesis. Aflatoxin production was observed to be greater when *A. parasiticus* was grown in YES (yeast extract sucrose) medium, as compared to Czapek's based liquid medium (Klich 2007, Huynh and Lloyd 1984). Aflatoxin biosynthesis was found to be greater in YES liquid static culture than YES agar medium (Gqaleni, Smith and Lacey 1996).

Effect of climate: Aflatoxin contamination is mostly observed during drought or humid and warmer seasons (Cotty and Jaime-Garcia 2007). Change in weather conditions

may influence the growth of the mycotoxin producers; in cooler temperature (<20^0C) *A. flavus* growth is minimal compared to warmer temperature. Climate also influences the type of fungi community present in the soil. It was found that major aflatoxin B_1 producer, *A. flavus,* was present in crops of any geographical region but other *Aspergillus* species are not common in different geographical regions (Cotty 1997). It is reported that people in developing countries in tropical and subtropical areas are exposed to moderate to high levels of aflatoxin (Liu and Wu 2010). The farming lands in these regions are favorable for the growth of *A. parasiticus*/*A. flavus*.

1.5 EFFECT OF AFLATOXIN & OTHER MYCOTOXIN & THEIR PRODUCRES ON MICROBIAL INTERACTIONS IN THE ENVIRONMENT

It has been a challenge to protect food and animal feed from mycotoxins and to inhibit the growth of the fungi producing them. Agricultural products completely depend on the chemicals to get a high crop yield, as they are cheap and very effective. That is why synthetic compounds are used extensively to control the fungal infestation, but there are concerns about the environmental health hazards of using these chemicals. Most pesticides contaminate soil and water and most of them do not have adequate toxicological data (Weisenburger 1993). Hence there is an urgent need to discover a novel drug which can successfully inhibit mycotoxin accumulation in food without the health concerns. Researchers have tried different methods and the long-term goal is to understand aflatoxin biosynthesis to discover novel molecules to eliminate aflatoxin accumulation in nature.

There are several methods listed in the literature. Ethylene and carbon dioxide can inhibit aflatoxin synthesis in the laboratory-grown *A. parasiticus* on peanuts (Gunterus et al. 2007). This study also showed that while aflatoxin inhibition by ethylene gas is dose dependent, the effect of carbon dioxide has a very narrow range of inhibition effect, and it does not affect the growth of molds.

Some phenolic compounds such as acetosyringone, and syringaldehyde can inhibit aflatoxin biosynthesis in *A. flavus* efficiently (Hua, Grosjean and Baker 1999). There are some studies on using plant extracts such as asafoetida, turmeric and *Azadirachta indica* leaf extract to prevent aflatoxin production in ground nuts (Ghewande and Nagaraj 1987).

In several studies, it has been reported that aflastatin, a chemical produced by Streptomyces species, can inhibit aflatoxin production completely without inhibiting the fungal growth (Ono et al. 1997, Sakuda et al. 1996, Kondo et al. 2001). Aflastatin A (0.5µg/ml) inhibits aflatoxin production in *A. parasiticus* by increasing glucose consumption and ethanol accumulation in the cell. It can also significantly reduce expression of aflatoxin producing genes such as *nor-1*, *ver-1*, *omtA*, as well as repress transcriptional activator *aflR*. Another compound, blasticidin A, biosynthesized by *Streptomyces* species also inhibits aflatoxin biosynthesis (Sakuda et al. 2000, Yoshinari et al. 2010) but the environmental toxicity data of these antibiotics are not adequately studied yet.

Several bacterial species are tested against fungi that produce aflatoxins. It was reported that bacterium *Nannocystis exedens* produces antifungal metabolites which were found to inhibit growth and sporulation of the two fungal species such as *A. flavus* and *A. parasiticus* (Taylor and Draughon 2001). *Lactobacillus casei* and *L. rhamnosus* are two

bacterial species that were found to reduce the growth of *A. flavus* in liquid culture (Bueno et al. 2006). Several strains of Bacillus were tested against *A. flavus* and *A. parasiticus* and it was found that the bacterial strain inhibited fungal population by 30% and reduced aflatoxin production as well (Bluma and Etcheverry 2006).

Recently we discovered that a non-pathogenic estuarine bacteria *Vibrio gazogenes* produces aflatoxin response metabolites (ARMs) upon exposure to a non-toxic dose of aflatoxin, which can prevent aflatoxin biosynthesis by *A. parasiticus* without inhibiting the fungal growth (Gummadidala et al. 2016).

1.6 NANOPARTICLES: BACKGROUND, ANTIMICROBIAL ACTIVITY, EXPOSURE, AND RISK ASSESSMENT

Background:

Nanotechnology has gaining popularity in recent years and it is considered to be a modern discovery. But, nanoparticles have a surprisingly long history. The use of nanoparticles began back in the ninth century in Mesopotamia (Sciau et al. 2009, Sattler 2010), where gold, silver or copper nanoparticles were used to glitter the pots. Nowadays, manufactured or engineered nanomaterials are used extensively in different areas such as electronic, textiles, cosmetics, in wound dressings, implant surfaces, as antiseptic and disinfectant in innumerable consumer goods, targeted drug delivery, and diagnostic imaging due to their unique physical and chemical properties (Dobson 2006, Rudge et al. 2001, Praetorius and Mandal 2007). With the rapid developments in nanoscience, and nanotechnologies, there is an urgent need for an internationally accepted definition for

nanomaterials. Currently a few definitions are available to serve the purpose. Definitions are as follows:

OSHA (USA): "Engineered nanoscale materials or nanomaterials that have been purposefully manufactured, synthesized, or manipulated to have a size with at least one dimension in the range of approximately 1 to 100 nanometers and that exhibit unique properties determined by their size".

European Commission: "A natural or manufactured materials containing particles, in an unbound state or as an aggregate or as an agglomerate and where, for 50% or more of the particles in the number size distribution, one or more external dimensions is in the size range 1nm -100nm. In specific cases and where warranted by concerns for the environment, health, safety or competitiveness the number size distribution threshold of 50% may be replaced by a threshold between 1% and 50%. By derogation from the above, fullerenes, graphene flakes and single wall carbon nanotubes with one or more external dimensions below 1nm should be considered as nanomaterials".

NNI (USA): "Nanomaterials are all nanoscale materials or materials that contain nanoscale structures internally or on their surfaces. These can include engineered nano-objects, such as nanoparticles, nanotubes, and nanoplates, and naturally occurring nanoparticles, such as volcanic ash, sea spray, and smoke".

However, the definitions are mainly based on size parameters and the definition given by the European Commission is more specific than other existing international definitions.

Based on the origin of nanomaterial, there are three main categories of nanomaterials or nano-sized particles listed in the literature, namely, naturally occurring, man-induced, and engineered or manufactured nanomaterials (SCENIHR). Examples of

naturally occurring nanomaterials are gas-phase condensation products, ash, minerals, colloids, etc., and they can be produced by different natural processes such as volcanic eruptions, micro-biosynthesis, geochemical reactions, and drastic weather conditions (Lead and Wilkinson 2006, Hough, Noble and Reich 2011, Heiligtag and Niederberger 2013). Naturally occurring nanoparticles can be divided into two groups – organic and inorganic. Polysaccharides and proteins are examples of organic nanoparticles and inorganic includes different metal nanoparticles (Heiligtag and Niederberger 2013). Man-induced nanomaterials are produced as by-products of human activities such as industrial processes, combustion, landfills, and from other point and nonpoint sources. Engineered or manufactured nanomaterials are intentionally produced to possess unique physico-chemical properties.

Nanoparticles as antimicrobial agent

In recent years, microbial infections have become life-threatening events because of emerging or re-emerging resistant strains of bacteria, pathogenic and opportunistic fungi, viruses, and protozoa (Galdiero et al. 2011, Tanwar et al. 2014, Sharma and Ghose 2015, Yah and Simate 2015). Development of effective antimicrobial agents is very important. Recently engineered nanomaterials have shown better activity against various types of microorganisms (Yah and Simate 2015). Metal and metal oxide nanoparticles such as silver, gold, titanium, zinc, silica, and magnesium have been used for therapeutic purposes (Seil and Webster 2012). Particle size, coating, stability, and concentration of nanoparticles are the key factors that govern the effectiveness (Azam et al. 2012, Dizaj et al. 2014). The accurate mechanism of antimicrobial action is yet to be understood

completely. Some studies have reported that nanoparticles can generate reactive oxygen species (ROS), which in turn exerts toxicity or cells undergo oxidative stress (Besinis, De Peralta and Handy 2014). Studies showed that nanoparticles also can efficiently get inside the living cells by pinocytosis and can cause cellular damage by binding to the different organelles in the cell (Usman et al. 2013, Lunov et al. 2010, AshaRani et al. 2009, Wang et al. 2012).

Effect on bacteria

Engineered nanoparticles are found to be effective against different pathogenic bacteria. The mechanism of action is not fully understood yet. Zinc oxide nanoparticle is well known for its bactericidal activity, even possessing the capability to kill spores (Azam et al. 2012), and it does not show any adverse effect when in contact with the human body (Saraf 2013, Liu et al. 2014). Zinc nanoparticles have been found to disrupt bacterial cell membrane along with the generation of a lot of oxidative stress which leads to cell damage (Xie et al. 2011). Anti-bacterial activity is related to the size of the particle; the smaller the particle, the better the activity (Emami-Karvani and Chehrazi 2011).

Gold nanoparticles are widely used antimicrobial nanoparticles because of their stability, easy detection, easy functionalization abilities (Lima et al. 2013). Gold nanoparticles do not induce ROS production in the cell unlike zinc nanoparticles but they can bind and modify bacterial cell membrane, and can reduce ATP generation and hinder tRNA binding process to the ribosome which is necessary for protein synthesis (Cui et al.

2012). Gold nanoparticles have been found to be effective against bacteria like *E. coli*, *S. typhi*.

Silicon dioxide nanoparticle is non-toxic in nature, and it does not have any detrimental effect on the microbes when it is used alone. But silica based nanostructure or modified silica nanoparticles can significantly reduce microbial growth (Camporotondia et al. 2013). Silver nanoparticle-silicon nanowire is found to inhibit the bacterial cellular growth (Lv et al. 2010). It was observed in one of the studies that silica nanoparticles can hinder biofilm growth and reduce bacterial adherence which disturbs bacterial cell proliferation (Besinis et al. 2014).

Calcium and magnesium nanoparticles are very stable and they have excellent antimicrobial properties (Yamamoto et al. 2010, Jin and He 2011). These nanoparticles are safe to humans, especially magnesium nanoparticles which are used to treat cancer (Krishnamoorthy et al. 2012 , Tang and Lv 2014). It is reported that, like zinc nanoparticles, magnesium and calcium nanoparticles also produce reactive oxygen species which most likely cause bacterial cell damage (Jin and He 2011, Hewitt et al. 2001). Magnesium alone or in combination with calcium nanoparticles can also be used in medical treatments. Calcium phosphate nanoparticles are extremely useful in targeted drug delivery treatment (Roy et al. 2003).

Titanium dioxide is one of the most abundantly found naturally occurring compounds. It is extensively used in paints, varnish, textiles, and cosmetic products such as sunscreen because of its UV light absorbing abilities (Fujishima and Honda 1972). In one of the studies, it was found that titanium dioxide nanoparticle could inhibit the bacterial growth and biofilm production by methicillin-resistant *S. aureus* isolates

(Jesline et al. 2015). Titanium dioxide is known for its photocatalytic action. This particular property is used to remove contaminants from ground water, disinfect air or water, and it is used as a potential antimicrobial agent. It is effective against a wide range of microbes including fungal spores that are very resistant to harsh conditions (Jang, Kim and Kim 2001, Foster et al. 2011).

Copper nanoparticles are effective against a wide range of microorganisms including methicillin-resistant *S. aureus* (Usman et al. 2013). The effectiveness of copper nanoparticles is size, concentration, and stability dependent. Copper gets oxidized very easily which limits the usability. Copper nanoparticles are believed to interact with the bacterial cell, causing a severe damage to the cell (Mahapatra et al. 2008). Cupric oxide nanoparticles and cuprous nanoparticles work via two different pathways. Cupric oxide generates free radical and cuprous oxide alters the protein complex in the microorganism (Meghana et al. 2015). Both the oxides are capable of causing damage to the microorganism.

Many studies suggested that, among other nanoparticles, silver-nanoparticles are one of the most studied and widely used antimicrobial (Kim et al. 2007, Rai, Yadav and Gade 2009, Pal, Tak and Song 2007) and antimicrobial activity is size and particle charge dependent (Panacek et al. 2006, Carlson et al. 2008, Ivask et al. 2014, Sail and Webster 2012). The smaller the particles, the better the activity. Smaller particles (1 - 10nm) have greater specific surface area, are capable of attaching to the bacterial cell membrane and prevent cellular functionality (Pal et al. 2007, Morones et al. 2005). Silver nanoparticles have proved their efficacy in controlling multi-drug resistant strains and they are effective against gram positive and gram-negative bacteria (Panacek et al. 2006, Allahverdiyev et

al. 2011a, Lunov et al. 2010). It was observed that these nanoparticles work in multi-mechanistic pathways in bacteria, such as the production of ROS, DNA damage to prevent replication process, and cell membrane damage. It has been reported that ionic silver is more reactive, interacts with the thiol group of some essential enzymes and those enzymes get inactivated (Morones et al. 2005). It also hinders expression of some ribosomal proteins and cellular proteins essential for ATP synthesis (Pal et al. 2007, Yamanaka, Hara and Kudo 2005). On the other hand, silver nanoparticles tend to bind to sulfur-containing membrane protein and phosphorus containing DNA, and hinder the cell division process (Pal et al. 2007, Sail and Webster 2012). Damaged cell membrane might cause increased and uncontrolled cellular permeability which may lead to cell death (Sail and Webster 2012). Because of its multi-functionality bacterial strains (except a few) have not yet developed any mechanisms to grow resistance against silver nanoparticles.

Effect on protozoan parasite

The conventional antiparasitic drugs are becoming less effective, highly toxic to the host, and they are too costly. Titanium and silver nanoparticles are proven to be very effective against parasites like giardia and leishmanial (Said, Elsamad and Gohar 2012, Allahverdiyev et al. 2011b, Allahverdiyev et al. 2011a). The exact mechanism of action is not yet known, but the possible anti-parasitic effect might be because silver nanoparticles cause the production of reactive oxygen species (ROS). Like a bacterial cell, parasites are also sensitive to ROS. It is reported that during silver nanoparticle treatment, nanoparticles showed no toxic effect on the experimental subjects with parasite infection (Said et al. 2012, Yah and Simate 2015). Metal nanoparticles have been

reported to have a toxic effect on the environment, minimizing their use in treating a human. If the toxicity issue is resolved, nanoparticles can be put into great use.

Effect on fungi

Fungi are eukaryotic organisms that are ubiquitously found in nature. Many of them are opportunistic pathogens. Several studies have investigated the efficacy of nanoparticles such as titanium dioxide, silver, gold and copper nanoparticles (Panácek et al. 2009, Jo, Kim and Jung 2009, Kathiravan et al. 2015, Nasrollahi, Pourshamsian and Mansourkiaee 2011) as potential antifungal compounds as a tool to combat life-threatening fungal infections.

The efficacy of ZnO nanoparticles was tested against mycotoxigenic molds (Hassan, Howayda and Mahmoud 2013). It was observed that ZnO nanoparticles at the concentration of 8µg/mL could inhibit growth and aflatoxin biosynthesis in molds. At 10µg/mL concentration of ZnO nanoparticles ochratoxin A and fumonisin B1 production was inhibited along with the molds producing them.

SDS (sodium dodecyl sulfate) stabilized silver nanoparticles at the concentration of 0.05mg/L showed a maximum growth inhibitory effect against pathogenic fungi *Candida albicans* (Panácek et al. 2009). This study also reveals that the antifungal effect of silver nanoparticle depends on the stabilizing agent used. Most importantly, stabilized silver nanoparticle showed no cytotoxicity to human fibroblast cell, unlike ionic silver. In another study, it was reported that gel containing silver nanoparticles (size distribution of 7-20 nm) inhibited *Candida albicans* and *Aspergillus niger* (Jain et al. 2009). In silver nanoparticles, the size of 3nm was found to be very effective against a total of 44

different strains of 6 different fungal species, among them, 30 are *T. mentagrophytes* and 14 are *Candida* species (Kim et al. 2008).

Catheter related nosocomial bloodstream infections are a very common cause of complications and morbidity. Catheters coated with silver nanoparticles, size distribution of 3-18nm, can successfully inhibit the growth and biofilm formation by the microorganisms which are related to nosocomial catheter-related bloodstream infections (Roe et al. 2008). In this study, it was observed that during the 10-day experimental period catheters released 16% of the silver nanoparticles and the majority of the nanoparticles got released in the feces. A silver nanoparticle accumulation study was conducted using heart, brain, kidney, lung, liver, blood, and skin, but no significant amount of silver nanoparticles accumulated in the specific organs and 96% of nanoparticles were recovered (Roe et al. 2008). When citrate coated silver nanoparticles were administered orally to the experimental mammals, the nanoparticles were not absorbed into the bloodstream, and it was observed that the nanoparticles mostly discharged via feces (Park et al. 2011b). These results suggest that orally administered silver nanoparticles are less bioavailable and hence may not have any toxic effect on the host.

Silver nanoparticles have been effective against plant pathogens as well, when grown on solid agar growth medium. The effect is silver nanoparticle concentration dependent (Kim et al. 2012a). For example, silver nanoparticles (stabilized raspberry extract) of size 60 nm inhibit the growth of *A. niger* and *C. cladosporioides* (Pulit et al. 2013). *A. niger* was more resistant than *C. cladosporioides* against nanoparticles. The

highest inhibitory effect was observed at a concentration of 50 ppm suggesting that antifungal activity of silver nanoparticle is concentration dependent.

It has been reported that concentration, chemical composition, and the particle size of silver nanoparticles have strong influences on the growth and mycotoxin biosynthesis in the filamentous fungi *Penicillium verrucosum*. It was found that silver nanoparticles with 0.65-5nm in size can get attached to the mycelial surface, and can be internalized within the fungal cell, and form aggregation in the cytoplasm and in different organelles (Kotzybik et al. 2016).

In a recent study published in reference to the effect of AgNps on the growth and aflatoxin biosynthesis in *A. parasiticus*, the reported MIC of AgNps against *A. parasiticus* was observed at 180µg/mL concentration, and AgNps inhibited aflatoxin biosynthesis by 50% at 90µg/mL (MIC) concentration (Mousavi and Pourtalebi 2015). How these nanoparticles interact with the fungal cells at concentrations that do not affect the growth of the fungi is yet to be elucidated.

Nanomaterial exposure

Applications of nanomaterials in different consumer products are currently available or imminent. Examples include titanium di-oxide nanoparticles in sunscreen and paints, fullerene nanotube composite in tires, and tennis rackets, protein based nanomaterials in soaps, and shampoos, metal nanoparticles in the ground water for remediation purposes, textiles, and food packaging (Handy et al. 2008). The Woodrow Wilson Database (http://www.nanotechproject.org) has listed 1814 consumer products containing nanoparticles with 438 containing silver nanoparticles as of March 2015. This is approximately a 30-fold increase in consumer products containing nanoparticles over

the 54 products originally listed in 2005. Many critical information such as nanomaterial size, shape, and concentration are unknown for most of the products listed on the consumer product inventory (CPI). Hence, it is difficult to assess the potential health risk of these products. There are concerns that, manufactured nanomaterials will get released from the consumer products over time and currently very little is known about the behavior of nanomaterials in the environment. For example, silver nanoparticles from textiles and cosmetics can enter the environment when water is used to wash them or rinse them off. Subsequently, silver gets released from the wastewater to the ground water and surface water. In the past rivers, lakes carried high amount of silver, which came from photographic industries. However, with the development of digital photography, silver concentration in the ground water has decreased measurably (Fabrega et al. 2011b). Furthermore, release of nanomaterials may also come from different sources such as factories, landfills, soil erosion, water runoff, atmospheric wet deposition, and erosion from products containing nanomaterials (Wiesner et al. 2006). Accidental spillage or release of engineered nanomaterials in industrial effluents in waterways and aquatic systems will result in direct exposure to human and other animals via direct ingestion (as contaminated drinking water), skin contact, inhalation (water aerosol), or adsorbed particles on food. Indirect exposure could arise from ingestion of aquatic organisms as a part of diet, using products containing nanomaterials. The production, use, and disposal of different nanomaterials will appear in the environment (Nowack and Bucheli 2007) along with already existing naturally occurring nanoparticles (such as colloids in fresh water), which could potentially lead to unexpected environmental health hazards.

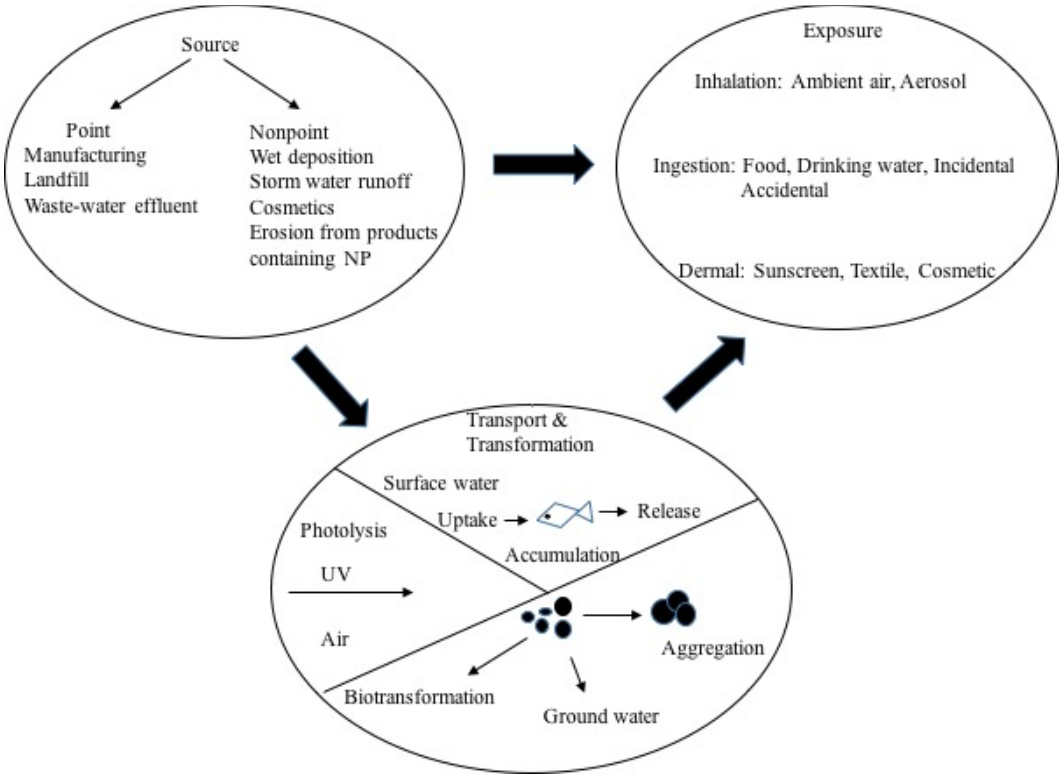

Figure 1.5: Exposure of nanomaterial in the environment

Hazard and risk assessment

An increased use of engineered nanomaterials in different commercial products may result in enhanced release in the environment (Fabrega et al. 2011a) and it has gained a multitude of concerns due to their toxic effects on experimental organisms (Bondarenko et al. 2013, Asharani et al. 2008, Manzo et al. 2011). To assess the risks associated with their release into the environment, a better understanding of their mobility, bioavailability and impacts on different organisms is required. The engineered nanomaterials are different from naturally occurring nanomaterials because they are

designed to possess particular surface properties and surface chemistry. The physico-chemical properties and reactivities of bulk materials also change as their size advances to nanoscale. Nanoparticles have higher specific surface area than their bulk counterparts and the percentage of atoms on the surface is also higher than the interior of the particle (Roduner 2006). These factors may explain their higher surface reactivity such as adsorption or catalytic activities. It is reported that the functionalization or the surface properties of engineered nanomaterials plays a crucial role in their aggregation, their mobility (as colloidal suspensions), deposition in the aquatic and terrestrial systems, as well as their interaction with other organisms in the environment (Navarro et al. 2008). Natural organic matter present in water and soil system plays an important role in nanomaterial aggregation behavior. Natural organic matter (NOM) influences the aggregation or deposition of nanomaterial by changing the surface speciation (Hug and Sulzberger 1994). Organic matters have different ways to interact with nanoparticles such as electrostatic force, hydrogen bonding or hydrophobic interaction (Ojamäe et al. 2006). This interaction is the deciding factor of the fate, stability, toxicity, and transportation of nanoparticles in the environment. Some studies have suggested that formation of larger aggregates by high molecular weight NOM will facilitate the removal of engineered nanoparticles from the sediment and will decrease the bioavailability (Navarro et al. 2008). On the contrary, solubilization by lower molecular weight NOM compounds will likely enhance the mobility and bioavailability of engineered nanoparticles (Navarro et al. 2008). The higher mobility of nanomaterials in the environment suggests higher possibility for exposure as they are dispersed over a greater distance and their persistence in the environment will also be enhanced. Organisms such as algae, plants, fungi, and

bacteria interact strongly with the environment; therefore, they are expected to get affected as a result of their exposure to engineered nanomaterials.

The ecological toxicity of nanomaterial and nanoparticles has been studied on different aquatic organisms, soil organisms, and mammals. In the biological systems of bacteria, fungi, and algae, the cell wall is mainly made up of carbohydrates and proteins which make the cell wall the active binding site (Navarro et al. 2008). Cell walls (thickness ranges from 5nm -20nm) are semipermeable with pores, thus smaller nanoparticles are permitted inside the cell (Navarro et al. 2008). Internalization of nanoparticles occurs mostly via endocytosis (Moore 2006). In this pathway, a cell might lead the nanoparticle to an endosome or lysosome or to cell-surface lipid raft associated domains (Moore 2006). Once the nanoparticles are inside the cell they might try to translocate to different organelles, and may interfere with the metabolic process and generate reactive oxygen species (ROS) (Jia et al. 2005). It is reported that the toxicity of titanium dioxide nanoparticles is size-dependent: smaller particles showed dose-dependent activity whereas larger particles were less toxic (Hund-Rinke and Simon 2006). Zinc oxide nanoparticles have shown phytotoxic effects and aluminum nanoparticles can hinder the growth of plants (Yang and Watts 2005). Engineered cerium oxide nanomaterials can translocate into plant tissue and alter germination, and thus, inhibit the growth of root and shoot (Holden et al. 2013). In an Aquatic environment, engineered zinc nanomaterials were found to cause toxicity in sea urchin embryo and chronic exposure to ZnO caused cellular damage in mussels (Fairbairn et al. 2011). Engineered silver nanoparticles are popular due to their antimicrobial properties but they also have toxic effects on environmental and human health. The chronic exposure to

silver nanoparticles causes argyria, which is irreversible skin discoloration (blue-grey coloration). On the cellular level, it may induce cell membrane alteration, enhance pore size in the cell wall, and disrupt the transport through the cell membrane (Pal et al. 2007). Many studies show that silver nanoparticle toxicity is due to the silver ion being released from the nanoparticles, and ionic silver is more toxic than the nano-silver (He et al. 2012a). Ionic silver (Ag^+) can inhibit respiratory enzymes and induce oxidative stress by generating ROS (Kim et al. 2007). It may also bind to sulfur containing proteins and inhibits important enzymatic reactions (Navarro et al. 2008). Ag^+ was also found to be responsible for the inhibition of cell-specific growth rate, photosystem II's quantum yield, and chlorophyll A's constant presence in marine phytoplankton and fresh water algae (Miao et al. 2007, Navarro et al. 2007). Silver nanoparticles may cause size-dependent cytotoxicity, genotoxicity, and may induce apoptosis in mammals (Park et al. 2010, Kim and Ryu 2013, Park et al. 2011a). Studies show that mouse embryonic stem cells when treated with polysaccharide coated silver nanoparticle, exhibit upregulation of protein p53, also known as TP53 or tumor protein (regulates cell cycle; functions as tumor suppressor) and Rad51 (repair DNA double strand breakage), which indicates genotoxic effect (Ahamed et al. 2008). Smaller silver nanoparticles (4 nm) were observed to induce significant levels of cytotoxicity, ROS generation, and IL-8 (immune response) secretion in mammalian cells (Park et al. 2011a). However, the specific mechanism and the factors affecting the toxicity are still not known. For the assessment of environmental health implementation of engineered nanomaterials, it is necessary to understand the potential exposure routes and their toxicological effects on the basis of chronic and acute exposures. Some may assume that engineered nanomaterials would have limited impacts

due to the environmental dilution. But these nanomaterials have a tendency to transform: aggregate, dissolve, or adsorb onto the NOM, deposit in sediment, or may remain suspended in water indefinitely (Lowry et al. 2012). The ecological nanotoxicology experiments are carried out using medium to high concentrations of engineered nanomaterials to determine the potential risks associated with these materials. The dose response relationship does not represent actual concentrations of nanomaterials in the environment. The complexities in relation to nanomaterial transformations and environmental toxicological concerns are required to be addressed on the basis of real world exposure scenarios.

1.7 GOAL OF MY STUDY

While several studies demonstrate that nanoparticles at specific threshold concentrations inhibit the growth of fungi, there are currently no studies that shed light on the response of fungi to nanoparticles present in the growth medium at concentrations that do not affect the growth of the fungi. The knowledge is especially essential to assess the effects of naturally occurring nanoparticles in ecosystems that harbor fungi with the ability to synthesize secondary metabolites such aflatoxins and other mycotoxins, which have significant impacts on public and environmental health. My thesis addresses this knowledge gap. In this work, I investigated the effect of a custom designed silver nanoparticle (20 nm sized citrate coated silver nanoparticles or 'AgNp-cit') on *Aspergillus parasiticus*, the popular plant pathogen, which produces aflatoxin B_1. The 20nm sized AgNp-cit have been used previously as model silver nanoparticles for studying nanoparticle fate and behavior in diverse environments (Römer et al. 2011). We

have mainly used a concentration of 50ng/mL to study the effect of AgNp-cit on *A. parasiticus* aflatoxin biosynthesis. As will be described later in the thesis, this is a concentration that was identified in our dose-response assay as one that displayed maximum inhibitory effects on aflatoxin biosynthesis but demonstrated no effect on *A. parasiticus* growth. In this thesis, we attempt to answer two fundamental questions:

(1) How does AgNp-cit affect aflatoxin biosynthesis at concentrations that do not affect the mycelial growth?

(2) What impact does nanoparticle concentration, size, and surface coating have on aflatoxin biosynthesis?

In this study we demonstrate that exposure of AgNp-cit elicits a transient intracellular response (a significant reduction in aflatoxin accumulation) in the fungus without causing any alteration in the cellular growth. The knowledge opens a new research direction that will investigate the mechanistic details of the nanoparticle-mediated inhibition of aflatoxin biosynthesis and will reveal new targets for modulation of fungal secondary metabolism

CHAPTER 2

SYNTHESIS AND CHARACTERIZATION OF CITRATE-COATED SILVER NANOPARTICLES

Silver nanoparticles are one of most popular and widely used metal nanoparticles. Silver nanoparticles are used abundantly in various fields, especially as antimicrobial agents. They are considered to be less toxic to humans (Fabrega et al. 2011a). There are several methods to synthesize silver nanoparticles, but the chemical reduction method is widely used. For the majority part of this study, citrate coated silver nanoparticles of size 20nm were used (here we call them AgNp-cit). To investigate the effect of nanoparticle size on our biological model, *Aspergillus parasiticus*, we used 15nm and 30 nm citrate coated silver nanoparticles as well. The nanoparticles were synthesized by chemical reduction of silver nitrate by using the reducing agent, sodium borohydride and were then stabilized with citrate. The synthesized silver nanoparticles were characterized by surface plasmon resonance UV-vis spectrophotometry (wavelength 200nm to 800nm) to verify the absorbance of the nanoparticles, dynamic light scattering spectroscopy to measure their hydrodynamic diameter and size distribution, and transmission electron microscopy to verify their morphological characteristics. The UV-vis spectroscopy demonstrated a typical surface plasmon absorption peak at 390nm for 15nm sized AgNp-cit, 395nm for 20nm sized

AgNp-cit, and 403nm for 30nm sized AgNp-cit. DLS measurements confirmed their *z* average size values. TEM images confirmed the formation of spherical shaped nanoparticles. Both DLS and TEM analysis demonstrated the size homogeneity of the synthesized nanoparticles. A part of our study also investigated the effect of nanoparticle coating on *A. parasiticus* for which we compared commercially obtained 20 nm sized polyvinyl pyrrolidone (PVP) coated silver nanoparticles with AgNp-cit. These nanoparticles were also characterized to confirm their structural and morphological characteristics. The UV-vis absorbance for AgNp-pvp was observed at 396 nm. TEM images showed that the particles are spherical in shape and homogenously distributed throughout the nanoparticle suspension, and the DLS data confirmed the hydrodynamic size of the AgNp-pvp was found to be ~20nm.

2.1 INTRODUCTION

National Industrial Chemicals Notification and Assessment Scheme (NICNAS) defines nanomaterials as "Industrial materials intentionally produced, manufactured or engineered to have unique properties or specific composition at the nanoscale, that is a size range typically between 1nm to 100 nm, and is either a nanoobject (that is confined in one, two or three dimensions at the nanoscale) or is nanostructured (that is having an internal or surface structure at the nanoscale)". Notes to this working definition are a) intentionally produced, manufactured or engineered materials are distinct from accidentally produced materials, b) 'unique properties' refers to the chemicals and/or physical properties that are different because of a material's nanoscale features when compared with the same material without nanoscale features, and result in unique

phenomena (e.g. increased strength, chemical reactivity or conductivity) that enable novel applicaltions, c) aggregates and agglomerates are considered to be nanostructured substances, and d) where a material includes 10% or more number of particles that meet the above definition (size, unique properties, intentionally produced) NICNAS will consider this to be a nanomaterial. These particles have relatively higher specific surface area, with unique physical and chemical characteristics as compared to their corresponding bulk materials. Metal nanoparticles, especially silver nanoparticles, are very popular for their broad-spectrum antimicrobial activity. There are several methods to synthesize metal nanoparticles of different sizes and shapes. Among the other methods, liquid phase synthesis of nanoparticles is a widely used the technique (Römer et al. 2011). Synthesis of spherical metal nanoparticles, and stabilization with citrate was previously established by J. Turkevich (Henglein and Giersig 1999, Turkevich, Stevenson and Hillier 1951). In this method, gold nanoparticles were synthesized in an aqueous solution at an elevated temperature, and sodium citrate was used as both a reducing agent and a capping agent. Many studies have reported that citrate can reduce the metal ion and, at the same time, stabilize the resulting metal nanoparticles. According to the Turkevich method, using different concentrations of metal salt and citrate as reducing agent can control the size of the particles. However, with an increase in particle size, aggregation and precipitation of nanoparticles may be observed. In another method established by Burst and Sciffrin, metal nanoparticles are made by using sodium borohydride as a reducing agent (Shirtcliffe, Nickel and Schneider 1999, Wuithschick et al. 2013). It is reported that previously it was difficult to synthesize homogeneous and stable particles less than 10nm size and larger than 50nm (Agnihotri, Mukherji and

Mukherji 2014). For smaller size particles, the use of a strong reducing agent (sodium borohydride) facilitates the growth of smaller particles and for larger particles, a weaker reducing agent (trisodium citrate) is helpful. In this study, silver nanoparticles of different sizes (15nm, 20nm, and 30nm) were synthesized by chemical reduction of silver nitrate salt by sodium borohydride (reducing agent), and then stabilized with citrate. This process is simple and reproducible. The particles size was manipulated by varying the solution temperature, the concentration of the metal salt, the reducing agent, and the reaction time (Römer et al. 2011, Agnihotri et al. 2014). The optical properties of the resulted AgNps were evaluated using surface plasmon UV-vis spectrophotometer at a wavelength range of 200nm to 800nm. It measures the ratio of the intensity of incident light at a given wavelength and intensity of transmitted light. The absorption phenomena of nanoparticles is because of the surface plasmon resonance. The surface plasmon resonance changes with a change in particle size and shape. Next, the silver nanoparticles were characterized by using TEM. It is a quintessential tool in analyzing morphological characters for the subject. Electrons pass through the specimen, resulting in a transmitted image, and the image is collected with a digital camera. The TEM image indicates that the particles are well dispersed, homogeneous and spherical in shape. The z-average size and particle size distribution were determined by DLS.

2.2 MATERIALS AND METHODS

Synthesis of citrate-coated silver nanoparticles:

Three different sizes of AgNps were prepared from a previously established chemical reduction method (Römer et al. 2011, Cumberland and Lead 2009, Afshinnia et al. 2016). A 100mL aqueous solution of silver nitrate (0.25mM), a 100mL aqueous solution of sodium citrate (0.31mM), and a 10mM sodium borohydride solution were prepared in nanopure water and kept in 4^0C for 30 minutes. Then silver nitrate solution and sodium citrate solution were mixed together in a conical flask and stirred vigorously. After a few minutes, 6mL of sodium borohydride (0.25mM for 20nm AgNp-cit, and 10mM for 15nm and 30nm AgNp-cit) (reducing agent) were added. The reaction mixture was slowly brought to a boil. After heating for 90 minutes, the mixture was kept at room temperature, overnight, in the absence of light. To obtain the 15nm AgNp-cit, the heating process was performed without sodium borohydride and towards the end, 6mL of 10mM sodium borohydride was added. After adding the reducing agent, the mixture was heated for an extra 10 minutes. The AgNps were cleaned to remove excess amounts of dissolved ions from the suspension by ultrafiltration with 1kDa regenerated cellulose membrane (Millipore) using diafiltration the method, to prevent nanoparticle aggregation and drying. Then the nanoparticle suspensions were redispersed in 0.31nM sodium citrate solution to prevent any further growth. This process was repeated three times. Then the AgNps were stored at 4^0C (away from light) for future use.

Pvp coated silver nanoparticles (AgNp-pvp) suspension was purchased from Sigma-aldrich (product # 795933). According to the manufacturer, the concentration of

the suspension is 0.02mg/mL, and the average size of the AgNp is 20nm. AgNp-pvp characterization was carried out to confirm the size and shape by UV-vis, TEM, and DLS, and the data is described later in detail.

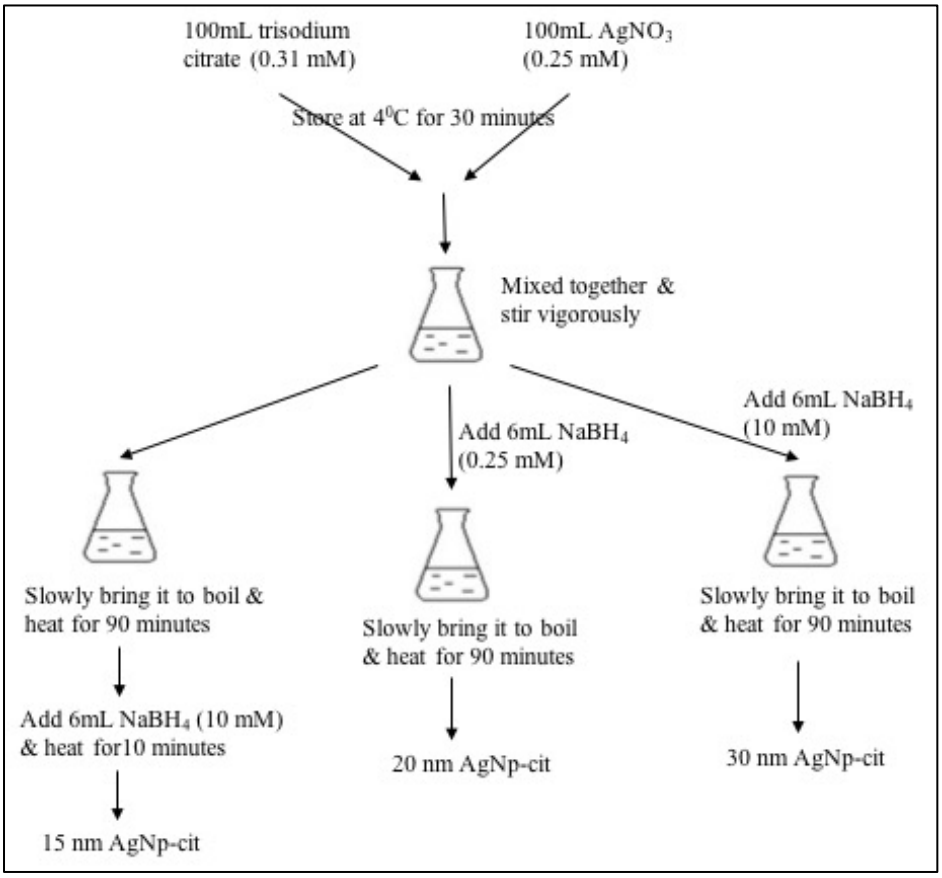

Figure 2.1: Schematic diagram of synthesis of citrate coated silver nanoparticles of different sizes.

Characterization of AgNps:

(a) Surface plasmon resonance: AgNps were characterized using multiple methods to ensure particle size, shape, and size distribution. AgNp suspensions were characterized using surface plasmon UV-Vis spectrophotometry at a wavelength range

from 200nm to 800nm. All the measurements were done in triplicates and were corrected with a blank.

(b) Transmission electron microscopy: Carbon coated copper grid (mesh# 300, Ted Pella) was used for TEM study. The samples were prepared by using the drop method (Bonevich and Haller 2010). The grids were covered with 15 µl of poly-L-lysine and left for 15 minutes. Grids were washed gently with nano-pure water and dried. Then 15 µl of undiluted AgNp-cit suspension was added to the grid. After 15 min, excess amounts of the suspension were soaked from the grid by filter paper, dried, and the images were obtained using TEM (Hitachi 8000) operating at 200kv accelerating voltage.

(c) Dynamic light scattering (DLS): DLS was carried out at 25^0 C with Malvern Zetasizer using a 1cm pathway disposable polystyrene cuvette. The z average diameter and polydispersity index (PDI) were provided by the instrument. The z average diameter and PDI were measured three times to calculate the mean diameter of the particles.

(d) Measurement of total silver concentration: Inductively Coupled Plasma Optical Emission Spectroscopy (ICP-OES) (Varian 710-ES) was performed as described previously (Shameli et al. 2011) to determine the total silver concentration (includes silver present as ions as well as nanoparticles) in AgNp-cit suspension. 1mL of AgNp-cit solution was acid digested with 67-70% nitric acid (Fisher Chemalert) prior to ICP-OES measurements. Silver concentrations in the sample were determined using a standard calibration curve that was plotted using known concentrations of silver solutions.

2.3 RESULT & DISCUSSION

Characterization of synthesized AgNps:

There are several methods to synthesize silver nanoparticles such as physical techniques, chemical synthesis, biological, electrochemical, photochemical, *y*-radiation, laser ablation, etc. The most popular preparation of silver colloid is chemical reduction of silver salt with a reducing agent such as sodium citrate or sodium borohydride. It is a simple, straightforward, and reproducible method in which solution temperature, reaction time, concentrations of reducing agents, and metal salt influences particle size (Šileikaitė et al. 2006). In this study silver nanoparticles of different sizes were synthesized by using sodium borohydride and sodium citrate as a reducing agent. There are several steps involved in the formation of the nanoparticles such as reduction, nucleation, growth, agglomeration (Pacioni et al. 2015). The possible first step for generation of AgNps is the reduction of Ag^{+} to metallic silver (Ag^{0}), followed by agglomeration into oligomeric clusters. Then the clusters lead to the formation of silver nanoparticle suspension (Agnihotri et al. 2014, Pacioni et al. 2015, Iravani et al. 2014). Citrate also acts as a stabilizing agent. It interacts with the particle surface and stabilizes particle growth, and protects particles from sedimentation, agglomeration or aggregation.

As an initial step of characterization of AgNp-cit, we first analyzed the absorbance spectra of the freshly synthesized nanoparticle solution using surface plasmon resonance UV-Vis spectrophotometry (wavelength 200nm to 800nm). Surface plasmon resonance UV-vis spectroscopy is a very sensitive technique, which shows absorption spectra for specific nanoparticles. This technique is also sensitive towards the size of the

nanoparticles; the SPR peak position shifts to longer wavelengths as the particle size increases. As shown in Fig 2.2 a) AgNp-cit-15nm, 2.3 a) AgNp-cit-20nm, 2.4 a) AgNp-cit-30nm, and 2.5 a) AgNp-pvp-20nm, the nanoparticle solution demonstrated an absorbance peak at 391nm, 395 nm, 403, and 396nm respectively (table 2.1), which was suggestive of the successful synthesis of respective silver nanospheres. The spectroscopic observations of the AgNp-cit of different sizes indicate that, as the particle size increases, the SPR peak shifts towards the higher wavelengths. To determine the size and shape of the nanoparticles, we have performed a transmission electron microscopy (TEM) of the AgNp-cit and AgNp-pvp suspensions by placing a droplet of the solution on a carbon-coated grid coated with Poly-L-lysine, followed by gentle washing and drying. The representative images of the nanoparticles as observed under TEM is shown in Fig. 2.2 b (AgNp-cit 15nm), 2.3 b (AgNp-cit 20nm), 2.4 b (AgNp-cit 30nm), and 2.5 b (AgNp-pvp 20nm). The TEM images of all the AgNps indicate well-dispersed particles in the resulting suspension, and the particles are spherical in shape. The mean hydrodynamic diameter and the size distribution of the nanoparticles were performed using dynamic light scattering (DLS) spectroscopy. It is a very common technique used to determine the hydrodynamic size and size distribution of particles. Particles in solution undergo random movement called Brownian movement. Larger particles have slower Brownian motion, and the distance between particles changes constantly with time. When light hits particles, the light scatters in all directions due to their random movements and the scattering intensity fluctuates over time. This scattered light then undergoes either constructive or destructive interference with the surrounding particles. The rate at which the intensity of the scattered light fluctuates is measured and the data is evaluated as

autocorrelation function. However, this technique is biased to bigger particles because according to Rayleigh's scattering equation, the intensity is proportional to the diameter of particle to the sixth power. Therefore, even a very small portion of aggregate will have a large bias on the signal. Hence, the machine cannot measure mixture of particles with different sizes accurately. Fig 2.2 c, 2.3 c, 2.4 c and 2.5 c show the size distribution by intensity with DLS for different particles in their undiluted state. As shown in table 2.1, the size obtained by the DLS is larger than the size obtained by TEM because DLS measures hydrodynamic size rather than physical size and DLS is biased towards larger particles.

Table 2.1: A comparison of UV-vis spectrophotometer absorbance, DLS z-average size, PDI, TEM average size, and ICPOES values for different AgNp particles

	AgNp-cit 15nm	AgNp-cit 20nm	AgNp-cit 30nm	AgNp-pvp 20nm
λ max from UV-vis	391nm	395nm	403nm	396nm
z average diameter	15.11 ± 1.27	20.13 ± 0.95	30.42 ± 2.06	36.9 ± 0.8
PDI	0.184 ± 0.01	0.109 ± 0.03	0.252 ± 0.05	0.297 ± 0.04
Average size by TEM (n=100 particles)	6.82 ± 2.61	13.8 ± 2.25	25.06 ± 5.92	19.56 ± 5.87
ICPOES (ppb)	9289.67 ± 236.9	9671.56 ± 100.04	9651.69 ± 96.83	18877.33 ± 241.93

2.4 CONCLUSION

In this study, three different sizes of silver nanoparticles were synthesized using the chemical reduction method and all the nanoparticles were stabilized with citrate. All the AgNps (AgNp-cit of 3 different sizes and AgNp-pvp) were characterized by surface plasmon UV-vis spectrophotometry, TEM, and DLS. The characterization data confirms the successful synthesis of three different sizes of citrate-coated AgNps.

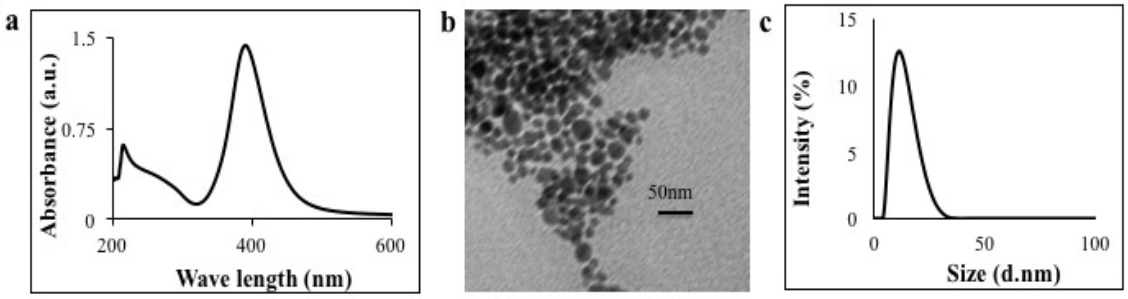

Figure 2.2: Characterization of AgNp-cit size of 15nm: (a) surface plasmon UV-vis spectrophotometry, peak is at 391nm, (b) Transmission electron microscope image of AgNp-cit-15nm of size, the scale bar is 50nm, (c) Dynamic light scattering graph; size distribution by intensity of AgNp-cit-15nm

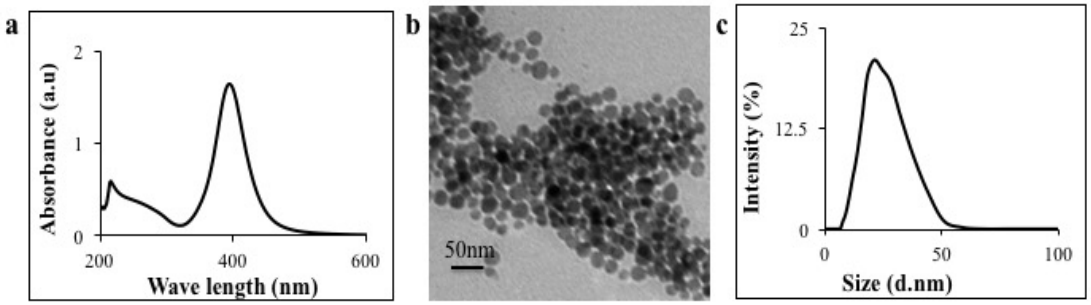

Figure 2.3: Characterization of AgNp-cit size of 20nm: (a) surface plasmon UV-vis spectrophotometry, peak is at 395nm, (b) Transmission electron microscope image of AgNp-cit-20nm of size, the scale bar is 50nm, (c) Dynamic light scattering graph; size distribution by intensity of AgNp-cit-20nm.

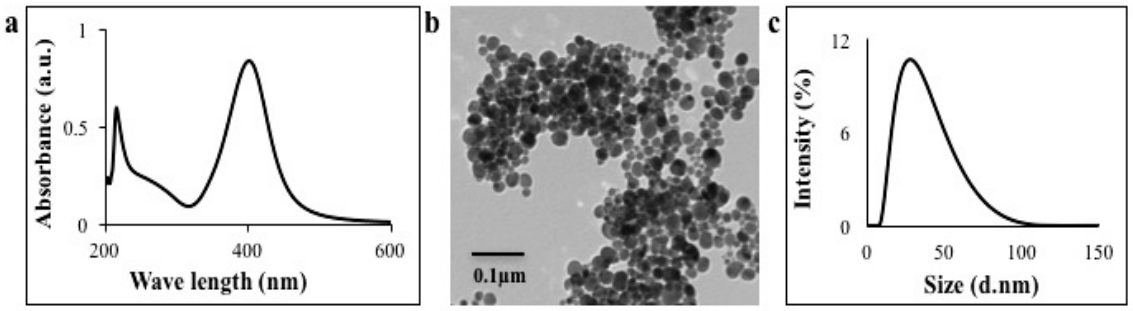

Figure 2.4: Characterization of AgNp-cit size of 30nm: (a) surface plasmon UV-vis spectrophotometry, peak is at 403nm, (b) Transmission electron microscope image of AgNp-cit-30nm of size, the scale bar is 0.1µm, (c) Dynamic light scattering graph; size distribution by intensity of AgNp-cit-30nm.

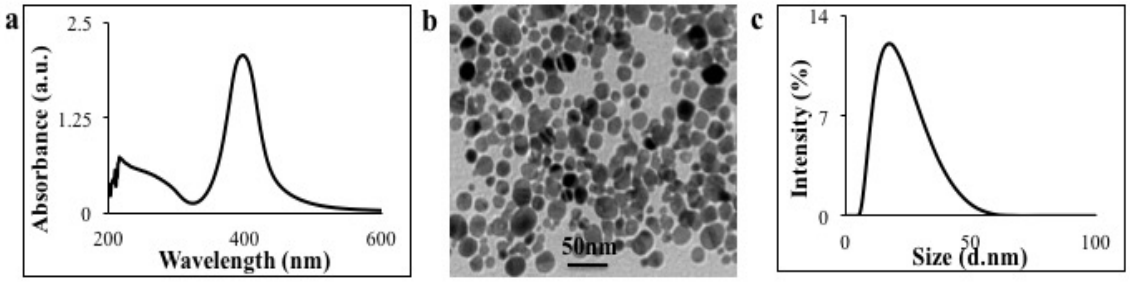

Figure 2.5: Characterization of AgNp-pvp size of 20nm: (a) surface plasmon UV-vis spectrophotometry, peak is at 403nm, (b) Transmission electron microscope image of AgNp-cit-30nm of size, the scale bar is 50nm, (c) Dynamic light scattering graph; size distribution by intensity of AgNp-pvp-20nm.

CHAPTER 3

EFFECT OF CITRATE COATED SILVER NANOPARTICLES ON THE GROWTH AND AFLATOXIN BIOSYNTHESIS IN *ASPERGILLUS PARASITICUS*

The manufacturing and usage of silver nanoparticles have increased in recent years because of their broad-spectrum antimicrobial properties. However, their effect on microbial natural product synthesis at concentrations that have no effect on microbial growth remains unclear. In this study, we evaluated the effect of 20nm citrate coated silver nanoparticles (AgNp-cit), on the growth and aflatoxin biosynthesis in *Aspergillus parasiticus*. This fungus is a well-characterized model for fungal secondary metabolism and the producer of the hepatocarcinogenic mycotoxin, aflatoxin B_1. We demonstrate here that exposure and uptake of AgNp-cit at 50ng/mL concentration elicits a significant reduction in intracellular reactive oxygen species in the fungus resulting in a greater than two-fold decrease in aflatoxin biosynthesis as compared to the untreated mycelia. No effect on fungal growth was observed. Our results also suggest that AgNp-cit mediated aflatoxin inhibition was a result of transcriptional inhibition of the aflatoxin gene cluster and two global regulators of secondary metabolism, *laeA,* and *veA*. We also observed that at 30-hour post inoculation, approximately ~85% of AgNp-cit was removed from the growth

medium, and around 40-48-hour post inoculation, the ROS level, as well as the aflatoxin biosynthesis in the mycelia, reverts back to the levels observed in the wild type.

3.1 INTRODUCTION

Nanoparticles are studied and used extensively because of their usage in different fields such as biomedical, electronic, textile industries, cosmetic industries. Many studies also have suggested that, among other nanoparticles, especially silver nanoparticles have excellent anti-microbial properties (Rai et al. 2009, Kim et al. 2007, Pal et al. 2007). Silver nanoparticles have proven their efficacy in controlling the resistant microbial communities and they are effective against gram-positive and gram-negative bacterial strains (Panacek et al. 2006, Morones et al. 2005). The antifungal effect of silver nanoparticles has not received the attention it needs; furthermore, some studies suggested the antifungal activity of silver nanoparticles is not reliable because of its inconsistency (Kim et al. 2008, Panácek et al. 2009). It has been reported that surface coating, concentration, and particle size of silver nanoparticles have strong influence on the growth and mycotoxin biosynthesis in fungi. SDS coated silver nanoparticles size of 25nm, at concentration 0.05mg/L, demonstrated better fungistatic activity against candida species than did ionic silver, non-stabilized silver, pvp, tween 80, and brij coated silver nanoparticles of same size (Panácek et al. 2009). It was observed that silver nanoparticles, size of 0.65nm-5nm can get internalized within the *Penicillium verrucosum* mycelial filaments and form aggregations in the cytoplasm (Kotzybik et al. 2016), and particles size 50nm-200nm attached strongly to the cell wall of the mycelium. Silver nanoparticles, size of 5nm, significantly inhibited fungal growth and germination

at concentration of 5mg/L whereas 50nm particles showed weak inhibition and 200nm particles showed no effect on growth and germination at concentrations up to 100mg/L (Kotzybik et al. 2016). Few recent studies have been published in reference to the effect of AgNps on the growth and aflatoxin biosynthesis in *A. parasiticus.* The reported MIC of AgNps against *A. parasiticus* was observed at 180µg/mL concentration, and AgNps inhibited aflatoxin biosynthesis by 50% at 90µg/mL (MIC) concentration (Mousavi and Pourtalebi 2015). How these nanoparticles interact with the fungal cells at nontoxic concentrations is yet to be elucidated.

In this study, we examined the effect of 20nm-sized AgNp-cit on growth and aflatoxin B_1 biosynthesis in the filamentous fungus, *Aspergillus parasiticus*. Aflatoxin B_1 is a potent naturally occurring carcinogenic mycotoxin that contaminates crops such as corn, tree nuts, peanuts, cotton seeds and much more. Every year billions of dollars are invested in preventing aflatoxin contamination in the food commodities. *A. parasiticus* is a well characterized and established model for investigating the molecular mechanism underlying aflatoxin biosynthesis. The current study aims to investigate:

- The effect of AgNp-cit of size 20nm on aflatoxin biosynthesis in *A. parasiticus* at concentrations that do not affect growth of mycelia.
- The molecular mechanism of AgNp-cit on *A. parasiticus* through aflatoxin pathway gene expression, gene expression of global regulators of secondary metabolism, ROS generation by the mycelia upon exposure to AgNp-cit, and SOD gene expression to validate the ROS generation by the mycelia.
- The interaction of AgNp-cit in the fungal growth medium (yeast extract sucrose).

3.2 MATERIALS AND METHODS

Synthesis and characterization of citrate coated silver nanoparticles:

The synthesis and characterization of AgNp-cit are described in detail in chapter 2.

AgNp-cit interaction with the fungal growth medium:

The possible interaction of the AgNp-cit with the fungal growth medium (YES; yeast extract sucrose) is an important step to understanding the possible aflatoxin inhibitory effect of AgNps in the medium. For the interaction study, the fungal growth medium (YES) was inoculated with AgNp-cit (50ng/mL) along with 10^6/mL *A. parasiticus* spores (treated group), and in another flask, fungal growth medium was inoculated only with AgNp-cit (50ng/mL) and grown under standard growth condition (29^0C, in a dark shaker with rpm 150). At different time points (0 hour, 12 hours, 24 hours, and 30 hours) the medium was harvested and studied under surface plasmon UV-vis spectroscopy.

Fungal strain, medium and growth conditions:

For the current study, wild-type aflatoxin producer, *Aspergillus parasiticus,* SU-1 (NRRL 5862) was used. For nanoparticle exposure experiments, 10^6 spores of *A. parasiticus* were inoculated in 100 mL Yeast Extract Sucrose (YES) liquid growth medium containing AgNp-cit (10, 25, 40, 50, 60, 75, and 100 ppb), and grown under standard growing condition (29^0C, in a dark shaker with rpm 150). Control groups were grown under the same growing conditions but in the absence of AgNp-cit. For this study, we have selected 50ng/mL concentration, because at this concentration mycelia growth

was unaffected and it showed maximum aflatoxin inhibitory effect. Mycelia were harvested for analyses of growth, nanoparticle uptake, and gene expression analysis at 24h, 30h, 40h, and 48h from the time point of inoculation. At the same time points, growth medium was harvested as well for determination of aflatoxin accumulation in the medium and nanoparticle concentration at each time-point.

Fungal growth and aflatoxin measurements:

Dry weight measurements of harvested mycelia were performed as described previously (Liang, Skory and Linz 1996). Briefly, at different time point, mycelia were harvested and stored at -80^{0}C. The next day mycelia were incinerated in a hot air oven (85^0 to 90^{0}C) for 8-10 hours. After 8 hours, all the mycelia were collected and the dry weight was calculated by deducting the final weight (after incineration) from the initial weight (before incineration). Since previous studies (Chanda et al. 2010) that have employed the fungal growth conditions used in the current study have shown that aflatoxin biosynthesis and export into the growth medium occurs at peak levels at 40h from the point of inoculation of fungal spores, we have performed all aflatoxin measurements in this study at 40h time-point. We compared aflatoxin B_1 accumulated in the growth medium normalized to the dry weight of the mycelia in the presence of AgNp-cit with the untreated control. Aflatoxin accumulation in the growth medium was determined using both thin-layer chromatography (TLC) and Enzyme Linked Immunosorbent Assay (ELISA) as described previously (Pestka 1988). Aflatoxin B_1 was measured using Neogen veratox aflatoxin (total) quantitative test kit (cat# 8030) and Neogen reader 4700.

Nanoparticle interaction with aflatoxin:

Interaction of citrate coated silver nanoparticles with aflatoxin was determined by ELISA as described above. Aflatoxin was extracted with 70% methanol from the fungal growth medium and incubated with AgNp-cit at 50ng/mL and 100ng/mL concentrations for 4 hours. After 4-hours aflatoxin was measured. In another experiment the aflatoxin-AgNp-cit mixture (after 4 hours of incubation) was ultra-filtered/ultra-centrifuged using Amicon ultra-centrifugal filter unit (3Kda). The filtrate was the acid digested and the concentration of aflatoxin was determined using ELISA.

Nanoparticle uptake measurements:

Uptake of AgNp-cit from the growth medium was determined by performing time-course (24h, 30h, 40h, and 48h) ICP-OES measurements of total silver in the growth medium and harvested mycelia in parallel. To determine the amount of total silver in the mycelia, the required amount (50mg) of mycelia was harvested from the AgNp-cit treated growth medium at different time points. The harvested cells were then washed with nanopure water several times to remove remaining growth media and acid digested in 2% HNO_3 for ICPOES study.

Quantification of ROS:

A quantitative comparison of ROS between wild-type strain, *A. parasiticus* SU-1 untreated, AgNp-cit, and $AgNO_3$ treated was conducted spectrophotometrically using 2', 7'-dichlorofluorescein diacetate (DCFH-DA) based on a protocol described previously (Wu and Yotnda 2011). An equal weight of mycelia from each sample was placed into 1mL freshly made 1 μM DCFH-DA in PBS. The yield of the fluorescent product

dichlorofluorescin (DCF) upon oxidation of DCFH-DA due to the generation of ROS was measured after 5h reaction at 37 °C using excitation/emission wavelength of 490/525 nm.

Gene expression studies:

a) RNA extraction, purification and cDNA synthesis:

Total RNA was extracted from cells harvested in triplicates using TRIzol (TRIzol Reagent; Invitrogen, Carlsbad, CA) based on a method previously described (Chanda et al. 2009). Within 24 hours of extraction, RNA cleanup was performed using a Qiagen® RNEasy Cleanup Kit (Qiagen, Valencia, CA), and samples were stored at -80°C. From the extracted RNA, samples complementary DNA (cDNA) was synthesized using a reverse transcription kit (New England BioLabs Inc., Ipswich, MA) according to manufacturer's instructions.

b) Real-time PCR assays:

Expressions of aflatoxin and superoxide dismutase genes were examined using quantitative real-time PCR assays using SsoAdvanced universal SYBR Green supermix (BioRad Laboratories, Hercules, CA) and gene-specific forward and reverse primers (**Table 1**). Superoxide gene-specific primers were designed using Primer3 online software (http://www.ncbi.nlm.nih.gov/tools/primer-blast/). Aflatoxin gene primers used were identical to those described previously (Roze et al. 2007). Reactions were performed in a CFX96 thermal cycler (Bio-Rad Laboratories, Hercules, CA). Similar to the previous gene expression studies in *A. parasiticus* (Roze et al. 2007), β-tubulin was used here as the housekeeping gene. The expression value of each gene was obtained from the threshold cycle values that were normalized against 18SrRNA expression in each sample. All RT-PCRs were performed in triplicates for each gene per sample. All

data and statistical analysis were performed using CFX Manager software (Bio-Rad Laboratories).

3.3 RESULTS AND DISCUSSION

Effect of AgNp-cit on aflatoxin biosynthesis:

To determine the effect of AgNp-cit on the mycelial growth of *A. parasiticus*, a series of different concentrations of AgNp-cit were selected. As shown in Figure 3.2 a, we observed a significant reduction in the dry-weight of *A. parasiticus* upon exposure to 500ng/mL concentration. AgNp-cit at the concentrations of 10ng/mL, 25ng/mL and 50ng/mL, did not inhibit the cellular growth of the fungus as compared to the untreated control. We also evaluated the effect of AgNp-cit on aflatoxin biosynthesis at different concentrations (10, 25, 40, 50, 60, 75, 100ng/mL). As shown in Figure 3.2 b, upon exposure to AgNp-cit at 50ng/mL concentration, *A. parasiticus* demonstrated a reduction of aflatoxin biosynthesis in the growth medium by greater than two-fold as compared to the untreated control. To ensure that inhibition of aflatoxin was not due to an initial growth inhibition effect, we also compared the growth rates of the fungus during the 48-hour time period by performing a time-course dry weight measurements at 24h, 30h, 40 and 48h. As shown in Figure 3.2 c, no significant difference in growth rate was observed between the AgNp-cit treated mycelia and untreated mycelia, suggesting that at the applied concentration, AgNp-cit was able to inhibit aflatoxin biosynthesis specifically, and this was not an indirect effect of an initial growth inhibition.

Effect of silver nitrate on aflatoxin biosynthesis:

We further explored the possibility of whether this inhibition of aflatoxin by nanoparticles was an effect of dissolution of nanoparticles into silver ions. Hence, we studied the effect of a panel of doses (10, 25, 40 and 50ng/mL) of silver nitrate, a salt that dissolves in the growth medium, resulting in the introduction of silver ions into the medium. We chose these doses to study the effect of silver ions at levels equivalent to or lower than the levels that would be generated if the silver nanoparticles dissolved fully or partially in the growth medium. As shown in Figure 3.2 d, unlike AgNp-cit, with silver nitrate at 50ng/mL concentration, aflatoxin accumulation was significantly enhanced (~1.5 fold). At 10ng/mL and 25ng/mL we observed no significant effect on aflatoxin accumulation. A previous study showed that silver ion (silver nitrate solution) at concentrations 8µg/mL and 12µg/mL enhanced the growth of *A. flavus* (another major aflatoxin producer) by 2.56% and 4.91% respectively and reduced aflatoxin production by 27% and 40% respectively when *A. flavus* is grown on YES agar medium (Ismaiel and Tharwat 2014). The growth enhancement was described, as the smaller concentration of Ag^+ in the growth medium was insufficient to inhibit the mycelial growth but had a physiological effect on certain enzymes in the cell, which in turn inhibited aflatoxin production. It was reported that metal ions such as copper, iron, and zinc could stimulate mycelial growth, and aflatoxin showed a correlated increase in *A. flavus* culture as compared to the untreated control. RT-PCR experiment demonstrated that these metals ions also enhanced expression of the aflatoxin pathway gene *omtA* and OMST (*O-methylsterigmatocystin*- aflatoxin precursor) (Cuero et al. 2003). In the current study, it was observed that aflatoxin biosynthesis was enhanced in the presence of silver ion at

concentration 50ng/mL and mycelial growth rate was unaltered. Silver ion may have indirectly stimulated certain enzymes in the cell, which participate in the aflatoxin biosynthesis.

Nanoparticle interaction with aflatoxin:

The interaction between AgNp-cit and aflatoxin was determined using ELISA. Extracted aflatoxin was incubated along with AgNp-cit at 50ng/mL and 100ng/mL concentrations. After 4 hours of incubation, aflatoxin was measured directly using ELISA. Another portion of the mixture (aflatoxin + AgNp-cit) was ultra-filtered/ultra-centrifuged and the filtrate was measured using ELISA for the presence of aflatoxin. The data showed in the Figure 3.2, e that there was no significant difference between AgNp-cit-aflatoxin, and aflatoxin alone, and filtrate AgNp-cit-aflatoxin concentrations. The data suggests that AgNp-cit might not have interacted with aflatoxin at the given experimental conditions.

Stability of AgNp-cit in the fungal growth medium:

Citrate coated silver nanoparticles are known for their strong interactions with the biological medium and it is a complex process. Previous studies have shown that aggregation (Baalousha et al. 2013, Römer et al. 2011), dissolution (Zook et al. 2011), precipitation, phase transformation (Afshinnia et al. 2016), and corona formation (Moore et al. 2015) of stabilized AgNps have taken place in biological medium with consequent changes in bioavailability and toxicity (Maiorano et al. 2010).

UV-vis spectroscopy is an important method used widely to quantify the aggregation kinetics of nanoparticles. AgNp-cit exhibits a specific localized surface

plasmon resonance band (LSPR), and the intensity of the band depends on the particle size, shape, and dielectric constant of the medium (Cao et al. 2011). The band changes with the change in nanoparticle properties (physico-chemical) in the biological system. Nanoparticle-protein interactions may induce nanoparticle aggregation, and such interactions impact the LSPR of the nanoparticles, resulting in spectral red-shift and progressive broadening of their absorbance peak (Moore et al. 2015).

In this study, stability of AgNp-cit in the biological medium (yeast extract sucrose or YES medium) was investigated using UV-Vis absorption spectroscopy. The samples from flasks containing the growing mycelia along with AgNp-cit (50ng/mL concentration) and flasks containing the growth medium along with AgNp-cit (without mycelia) were analyzed at four different time-points (0-hour, 12-hour, 24-hour, and 30-hour).

The UV-vis spectra of pristine AgNp-cit, at the 0-hour time point (shown in Figure 3.3 a) showed an absorbance peak at 394-395 nm. AgNp-cit in YES medium at 0-hour time point showed an absorbance peak at 414nm and the peak broadened at longer wavelengths (400-600nm) which indicates scattered light from large aggregates. AgNp-cit in YES medium with *A. parasiticus* spores at the 0-hour time point showed a similar primary absorbance peak at 413-414 nm. No loss in the absorbance (λ_{max}) was observed at this point, but formation of shoulders at 466-473nm and at 529-569nm appeared, suggesting aggregation due to charge screening from inorganic entities in the medium, and shape transformation. The primary peak shifting at higher wavelength in both of the cases is significant and it may be due to the presence of organic molecules in the medium

that replaced the surface coating (citrate) or interaction between the AgNp surface and other medium components.

The SPR of AgNp-cit in YES medium at the 12-hour time point (Figure 3.3 b) showed broader absorbance peak at 400-420nm and AgNp-cit in YES medium with mycelium showed significant absorbance reduction at λ_{max} and the peak appeared to be broaden (398-457nm). The reduction in peak height may suggest possible uptake by the mycelium, dissolution, and precipitation of silver salt in the medium. At 24-hour (Figure 3.3 c) post inoculation AgNp-cit in YES medium showed the primary peak at 413-414nm and 2 shoulders appeared around 442-474nm, and 476-592nm. The primary peak at 414 nm significantly broadened at the 30-hour time point (figure 3.3 d) around 381-440nm and 2 shoulders appeared to be joined together to form bigger and broader shoulder around 446-600nm. For AgNp-cit in YES with mycelia, the distinctive peak (primary peak) disappeared completely at 30-hour post inoculation. The disappearance of SPR may be due to mycelial uptake, precipitation of silver salt, dissolution of AgNps, or probably all the above mentioned mechanisms.

We have also performed a similar experiment with one low concentration (10ng/mL) and one higher concentration (100ng/mL concentration) to understand the order of interaction of AgNp-cit in the growth medium in the presence of growing mycelia. At the lower concentration of AgNp-cit (10ng/mL) the peak was unidentifiable, suggesting maximum amount of Np dissolution and precipitation in the medium and /or uptake of Np by the mycelia. But at higher concentrations of AgNp-cit (100ng/mL) the peak broadening effect of AgNp-cit was very prominent, as shown in Figure 3.3 e, f, g, and h. The surface plasmon UV-vis data suggests that nanoparticle aggregation increases

with an increase in the concentration of AgNp in the growth medium. At 24-hour (Figure 3.3 g) post inoculation AgNp-cit in YES medium, the primary peak at 405nm - 414 nm disappeared and the formed shoulder appeared to be broader. Similarly the SPR of AgNp-cit in YES medium along with mycelia showed primary peak broadening and formation of a shoulder around 460 nm-600 nm, suggesting aggregation, the absorption of organic molecules released by the cells, or formation of AgCl coating on the surface of AgNp. The significant loss in SPR of AgNp-cit in YES with mycelia was observed at 30-hour post inoculation (Figure 3.3 h), suggesting that uptake of AgNp by the mycelia, dissolution, or precipitation of AgNp in the growth medium. Higher nanoparticle concentration may enhance the rate of aggregation and/or AgNp-medium interaction.

YES medium broadly contains organic molecules such as yeast extract, glutamic acid, and inorganic salts such as magnesium sulfate, calcium chloride, and sodium bisulfite. It is possible that charged stabilized AgNp-cit will interact with the inorganic and organic components in the medium. Sodium is monovalent, and calcium and magnesium are bivalent cations and their aggregation kinetics in presence of AgNp-cit are controlled by electrostatic interactions. In previous study it was shown that NaCl is more efficient in aggregating AgNp-cit compared to other Na-salts ($NaNO_3$, $Na2SO_4$). Magnesium and calcium are efficient in neutralizing the surface charge of AgNp-cit inducing AgNp-aggregation (Baalousha et al. 2013). It is also suggested that calcium has greater affinity toward citrate ion to form the Ca-citrate complex (Moore et al. 2015). Glutamic acid is classified as a polar negatively charged aliphatic amino acid with a carboxyl acid and an amine as functional groups. The NH_3^+ group of glutamic acid may interact with the negatively charged citrate on the AgNp surface. As a consequence, the

surface charge of AgNp will decrease and may induce AgNp aggregation. Glutamic acid and other amino acids or proteins secreted by the fungal cell can replace, get bound, or adsorbed on the surface of AgNps and form a corona-like structure (Miclăuş et al. 2016). This may result in larger AgNp aggregates and the formation of a second absorbance peak at higher wavelengths (475nm-600nm). Sometimes due to the presence of chloride ion, small size (<5 nm) AgCl particles will form from the dissolved silver ions. Small size silver carbonate and silver phosphate particles formation is also possible from the dissolved silver ions. Decrease in peak height or loss of absorbance may be due to the formation AgCl particles, because these very small AgCl particles do not have an associated LSPR absorbance (Zook et al. 2011). The SPR peak shifting to a higher wavelength may result from formation of AgCl nanoparticles and/or the formation of AgCl coating on the surface of AgNp; formation of an aggregation of AgNp-cit due to specific chemical interactions with calcium chloride, magnesium sulfate, and sodium bisulfite; replacement of surface coating by organic molecules; or interaction of AgNp surface with other media components. Understanding the dynamic interaction between nanoparticles in biological systems is necessary because it will govern the uptake and toxicity in the cell.

Uptake of AgNp-cit by *A. parasiticus*:

Recent studies have reported electrostatic attractions/interactions between the cell wall-cell membrane of microorganisms and nanoparticles resulting in membrane wrapping of nanoparticles followed by cellular uptake (Kotzybik et al. 2016, Xia et al. 2016, Kosman 2003). The possible mechanism of nanoparticle uptake by eukaryotic cell

was suggested in several studies (Moore 2006, Kuhn et al. 2014) and cellular uptake followed by internalization of nanoparticles is governed by an endocytosis process (Wang, Xia and Liu 2015, Zhang, Gao and Bao 2015). The endocytic pathway is divided into different groups such as a) clathrin-dependent, b) caveolin-mediated, c) clathrin and caveolin-independent, and d) micropinocytosis (Wang et al. 2015). Via the endocytic pathway, nanoparticles either translocate to endosomal and lysosomal compartments or nanoparticles can also enter the cell via a cell surface lipid raft associated domain (cavaolae), and therefore avoid degradation by lysosomes (Na et al. 2003). Clathrin dependent endocytosis is a receptor mediated process, and receptor-ligand binding initiates formation of "coated pits" on the plasma membrane which promotes endocytosis (Zhang et al. 2015, Brodsky et al. 2001). A flask like structure (~50nm -80 nm diameter) forms at the plasma membrane during the caveolin mediated endocytosis process, and it involves biochemical signaling cascades. AgNp uptake may involve combinations of different endocytic processes. A previous study has reported that both clathrin-dependent and micropinocytosis coexisted for AgNp uptake by human mesenchymal stem cells (Wang et al. 2015). It was also observed that AgNp was bound to the scavenger receptor on the cell surface and phagocytosed by the clathrin and actin-dependent endocytosis process (Asharani et al. 2009). Engineered nanoparticles are able to bind to receptors and proteins on cell membrane. The involvement of Rab family GTPase in intracellular trafficking of nanoparticles was observed (Treuel, Jiang and Nienhaus 2013). The Rab family of GTPase is a major class of proteins which regulates intracellular trafficking. Rab 5A appears during endocytosis and facilitates early endosome fusion (Stenmark 2009). Rab 7 is responsible for maturation of late endosome followed by fusion with

lysosome (Vanlandingham and Ceresa 2009). Rab 9 and Rab 11A are involved in the endocytic recycling process (Treuel et al. 2013, Vanlandingham and Ceresa 2009). Others have reported that formation of early endosome in clathrin mediated endocytosis is important for AgNp-cit size of 25nm uptake in C. elegans (Maurer et al. 2016).

Fungal cell wall contains glucan and chitin (microfibrillar polysaccharide), appears mostly at the inner cell wall and at the outer cell wall proteins and mannoproteins predominates. It is possible that nanoparticles could interact/bind with the components of the cell wall (Chwalibog et al. 2010, Kotzybik et al. 2016). The interaction between nanoparticles and proteins is governed by several different mechanisms such as hydrogen bonding, solvation, van der Waals, electrostatic, charges, and steric (Nel et al. 2009). For example, silver has a higher affinity toward the thiol group to form silver-sulfide (features covalent bond). Silver nanoparticles also bind to the sulfur containing protein on the cell membrane. Protein molecules forms a layer on the surface of nanoparticles called the protein corona (Saptarshi, Duschl and Lopata 2013). Adsorbed protein on the nanoparticle surface may undergo structural and functional changes which may affect particle interaction with receptors and other proteins on the cell surface and will determine the cellular uptake and fate of nanoparticles in the biological system.

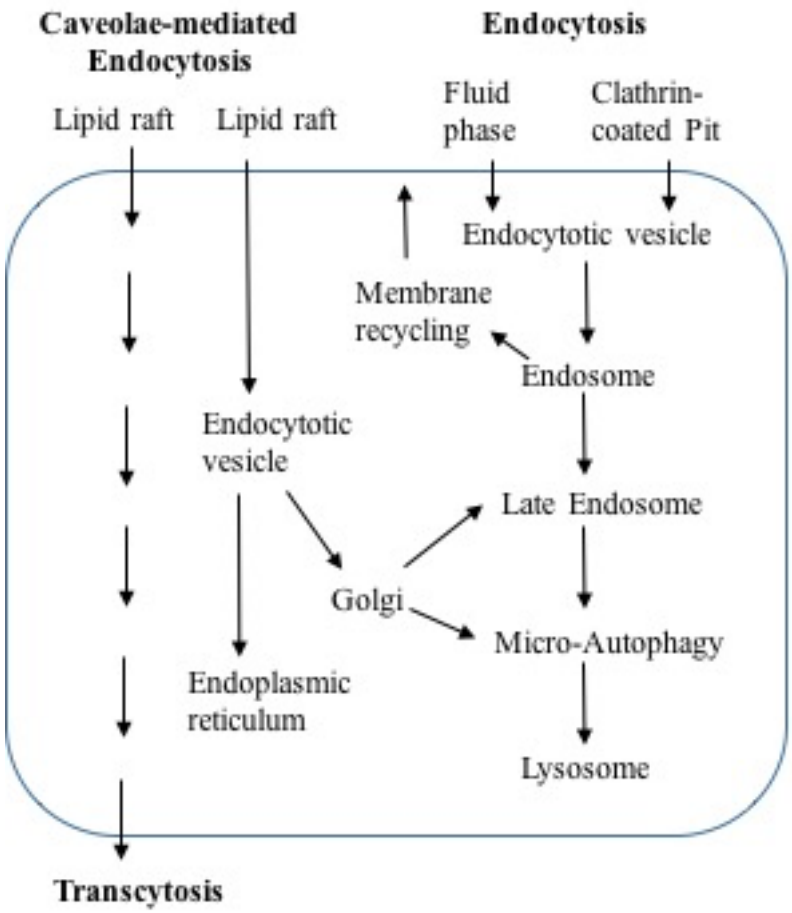

Figure 3.1: Possible mechanisms of nanoparticle uptake by eukaryotic cell.

Since fungal spores were inoculated in the medium containing the nanoparticles, uptake of nanoparticles by the mycelia along with nutrients in the growth medium would allow the nanoparticles to enter the cells and interfere with the cellular processes responsible for aflatoxin biosynthesis. To assess the uptake of AgNp-cit by the mycelia, we performed a time-course ICP-OES of the growth medium (after filtering the mycelia from the medium). We reasoned that if AgNp-cit was taken up by the mycelia, we would observe a drop in the amount of total silver in growth medium with time (loss of silver in the medium can also be caused by other reasons such as sedimentation and/or precipitation of Ag salts). As shown in Figure 3.4 a, our ICP-OES data demonstrated that

by 24h, the amount of total silver in the growth medium decreased by approximately 85% (blank corrected), suggesting that most of the AgNp-cit uptake into the mycelia occurred by 24h of fungal growth. Also, as expected the amount of total silver remained unchanged in an un-inoculated growth medium suggesting that the removal of total silver with time in the inoculated growth medium was dependent on the mycelia and not the growth medium. To collect further evidence to support our theory of uptake of AgNp-cit by the mycelia, we also performed a time-course ICP-OES of mycelia to quantify the total amount of silver accumulated in the mycelia with time. As shown in Figure 3.4 b, in parallel with the decrease of total silver in the growth medium, we observed a drastic increase of total silver in the mycelia during the period of 30h, within which, the maximum increase in total mycelial silver occurred by the first 24h of growth. Overall, these data suggest that approximately 80% of the total AgNp-cit was taken up by the fungus from the growth medium during the first 24h of growth. We also carried out a similar experiment with untreated mycelia to prove that silver did not come from the mycelia as a contaminant. Our ICPOES data suggests that the untreated mycelia do not contain any silver ions. Next, we evaluated the amount of AgNp-cit getting dissolved in the growth medium with or without mycelia, by ultra-filtration/ultra-centrifugation method using amicon ultra-centrifugal filter unit (3kDa). The filtrate (AgNp-cit exposed medium) containing only the dissolved silver was acid digested for ICPOES to measure the total amount of dissolved silver left in the medium at different time points. As shown in Figure 3.4 c, no evidence of dissolution of AgNp-cit when introduced in the growth medium is provided but there is a possibility of dissolution of AgNp-cit in the medium that remains undetected by ICPOES (detection limit was 5ng/mL). Another possibility is

AgNp-cit was interacting with the organic and inorganic components in the growth medium. As discussed earlier as UV-vis data suggested, that AgNp-cit had undergone certain changes such as aggregation, precipitation/re-precipitation, phase transformation, and corona formation in biological medium. Due to these changes there was no available dissolved silver ion present in the growth medium. We have also performed ultracentrifugation-ultrafiltration with dissolved silver ion to determine the amount of silver ion that can pass through the ultrafilter unit (3kDa). The filtrate was acid digested for ICPOES. Our ICPOES data suggests that the maximum amount (80-90%) of dissolved silver ion can pass through the filter and rest of the dissolved ion can get clogged in the filter of the filtering unit, or might get lost during the experimental process.

Effect of AgNp-cit on transcript accumulation of aflatoxin regulatory genes:

To investigate the molecular mechanism by which this nanoparticle inhibits aflatoxin biosynthesis, we examined the effect of AgNp-cit on genes of the aflatoxin biosynthesis gene cluster. We have quantified the transcript accumulation of the aflatoxin pathway transcription factor, *aflR*, one early pathway gene, *nor-1*, one middle pathway gene, *vbs,* and two late pathway genes, *ver-1* and *omtA*. Our results are shown in Figure 3.5. Unlike the housekeeping gene *β-tubulin*, which showed no effect in transcriptional activation upon exposure to AgNp-cit, the transcript of all five aflatoxin genes were significantly downregulated ($p<0.05$) upon exposure to AgNp-cit (approximately a two-fold reduction in transcript levels), thereby demonstrating that the AgNp-cit mediated

inhibition of aflatoxin biosynthesis was a result of transcriptional inhibition of the aflatoxin gene cluster. We further investigated whether the AgNp-cit could result in transcriptional inhibition of two global regulators of secondary metabolism, *laeA,* and *veA*, which, as reported previously (Strauss and Reyes-Dominguez 2011, Duran, Cary and Calvo 2007), regulate the activation of the aflatoxin gene cluster. As shown in Figure 3.6, mycelia exposed to AgNp-cit displayed in two-fold reduction in transcripts of both *laeA* and *veA*, thereby demonstrating the ability of AgNp-cit to inhibit the activation of secondary metabolism in *A. parasiticus*. LaeA and VeA proteins are both a part of the Velvet transcriptional complex that activates several secondary metabolite pathways including aflatoxin biosynthesis (Sarikaya Bayram et al. 2010). Hence the AgNp-cit mediated inhibition of transcriptional activation of *laeA* and *veA* suggests the feasibility of AgNp-cit mediated inhibition of the Velvet complex and the inhibition of other secondary metabolite pathways as well.

Effect of AgNp-cit on ROS generation:

Multiple studies (Roze et al. 2011) reported that activation of secondary metabolism is a response to an increase in intracellular oxidative stress. Previous reports (He et al. 2012a) on AgNp-cit-induced toxicity in biological systems indicate that nanoparticles increase intracellular reactive oxygen species (ROS), which in turn, increases intracellular oxidative stress. The effect of the nanoparticles on ROS build-up in such biological systems, when applied at nontoxic doses, such as in this study, has not been reported yet to the best of our knowledge. To evaluate the effect of AgNp-cit on total ROS in *A. parasiticus* in the current study, we adopted a DCFH-DA based protocol as described previously. Since activation of aflatoxin biosynthesis in the current growth

conditions occurs at 24h, we performed a quantitative comparison of total ROS in *A. parasiticus* at this time-point in presence and absence of AgNp-cit. As shown in Figure 3.7, the nanoparticle exposure resulted in a significant reduction by ~30% of total ROS. On the other hand, ROS generated upon exposure to $AgNO_3$ was comparable to the untreated ROS generation. We also examined whether a AgNp-cit mediated drop in total ROS resulted in reduction of transcriptional activation of the superoxide dismutase genes (SOD genes). Reactive oxygen species such as superoxide, hydroxyl radical, and hydrogen peroxide are continuously generated as byproduct during variety of enzymatic and nonenzymatic process in the cell. ROS plays an important role in number of cellular processes. But an excess amount of ROS can lead to cellular damage, oxidative stress, DNA damage or even cell death (Kisselev et al. 2016). To cope with the harmful effects of ROS, cells have developed a defense system of enzymatic and nonenzymatic antioxidants. SOD is a family of enzymes that catalyze superoxides (one class of ROS) through dismutation reactions (Miao and St Clair 2009). Here we measure the transcript accumulation of the five SOD genes named *CuSOD*, *Cu/ZnSOD*, *Cu/ZnSOD* cytosol, *MnSOD*, and *FeSOD* for AgNp-cit treated and $AgNO_3$ treated and untreated *A. parasiticus* SU-1 strains at 24 hours (post inoculation) as shown in Figure 3.8. Our results showed that four of these sod genes showed no effect, but *Cu/ZnSOD* cytosol showed a significant reduction (~2.5 fold) at transcriptional level upon exposure to AgNp-cit, suggesting that AgNp-cit possibly resulted in the reduction of ROS build up in the cytosol. On the contrary *Cu/ZnSOD* cytosol and *MnSOD* showed a significant increase (~11 fold and ~12 fold respectively) in the transcriptional level upon exposure to $AgNO_3$

as shown in Figure 3.8. The SOD gene expression data suggests that $AgNO_3$ probably enhances the ROS build up in the cytosol and in the mitochondria.

Effect of AgNp-cit on growth and aflatoxin biosynthesis after removal of nanoparticle from the growth medium:

We further explored the effect of AgNp-cit on growth and aflatoxin biosynthesis upon completion of AgNp-cit uptake by the mycelia. As shown in Figure 3.9 a, aflatoxin accumulation in the fungal growth medium was quantified by ELISA (described previously) at 48-hour (post inoculation) and normalized by 48-hour dry weight of the mycelia. AgNp-cit mediated aflatoxin biosynthesis (normalized by dry weight of the mycelia) is comparable to the untreated control. There is no significant difference in growth rate (expressed as dry weight per unit time (mg/h)) observed between AgNp-cit treated and untreated control as shown in Figure 3.9 b. Our ICPOES data of the AgNp-cit treated mycelia suggest that the maximum number of nanoparticles get taken up by the mycelia at 30-hour post inoculation, and we observe aflatoxin inhibitory effect at 40-hour post inoculation. But at 48-hour post inoculation the mycelia revert back to synthesize aflatoxin at the normal level due to lack of AgNp-cit in the growth medium. To assess the uptake of Ag from the medium by the mycelia, a time course ICPOES was performed with the treated harvested mycelia. Results suggested that mycelial Ag increased with time from 24-hour to 30-hour post inoculation, but Ag concentration decreased significantly from 48-hour to 72-hour post inoculation (greater than two-fold reduction). The reduction of Ag in the mycelia may suggest that the Ag was unavailable due to interaction with the medium or already taken up by the older cells.

Effect of AgNp-cit on transcript accumulation of aflatoxin regulatory genes at 40-hour post inoculation:

To explore whether the aflatoxin increase at 48h corresponds to the increase in the transcriptional accumulation of aflatoxin regulatory genes at an earlier time point, we quantified the RNA transcript levels of the aflatoxin genes at 40-hour post inoculation. Our results, shown in Figure 3.10, suggest that there is no effect in transcriptional activation of aflatoxin biosynthetic pathway genes upon exposure to AgNp-cit at 40-hour post inoculation and the result is comparable to the untreated control. The data demonstrate that upon removal (~85%) of AgNp-cit by the mycelia from the growth medium, the aflatoxin genes express at levels equivalent to the untreated controls and bring aflatoxin synthesis at levels similar to the untreated controls.

Effect of AgNp-cit on ROS generation at 40-hour post inoculation:

We also quantified the total ROS generated at 40h. As shown in Figure 3.11, AgNp-cit exposure resulted in a ~1.3-fold increase and $AgNO_3$ exposure resulted in a ~1.4-fold increase in total ROS level as compared to the untreated control.

3.4 CONCLUSION

Many studies have demonstrated that AgNps are toxic to several organisms: examples include toxicity against bacterial cells (Kim et al. 2007), aquatic plants (He et al. 2012a), arthropods (Khan et al. 2015), fungal cells (Pulit et al. 2013), and mammalian cells (AshaRani et al. 2009), but our growth and aflatoxin inhibition results suggest that

at low concentrations (ng/mL), AgNp-cit can be envisioned as a potential tool to manipulate public health-related ecosystems for the betterment. In this study, we have evaluated the effect of AgNp-cit, 20nm in size, on aflatoxin biosynthesis in *A. parasiticus*, which is one of the major aflatoxin producers. Our results showed AgNp-cit at 50ng/mL concentration significantly reduced intracellular oxidative stress and downregulated aflatoxin biosynthesis at the level of gene expressions of aflatoxin pathway genes and the global regulatory genes of secondary metabolism. Our results also showed that AgNp-cit mediated inhibition of aflatoxin biosynthesis is a temporary effect, and it does not alter the fungal growth rate. Once AgNp-cit is removed significantly by the mycelia from the growth medium, the fungi are able to regenerate aflatoxin to a normal level. These findings will help us to understand the molecular mechanisms through which nanoparticles regulate microbial cellular stress and the secondary metabolites production, which are enormously significant to environmental and public health.

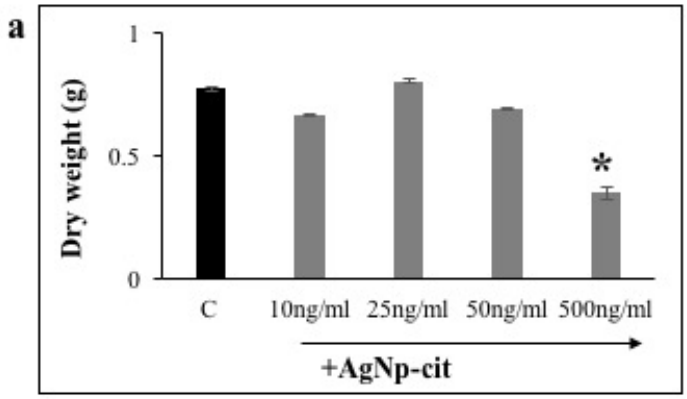

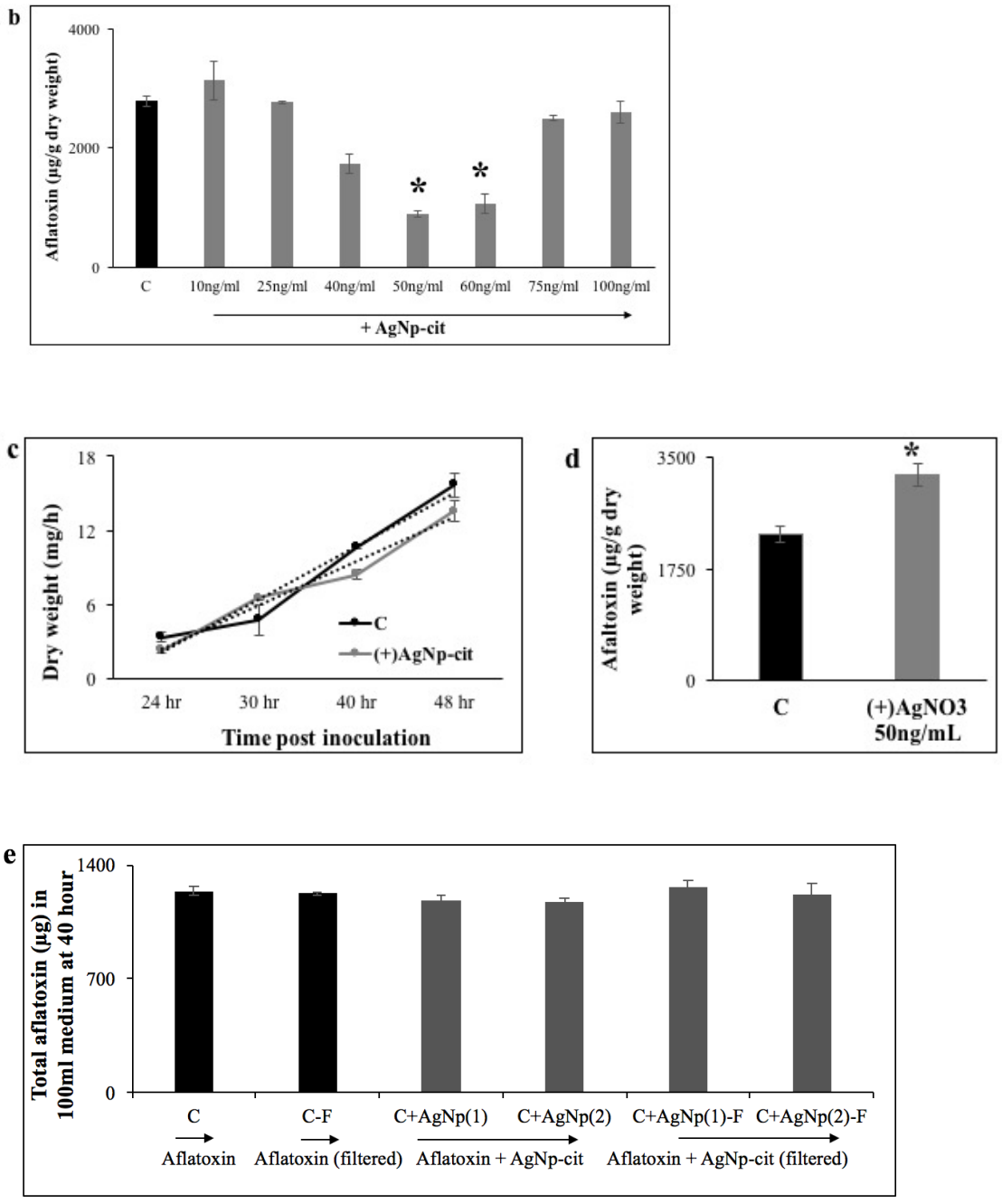

Figure 3.2: Effect of AgNp-cit on growth & aflatoxin biosynthesis in *A. parasiticus*: To carry out this experiment, 10^6 *A. parasiticus* spores were inoculated in 100ml YES (Yeast Extract Sucrose) media along with 20nm size AgNp-cit at different concentration and grown under standard growth conditions (mentioned above). The black bar indicates untreated control and gray bars indicate AgNp-cit treatment, * indicates significance as compared to the untreated control. (a) Determination of nontoxic dose of AgNp-cit at different concentrations by performing growth assay of *A. parasiticus* mycelia; 500ng/mL concentration significantly (p=0.004) reduced growth at 48 hours post

inoculation as compared to untreated, (b) Determination of Aflatoxin accumulation in the growth medium (normalized to dry weight of the mycelia) by ELISA between untreated and AgNp-cit treated (at different concentration); AgNp-cit treated (50ng/mL) mycelia had produced significant less (~>2 fold, p=0.002) aflatoxin when compared to untreated, (c) Determination of growth rate of untreated and 50ng/mL AgNp-cit treated mycelia at different times (post inoculation), (d) Determination of effect of $AgNO_3$ on aflatoxin biosynthesis by *A. parasiticus*, aflatoxin was quantified by ELISA and normalized to dry weight of the mycelia, result showed that $AgNO_3$ treated mycelia have produced an increased (~1.5 fold, p=0.05) amount of aflatoxin in the growth medium compared to the untreated. (Black bar indicates untreated control and gray bars indicate $AgNO_3$ treatment). e) AgNp-cit interaction with aflatoxin. C is the aflatoxin extracted from the growth medium a 40-hour, C-F is aflatoxin ultra-filtered, C + AgNp (1) is Aflatoxin + AgNp-cit (50ng/mL) and C + AgNp (2) is aflatoxin + AgNp-cit (100ng/mL). Both were incubated for 4 hours and aflatoxin was measured using ELISA. Aflatoxin + AgNp-cit (50ng/mL) and aflatoxin + AgNp-cit (100ng/mL) were ultra-filtered and aflatoxin in the filtrate from both were measured using ELISA. This data suggests that AgNp-cit might not have interacted with aflatoxin at the given experimental conditions.

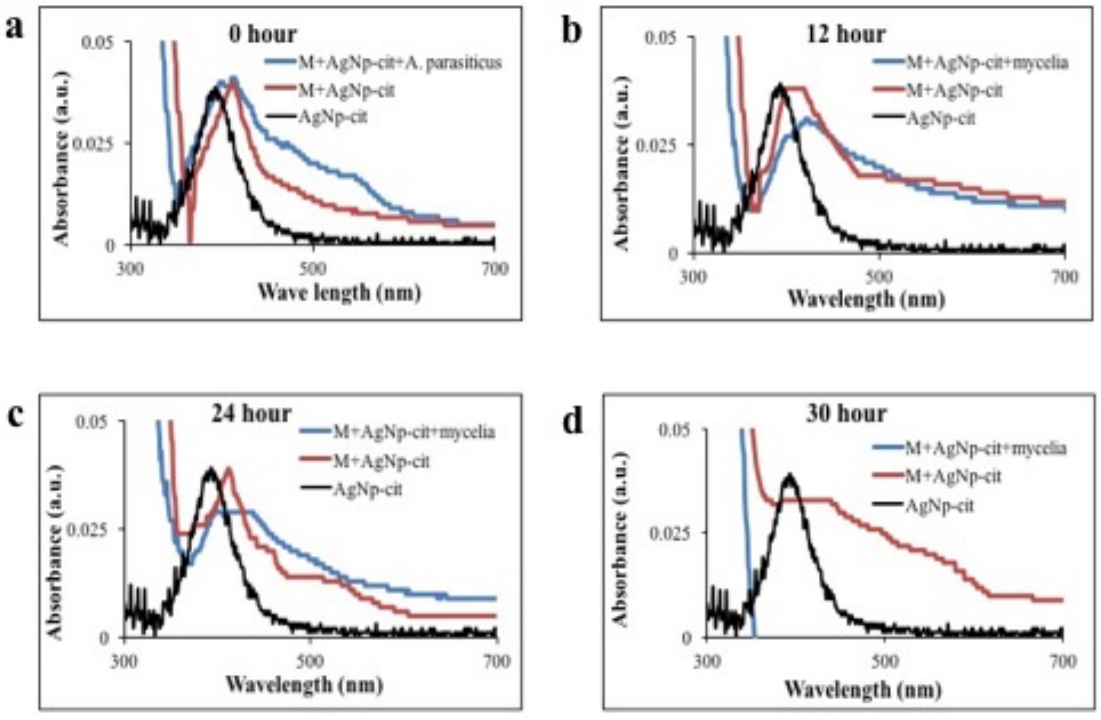

Figure 3.3: Interaction of AgNp-cit with the fungal growth medium with or without mycelia by surface plasmon UV-vis spectrophotometry. All the graphs were obtained at a different time (0, 12, 24, and 30 hours post inoculation) from the medium exposed to AgNp-cit at 50ng/mL concentration. AgNp-cit peak broadening effect was observed in all medium and in Figure 3.3 d, there was no AgNp-cit peak observed in the medium with

mycelia, suggesting the nanoparticles were taken up by the mycelia, precipitation of silver salts, and sedimentation of AgNps (as discussed earlier).

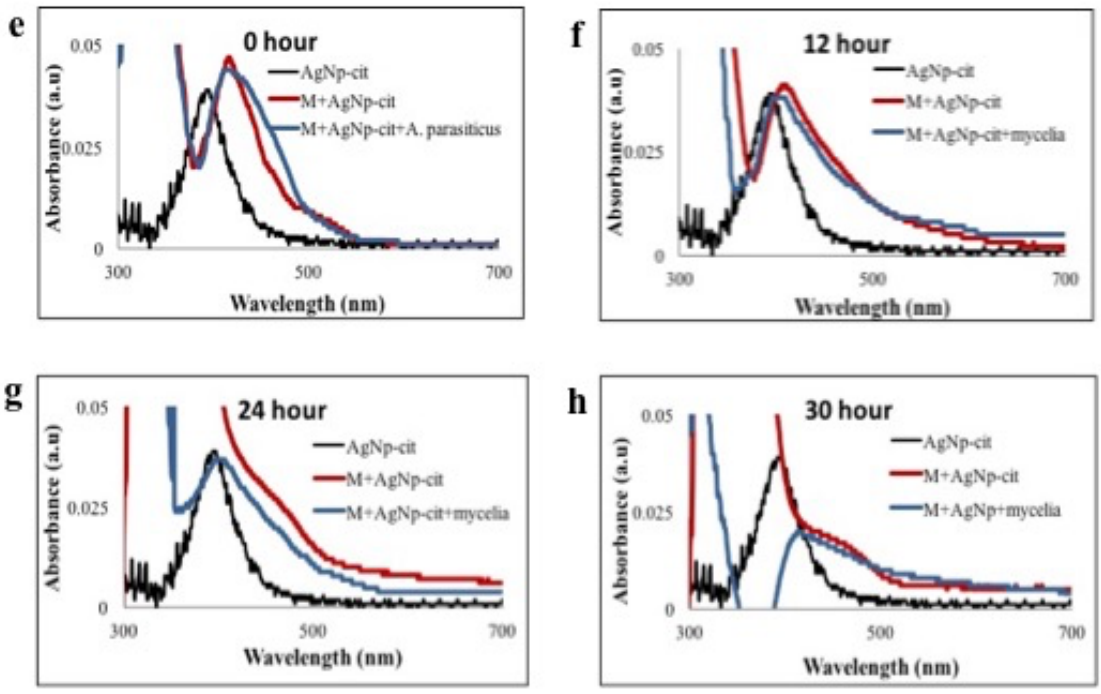

Figure 3.3: Interaction of AgNp-cit (at higher concentration (100ng/mL) with the growth medium with or without mycelia: AgNp-cit at 100ng/mL concentration was exposed to the fungal growth medium, with or without mycelia, and interaction was studied using surface plasmon UV-vis spectroscopy at different time point post inoculation. The results suggest nanoparticle interaction with the organic and inorganic components of the medium and the physicochemical properties of nanoparticles change with time (as discussed earlier).

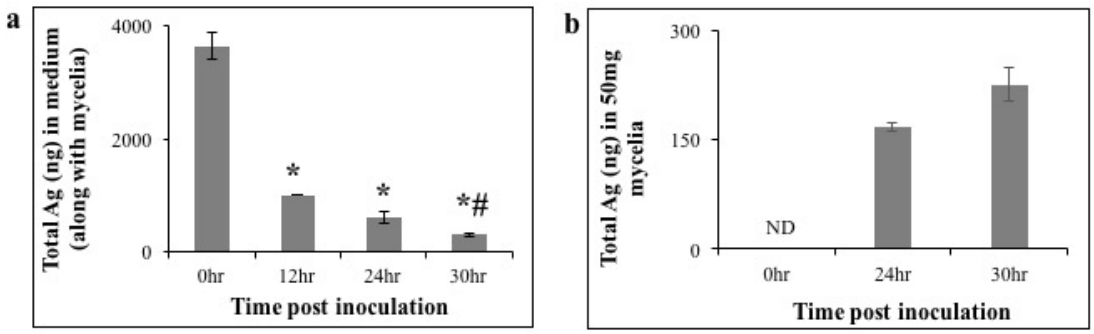

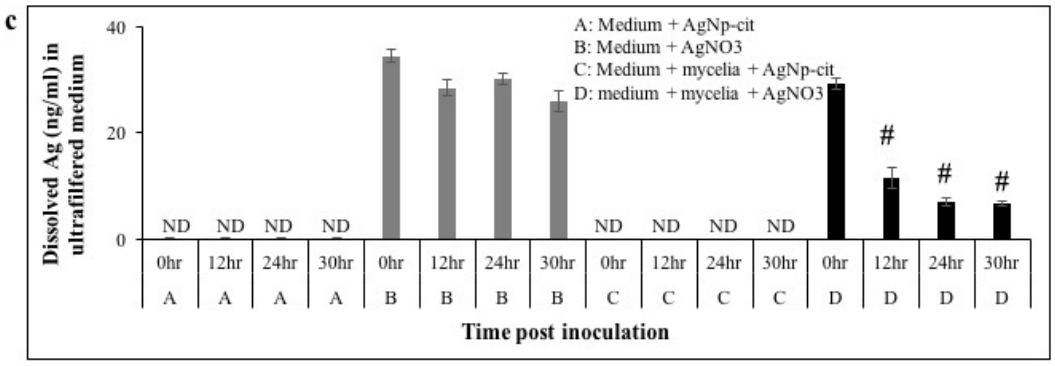

Figure 3.4: Uptake of AgNp-cit by *A. parasiticus*: (a) Determination of total silver left in the medium by ICPOES; the growth medium was inoculated with *A. parasiticus* (10^6 spores) along with AgNp-cit and grown under standard growth condition (mentioned above). At different times post inoculation, Ag level of the medium was quantified by ICPOES, at 24 hours post inoculation the total amount of Ag decreased by ~ 85% in the growth medium.(*indicates significance, as compared to 0 hours, and *#, indicates significance as compared to 12 hour ICPOES data), (b) Uptake of AgNp-cit by the mycelia; at different time points the 50 mg of AgNp-cit treated mycelia was harvested to carry out time course ICPOES, the results showed that presence of Ag in the mycelia and Ag level reaches maximum at 30 hours post inoculation. (c) Dissolution of AgNp-cit in the fungal growth medium; medium containing mycelia and AgNp-cit and medium only with AgNp-cit was collected, was ultra-filtered/ultra-centrifuged to obtain dissolved Ag+ as filtrate and measured by ICPOES. A similar experiment was done with $AgNO_3$ with and without mycelia in the growth medium, ultra-filtered/ultra-centrifuged and dissolved Ag was measured by ICPOES. (# indicates the significance compared to the 0 hour reading) Data suggests that there is no traceable amount of dissolved Ag in the medium upon exposure to AgNp-cit; on the contrary, 80% of the dissolved Ag was recovered from the medium. $AgNO_3$ exposed medium with mycelia showed significant less (~2 fold) amount of Ag+ in the medium at 12 hours, ~4 fold at 24 and 30 hours post inoculation, indicating uptake of $AgNO_3$ by the mycelia.

Table 3.1: List of Primer user for RT-PCR figure 3.4, 3.5, 3.7, and 3.9

Aflatoxin biosynthesis pathway Genes	**Primer Sequences**
aflR	F 5'-ACCTCATGCTCATACCGAGG-3' R 5'-GAAGACAGGGTGCTTTGCTC-3'
Nor-1	F 5'-CACTTAGCCAGCACGATCAA-3' R 5'-ATGATCATCCGACTGCCTTC-3'
Ver-1	F 5'-AACACTCGTGGCCAGTTCTT-3' R 5'-ATATACTCCCGCGACACAGC-3'
omtA	F 5'-CGAAGCCACTGGTAGAGGAG-3' R 5'-ACGAATGTCATGCTCCATCA-3'
Vbs	F 5'-TGGATAGGGCTCTCGCTAAA-3' R 5'-CTCCTGTTGCACGATTCTGA-3'
ß-tubulin	F 5'-TCTCCAAGATCCGTGAGGAG-3' R 5'-TTCAGGTCACCGTAAGAGGG-3'
VeA	F 5'-TCCAGCTATCCCAAGAATGG-3' R 5'-TAATCCCCCGATAGAGCCTT-3'
LaeA	F 5'-ATGGGGTGTGGAAGTGTGAT-3' R 5'-ATCGGTAAAACCAGCCTCCT-3'
FeSOD	F 5'-GAGATGGCCTCCGTATTCAA-3' R 5'-CATCAATCCTTCCCTCTCCA-3'
MnSOD	F 5'-CCACATCAACCACTCCCTCT-3' R 5'-TCCTGATCCTTCGTCGAAAC-3'
CuSOD	F 5'-GAGGCCGGAGATATTTCACA-3' R 5'-CCCTCTTTGCTCTTCGACAC-3'
CuZnSOD Cytosolic	F 5'-CCTCCTTGCAATACAACCGT-3' R 5'-GTCTTCCTTCGCCTCTTCCT-3'
CuZnSOD1	F 5'-CACCAGTTCGGTGACAACAC-3' R 5'-GTGTTCACTACGGCCAAGGT-3'

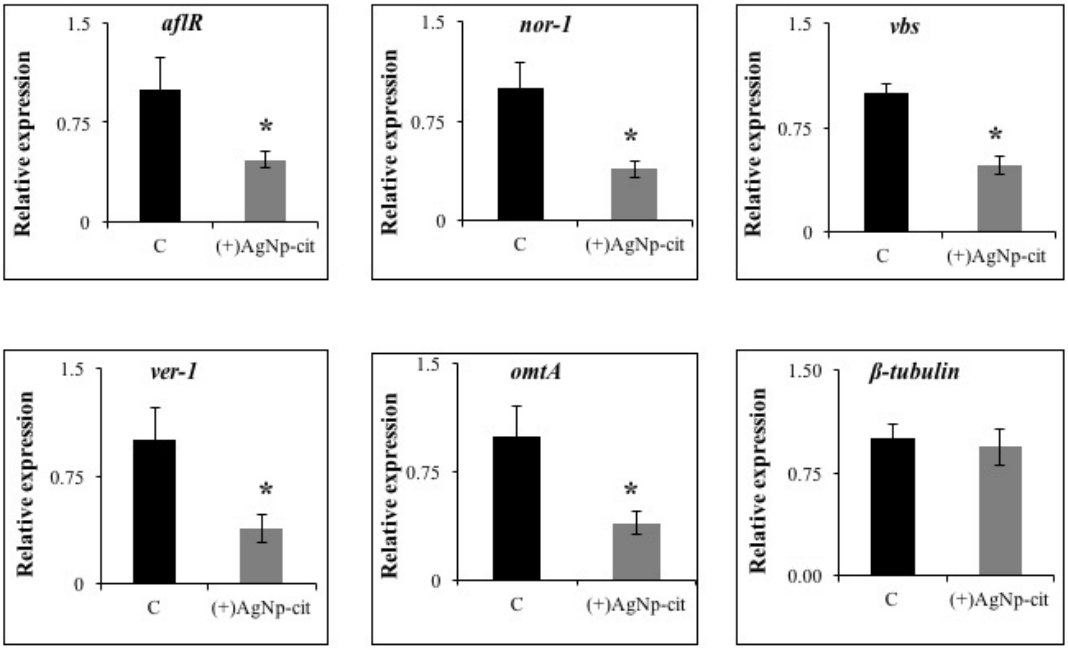

Figure 3.5: Effect of AgNp-cit on transcript accumulation of aflatoxin regulatory genes: *A. parasiticus* (10^6 spores) was inoculated in growth medium along with 20nm size AgNp-cit at 50ng/mL concentration and grown under standard growth conditions mentioned above. At 30-hours post, inoculation mycelia were harvested and Real-time PCR was carried out from the cDNA (extracted from RNA) of the harvested mycelia to study the regulation of aflatoxin producing gene expression. The black bar indicates untreated and the gray bar indicates AgNp-cit treated samples, and * indicates significance as compared with untreated. Result shows that the transcripts of all the 5 genes (*aflR*; p=0.05, *nor-1*; p=0.01, *vbs*; p=0.0001, *ver-1*; p=0.03, *omtA*; p=0.01) were significantly reduced (~2 fold) except the housekeeping gene *ß-tubulin* upon exposure to AgNp-cit.

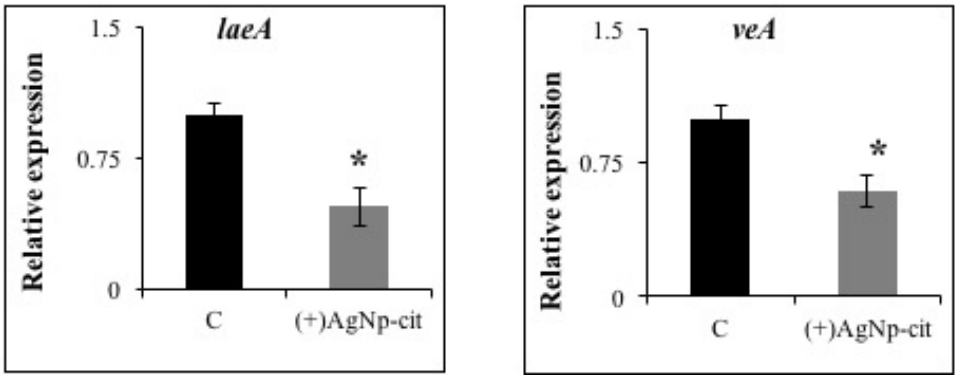

Figure 3.6: Effect of AgNp-cit on transcriptional inhibition of global regulators of secondary metabolism: Graphical representation of the relative gene expression levels of the global regulators of secondary metabolism *laeA* and *veA*. The black bar indicates

untreated and the gray bar indicates AgNp-cit treated samples and * indicates significance compared to untreated control. Mycelia exposed to AgNp-cit showed a ~2fold reduction in transcripts of both *Laea* (p=0.001) and *Vea* (p=0.004).

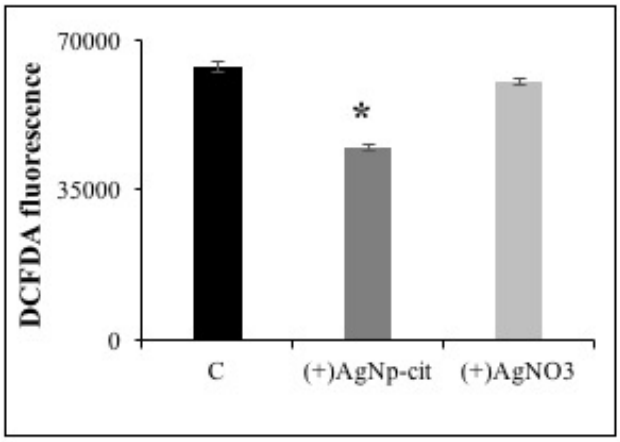

Figure 3.7: Effect of AgNp-cit on ROS generation: *A. parasiticus* (10^6 spores) was inoculated in fungal growth medium along with 20nm size AgNp-cit at 50ng/mL concentration and grown under standard growth conditions (mentioned above). At 24 hours post inoculation, mycelia were harvested and ROS was measured by a DCFDA based method. The black bar indicates untreated and dark gray bar indicates AgNp-cit treated and the light gray bar indicates $AgNO_3$ treated mycelia. AgNp-cit treated mycelia resulted a significantly less (p=0.01) amount of ROS generation in comparison to the untreated control and $AgNO_3$ exposed mycelia.

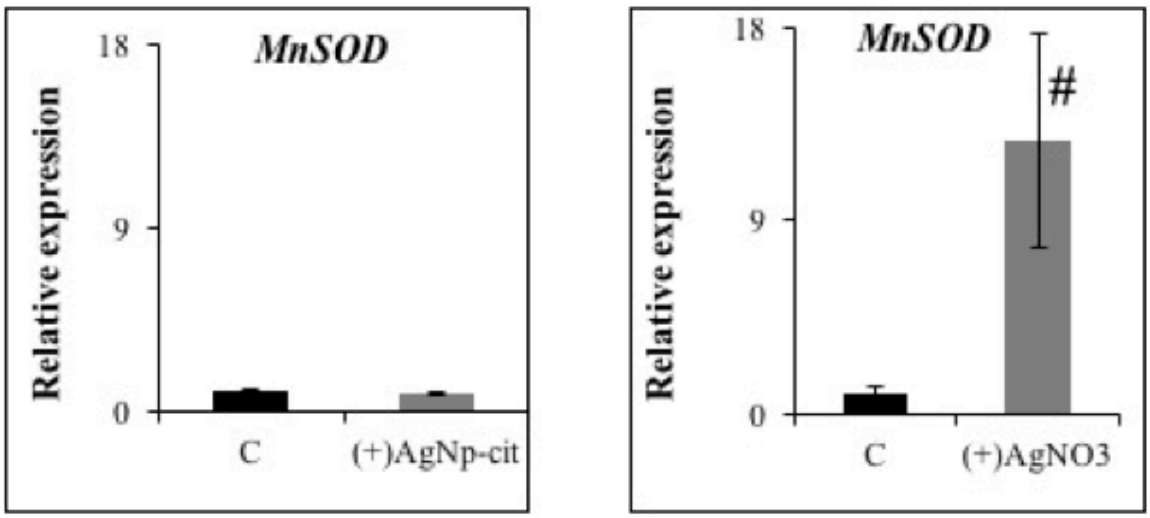

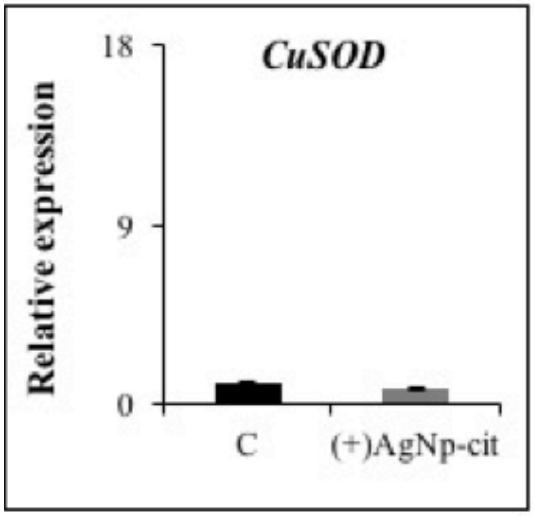
CuSOD
Relative expression
18
9
0
C
(+)AgNp-cit

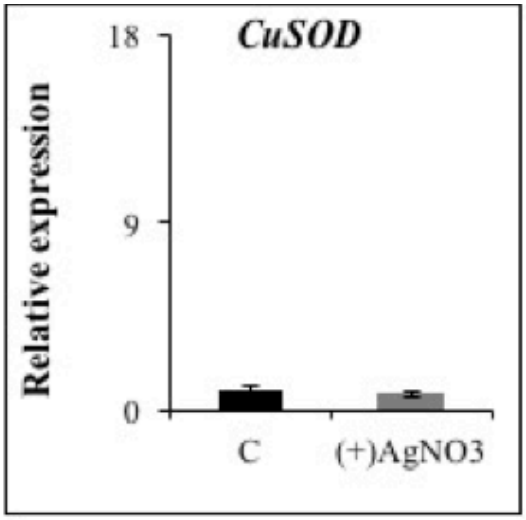
CuSOD
Relative expression
18
9
0
C
(+)AgNO3

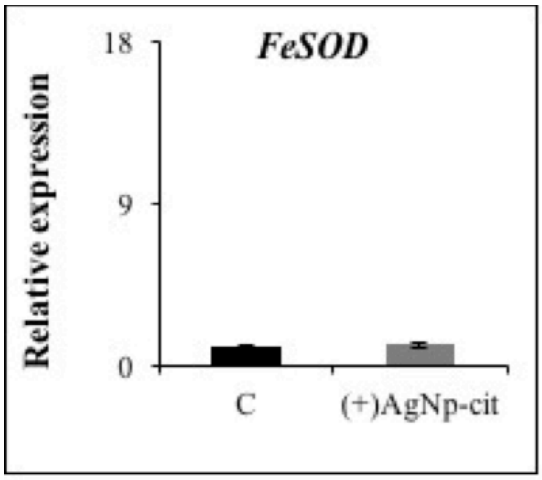
FeSOD
Relative expression
18
9
0
C
(+)AgNp-cit

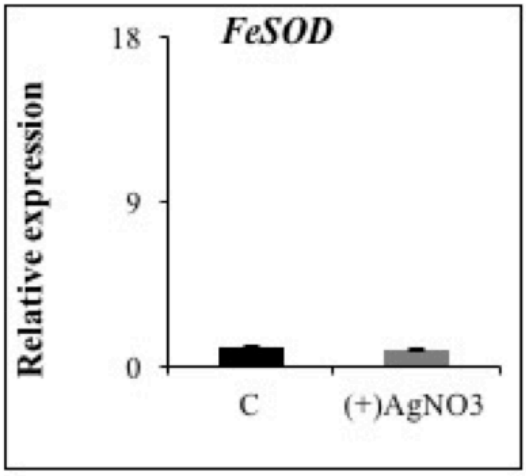
FeSOD
Relative expression
18
9
0
C
(+)AgNO3

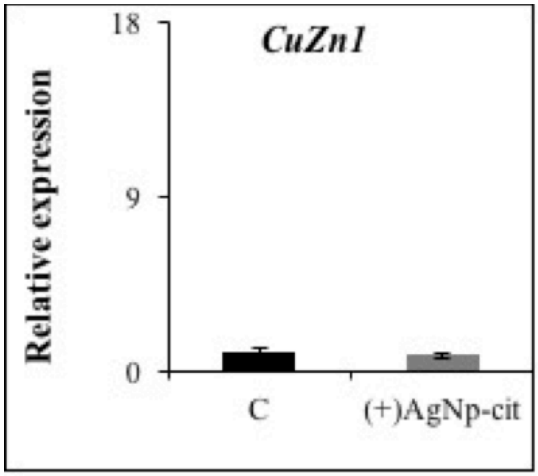
CuZn1
Relative expression
18
9
0
C
(+)AgNp-cit

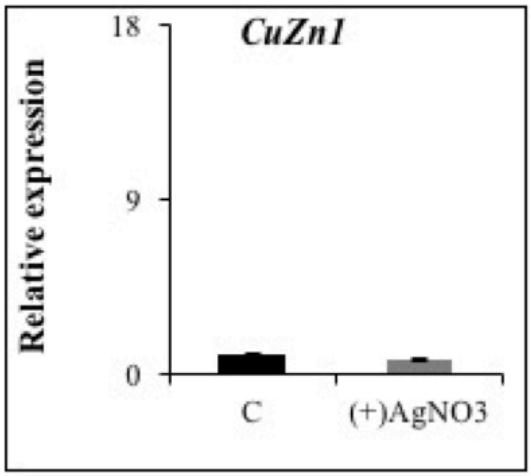
CuZn1
Relative expression
18
9
0
C
(+)AgNO3

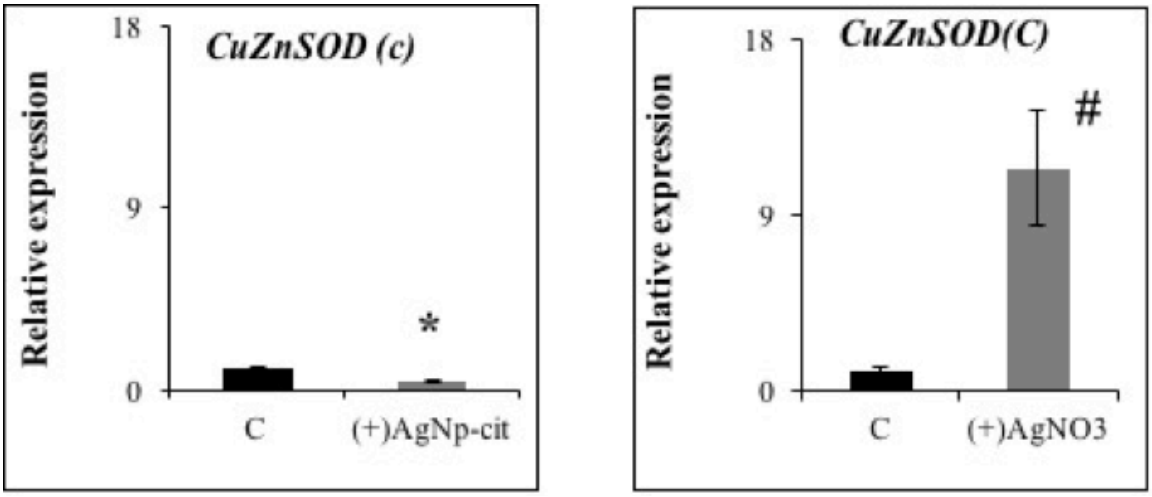

Figure 3.8: Effect of AgNp-cit and $AgNO_3$ on transcriptional inhibition of SOD genes: The cellular level of ROS is controlled by antioxidant enzymes superoxide dismutase (SODs). At 24 hours post inoculation, mycelia were harvested from the growth medium and RTPCR was carried out from the RNA of the harvested mycelia to study the regulation of SOD gene expression. The black bar indicates untreated and gray bar indicates AgNp-cit/$AgNO_3$ treated samples, * indicates the significance of AgNp-cit treated compared to untreated and # indicates the significance of $AgNO_3$ treated compared with untreated. AgNp-cit exposed mycelia showed significant reduction in CuZnSOD cytosol (p=0.01) gene expression indicating AgNp-cit might reduce intracellular oxidative stress. $AgNO_3$ exposed mycelia (on the right side) showed significant increase in MnSOD (p=0.03) and CuZnSOD cytosol (p=0.02) gene expression indicating $AgNO_3$ enhance intracellular oxidative stress.

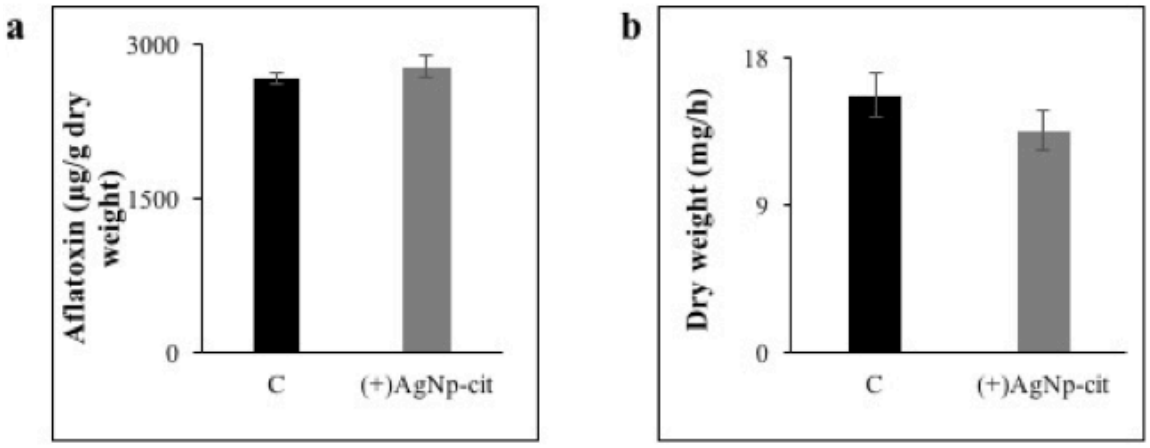

Figure 3.9: Effect of AgNp-cit on *A. parasiticus* growth and aflatoxin biosynthesis upon completion of AgNp-cit uptake: *A. parasiticus* (10^6 spores) was inoculated in fungal growth medium along with 20nm size AgNp-cit at 50ng/mL concentration and grown under standard growth conditions for 48 hours. (a) Determination of aflatoxin

accumulation in the growth medium (normalized to dry weight of the mycelia) by ELISA in untreated and AgNp-cit treated (50ng/mL concentration); the black bar indicates untreated control and the gray bar indicates AgNp-cit treated mycelia. The result showed that there is no significant difference in aflatoxin accumulation in the growth medium by untreated and AgNp-cit treated mycelia. (b) Growth rate (mg/h) of the harvested mycelia was carried out at 48 hours post inoculation. The black bar indicates untreated control and the gray bar indicates AgNp-cit treated mycelia. The result showed that there is no significant difference between the growth rate of untreated and AgNp-cit treated mycelia.

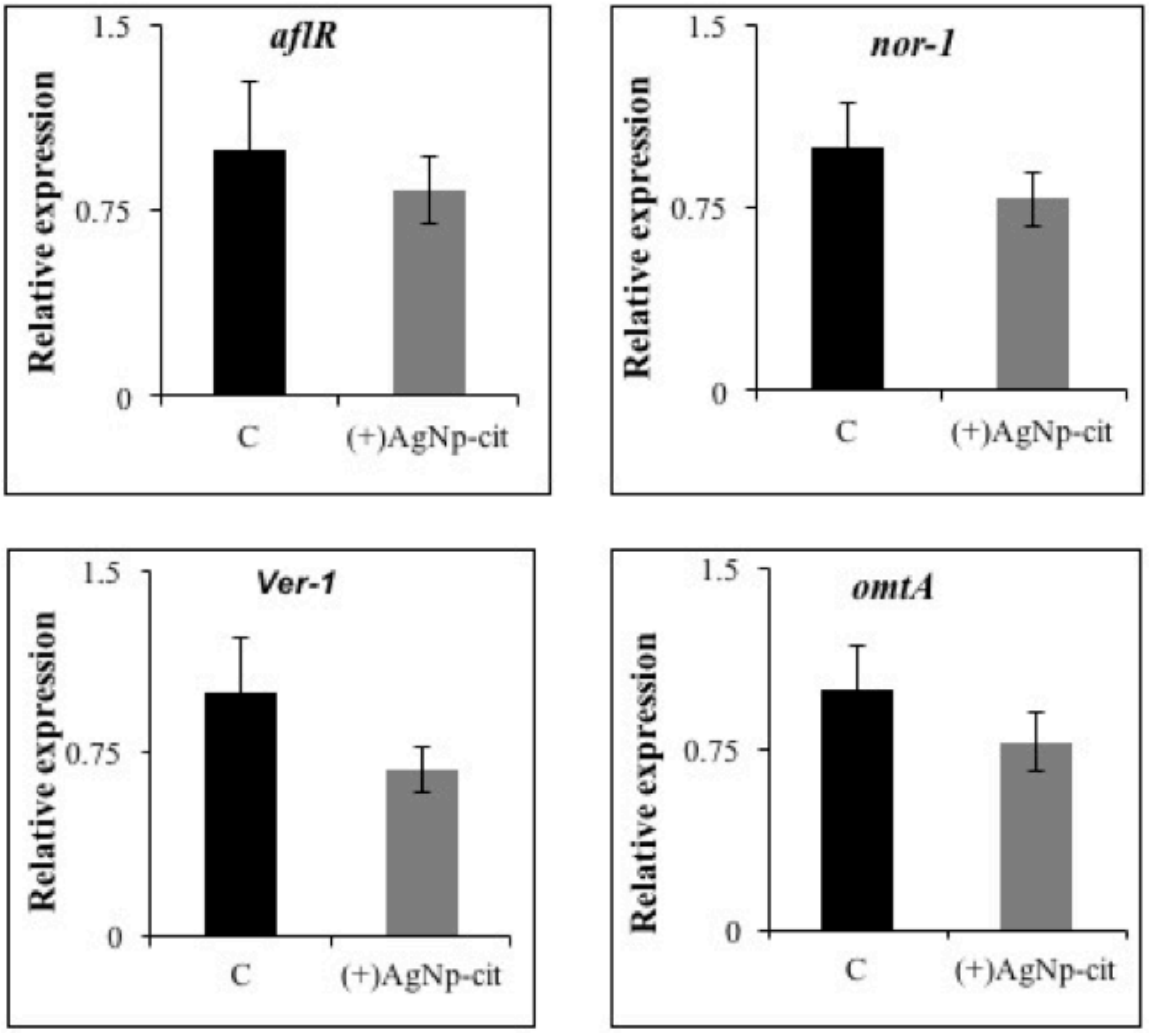

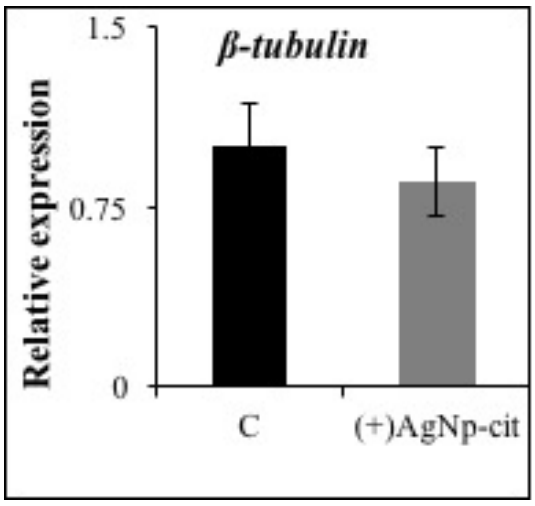

Figure 3.10: Effect of AgNp-cit on transcriptional activation of aflatoxin regulatory genes in aflatoxin biosynthesis at 40 hours post inoculation: At 40 hours post inoculation mycelia were harvested and Real-time PCR was carried out from the cDNA (extracted from RNA) of the harvested mycelia to study the regulation of aflatoxin producing gene expression. The black bar indicates untreated and the gray bar indicates AgNp-cit treated mycelia. The results show no effect in transcriptional activation of aflatoxin biosynthetic pathway genes upon completion of AgNp-cit uptake from the growth medium by the mycelia at 40 hours post inoculation.

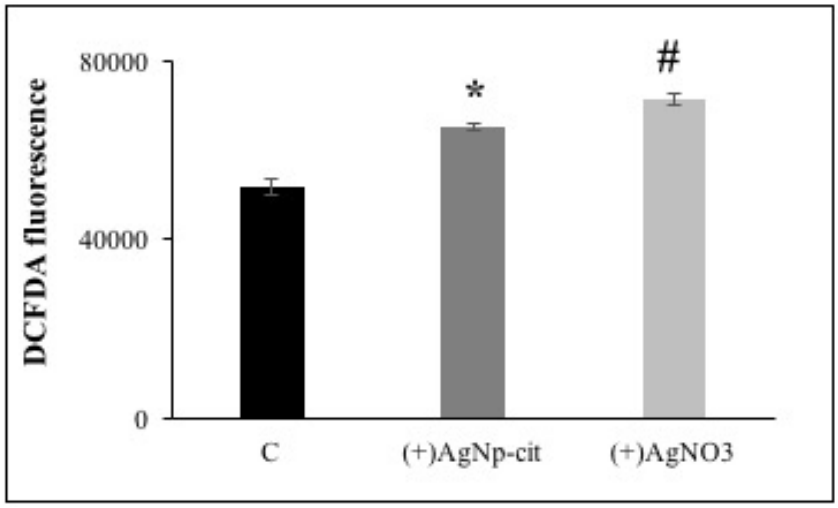

Figure 3.11: Effect of AgNp-cit and $AgNO_3$ on ROS generation at 40 hours post inoculation: Total ROS built up in the mycelia was quantified by DCF-DA based protocol (described above). The result showed a ~1.3-fold increase in total ROS level upon exposure to AgNp-cit and a ~1.4-fold increase in total ROS level upon exposure to $AgNO_3$ compared to the untreated control. The black bar indicates untreated, dark gray bar indicates AgNp-cit treated, the light gray bar indicates $AgNO_3$ treated mycelia, * indicates significance compared to the untreated, and # indicates significance compared with untreated.

CHAPTER 4

EFFECT OF SILVER NANOPARTICLE COATING AND SIZE ON AFLATOXIN BIOSYNTHESIS IN *A. PARASITICUS*

Engineered nanoparticles have emerged as a powerful device to design new antimicrobial agents. The antimicrobial effect of engineered silver nanoparticles was investigated in different microorganisms. However, there is very little information about the role of different coatings and sizes of silver nanoparticles on mycotoxin-producing fungi. Our previous study showed that citrate coated silver nanoparticles size of 20 nm at 50ng/mL concentration, can significantly decrease (approximately two fold) aflatoxin biosynthesis in *A. parasiticus* without altering the mycelial growth rate. It was observed that the aflatoxin inhibitory effect of AgNp-cit was mediated by a reduction in aflatoxin gene transcripts and a reduction in reactive oxygen species (ROS) as compared to the untreated control. In our current study, we have investigated the role of two different coatings (citrate and pvp) and three different sizes (15nm, 20nm, and 30nm) of citrate coated silver nanoparticles (using various concentrations ranging from 10ng/mL to 100ng/mL) on the growth and aflatoxin biosynthesis in *A. parasiticus*. Aflatoxin B_1 is a mycotoxin, biosynthesized by a few Aspergillus species when they grow on susceptible food and crops, and it is the most potent naturally occurring liver carcinogen. We have used *A. parasiticus* as it is one of the major aflatoxin producers and a well-studied fungal model for observing aflatoxin biosynthesis. Enzyme Linked Immunosorbent Assay

(ELISA) measured aflatoxin accumulation in the growth medium by *A. parasiticus* and cellular growth rate was measured by determining the dry weight (mg/h) of the mycelia. Our results suggest that the effect of AgNp-cit on aflatoxin B_1 biosynthesis is dependent on nanoparticles size. AgNp-cit size of 15 nm showed maximum inhibition at 25ng/mL (1.7-fold). For 20nm and 30nm AgNp-cit the strongest aflatoxin inhibition was observed at 50ng/mL concentration. However, 20nm AgNp-cit showed better aflatoxin inhibition than 30nm particles. For pvp coated silver nanoparticles (as AgNp-pvp) the maximum aflatoxin inhibition was observed at 60ng/mL concentration (2.3-fold). It was also observed that the growth rate of the mycelia was unaltered upon treatment with AgNps as compared to the untreated control. The result showed that aflatoxin inhibition is AgNp dose-dependent and the inhibition increased with an increase in AgNp concentration from 10ng/mL to 50ng/mL, then decreased beyond 60ng/mL concentration. An increased amount of silver nanoparticles in the growth medium may enhance nanoparticle interaction with the components of the medium leading to nanoparticle aggregation, as well as minimizing bioavailability of the particles. Hence, reduction in aflatoxin inhibition was observed at higher concentrations. Aflatoxin inhibitory effect was found to be AgNp size and coating dependent. Aflatoxin inhibitory effect of 20nm AgNp-cit is greater than those of 15nm and 30nm particles and the strongest aflatoxin inhibition by 20nm AgNp-cit was observed at 50ng/mL, while for 20nm AgNp-pvp, the maximum inhibition was observed at 60ng/mL.

4.1 INTRODUCTION

Engineered metal nanoparticles have been used in different fields for their unique physical and chemical properties. Their extremely small size is responsible for their activity (Ivask et al. 2014). The metal nanoparticles are used as novel antimicrobial agents, and some studies have reported their effectiveness against antibiotic resistance species (Morones et al. 2005, Panacek et al. 2006, Panácek et al. 2009, Yah and Simate 2015). Silver ions and, among other nanoparticles, silver nanoparticles are most widely studied and extensively used to control microbial invasions (Pal et al. 2007, Oka et al. 1994). It is also reported in the literature that, in lower doses, silver is nontoxic to humans (Fabrega et al. 2011a, Mousavi and Pourtalebi 2015). Many studies have also reported that the activity of AgNp is size and shape dependent (Morones et al. 2005, Elechiguerra et al. 2005). It is speculated that AgNps, with the same surface area but with a different shape and stabilized with different capping agents, may influence the interaction with biological systems differently (Tejamaya et al. 2012). The study showed that the highest antifungal activity was observed with PVP 360, SDS, Tween 80, Brij stabilized AgNps against Candida spp and the lowest MIC (minimum inhibitory concentration) equal to 0.05mg/L was observed with SDS-stabilized AgNp, (Panácek et al. 2009).

Our previous study demonstrated AgNp-cit, size of 20nm, and at a concentration of 50ng/mL, can inhibit aflatoxin biosynthesis by around two fold in *A. parasiticus*. This effect is mediated by the inhibition of aflatoxin pathway genes, and we have also observed, upon exposure of AgNp-cit, the intracellular ROS generation was reduced as compared to untreated and $AgNO_3$ treated mycelia. However, very little is known about

the coating, size, and dose-dependent activity of AgNps on aflatoxin biosynthesis by Aspergillus species.

In the current study, we investigate the effect of different sizes and coating of silver nanoparticles on the growth of and aflatoxin biosynthesis in *A. parasiticus*. Aflatoxin B_1 is a very potent hepatocarcinogen and its exposure is the third-leading cause of cancer death globally according to the WHO (2008). NIH statistics show that 16,600 new cases of aflatoxin induced liver cancer are reported per year in the US. The US Food and Drug Administration consider, aflatoxin B_1 as an unavoidable contaminants (Hamid et al. 2013). Besides causing liver cancer, aflatoxin can also suppress the immune system, and stunt growth in children (Cotty and Jaime-Garcia 2007). It is estimated by the Food and Agriculture Organization (FAO), that currently molds destroy more than 20% of world's crops each year; and pose a significant threat to food safety in the U.S. and to rest of the world (Schmale and Munkvold 2009). Aflatoxin related management costs in the U.S. are approximately $ 0.5 to $1.5 billion per year; furthermore, this report does not include the human health impact or loss due to reduced crop yield.

Plenty of research articles published each year (Rodriguez and Mahoney 1994, Reverberi et al. 2005, Ono et al. 1997) regarding new ways to inhibit aflatoxin production and inhibit the growth of the fungus producing it. Using nanomaterials to prevent aflatoxin biosynthesis is not yet explored. Few recent studies have been published in reference to the effect of AgNps on the growth of and aflatoxin biosynthesis in *A. parasiticus* (Mousavi and Pourtalebi 2015). It has been reported that the minimum inhibitory concentration (MIC) of AgNps against *A. parasiticus* was observed at 180µg/mL concentration, and AgNps inhibited aflatoxin biosynthesis by 50 % at

90µg/mL (MIC) concentration. But how different coatings and different sizes of silver nanoparticles affect the fungal biology at different concentrations which do not alter the mycelial growth is not known thus far. Therefore, the current study was undertaken to:

- Evaluate the effect of different sizes (15nm, 20nm, and 30nm) of AgNp-cit at different concentrations (that do not inhibit mycelia growth) on *A. parasiticus.*
- Evaluate the effect of AgNp-pvp size of 20nm at various concentrations (which do not affect the growth of the mycelia) on aflatoxin biosynthesis in *A. parasiticus*.

4.2 MATERIALS & METHODS

Silver nanoparticles synthesis and characterization:

Three different sizes of AgNps were prepared from a previously established chemical reduction method (Römer et al. 2011, Cumberland and Lead 2009). These silver nanoparticles were stabilized using citrate. Monodisperse pvp coated silver nanoparticles (AgNp-pvp) suspension was purchased from Sigma-Aldrich (product # 795933). All the silver nanoparticles were characterized by surface plasmon UV-vis spectrophotometry using wavelengths 200nm to 800 nm, dynamic light scattering spectroscopy was used to measure the average size of the particles, and transmission electron microscopy was used to evaluate the morphological characteristics of the silver nanoparticles (described in detail in chapter 2).

Fungal strain, medium and growth conditions:

In the current study, wild-type aflatoxin producer, *Aspergillus parasiticus,* SU-1 (NRRL 5862) was used. The effect of size on growth and aflatoxin biosynthesis was carried out using AgNp-cit of different sizes (15nm, 20nm, and 30nm) and for the effect of AgNp coating AgNp-cit size of 20nm and AgNp-pvp size of 20nm was selected. For AgNps exposure experiments, 10^6 spores of *A. parasiticus* were inoculated in 100 mL Yeast Extract Sucrose (YES) liquid growth medium containing AgNps at different concentrations (10ng/mL, 25ng/mL, 40ng/mL, 50ng/mL, 60ng/mL, 75ng/mL, and 100ng/mL) and grown under standard growing condition (29^0C, in a dark shaker at 150 rpm). The untreated control groups were grown under the same growing conditions but in the absence of AgNps. To determine the effect of dissolved silver on the growth and aflatoxin accumulation, silver nitrate ($AgNO_3$) salt was purchased from Sigma-Aldrich (product # 209139) and a 10 ppm solution was prepared. $AgNO_3$ solution (using 10ng/mL, 25ng/mL, 40ng/mL, 50ng/mL, 60ng/mL, 75ng/mL, and 100ng/mL concentrations) was inoculated along with 10^6 spores in YES medium and grown under the same growth conditions. Mycelia were harvested for analyses of growth, and YES medium was harvested for the determination of aflatoxin accumulation in the growth medium at 24h, 30h, 40h, and 48h from the time point of inoculation.

Fungal growth and aflatoxin measurements:

Dry weight measurements of harvested mycelia were performed as described previously (Liang et al. 1996). Briefly, at different time point, mycelia were harvested and stored at -80^0C. The next day, mycelia were dehydrated in a hot air oven (85^0 to

90^0C) for 8-10 hours. After 8 hours all the mycelia were collected and the dry weight was calculated by deducting the final weight (after incineration) from the initial weight (before incineration). Aflatoxin accumulation in the growth medium was determined using both thin-layer chromatography (TLC) and Enzyme Linked Immunosorbent Assay (ELISA) as described previously (Pestka 1988). Aflatoxin B_1 was measured using Neogen veratox aflatoxin (total) quantitative test kit (cat #8030) and Neogen reader 4700.

4.3 RESULT AND DISCUSSION

Characterization of AgNp-cit:

The optimized condition for successful AgNp synthesis of different sizes mainly depends on various factors such as temperature, reducing agent used, and concentration of the reducing agent. For this study silver nanoparticles of different sizes were synthesized by the manipulating reaction temperature, time, and concentration of reducing agent (sodium borohydride). Finally, all the AgNps were stabilized with citrate. Different sizes of AgNp-cit and AgNp-pvp were characterized with surface plasmon UV-vis spectroscopy, as the absorbance peak obtained from each AgNp is very specific. The characterization of all the AgNps by TEM was carried out (as discussed in chapter 2). The size distribution of intensity data was obtained using DLS, and the data suggests that all the AgNps have a narrow size distribution as discussed in chapter 2.

Aflatoxin inhibitory effect of stabilized silver nanoparticles:

Size dependent aflatoxin biosynthesis inhibition of citrate coated silver nanoparticles:

In the previous chapter we have observed that citrate coated silver nanoparticles (AgNp-cit) size of 20nm significantly inhibited aflatoxin biosynthesis in *A. parasiticus* without altering the growth rate of the mycelia. In this study we sought to determine the effect of different sizes of AgNp-cit (15nm, 20nm, and 30nm) on aflatoxin biosynthesis inhibition. We have used a series of different concentrations (10ng/mL, 25ng/mL, 40ng/mL, 50ng/mL, 60ng/mL, 75ng/mL, and 100ng/mL) for this study. Aflatoxin B_1 accumulation in the medium at 40 hour post inoculation was estimated by ELISA assay by a previously established method (Chanda et al. 2010) and normalized to the dry weight of the mycelia.

The results show that for particle size 20nm and 30nm, aflatoxin accumulation reduced with an increase in AgNp concentration from 10ng/mL to 50ng/mL (dose response relationship) and then increased beyond 60ng/mL to 100ng/mL concentrations. But for 15 nm particles, maximum aflatoxin inhibition occurred at 25ng/mL (by ~1.7 fold) concentration and aflatoxin accumulation increased with an increase in AgNp concentrations in the growth medium as compared to the untreated control (Figure 4.1). As illustrated in Figure 4.2, at 50ng/mL and 60ng/mL concentrations of AgNp-cit size of 20nm inhibited aflatoxin biosynthesis by ~3 fold and ~2.7 fold, respectively, as compared to the untreated control. As shown in Figure 4.3, 30nm AgNp-cit at 50ng/mL

concentration, inhibited aflatoxin accumulation in the growth medium by 1.9 folds as compared to the untreated control.

It is well documented that the size of nanoparticles has great effects on their uptake and impact on a biological system. It was observed that smaller sized nanoparticles (<50nm) are likely taken up by the cell through the intracellular membrane (Kim et al. 2012b). This process is called endocytosis. The size of a matured endosome is approximately 500nm, and it contains intraluminal vesicles with sizes ranging from 50nm to 100nm (Murk et al. 2003). It is possible that smaller nanoparticles are readily taken up by the eukaryotic cell during the endocytosis process. However, nanoparticles also tend to form aggregates during nano-bio interaction processes and they end up being aggregated at the cell wall or in the cell membrane (Treuel et al. 2013). Uptake of larger particles is more complicated and some studies have shown that endocytosis of bigger particles is thermodynamically possible (Zhang et al. 2015) but due to slower receptor diffusion rate, fewer nanoparticles are taken up by the cell.

In a nanoparticle stability study, it was observed that citrate coated silver nanoparticles strongly interact with the components of the fungal growth medium (described in the previous chapter). The interaction increased with an increased concentration of AgNp-cit and particles aggregated/precipitated/transformed quickly in the medium. At higher concentrations (of AgNp-cit), the maximum number of particles get aggregated and are made them unavailable for mycelial uptake. Some studies have suggested that protein corona formation on the surface of nanoparticles affects uptake efficiency (Treuel et al. 2013). The formation of protein corona by human transferrin protein on to carboxyl coated nanoparticles was found not to assist the endocytosis

process. The protein corona interferes in the interaction between nanoparticles and receptors on the cell membrane. Our current knowledge is still limited in understanding the effect of nanoparticle interaction with the biological medium followed by its uptake by the cell.

Coating dependent aflatoxin biosynthesis inhibition of silver nanoparticles:

In Figure 4.4, it was observed that, aflatoxin inhibition for AgNp-pvp, reached its maximum at 60ng/mL concentration (~2.3 fold), but 40ng/mL (~1.9 fold), 50ng/mL (2fold), and 75ng/mL (~2.2 fold) concentrations also showed significant amounts of aflatoxin inhibitory effect in the growth medium, as compared to the untreated sample at 40-hour time post inoculation. Many studies have suggested that different surface coatings of silver nanoparticles have variations in their biological activity (Li et al. 2013, Panácek et al. 2009). SDS stabilized silver nanoparticles (size of 25nm) showed better antifungal activity against *Candida albicans* than non-stabilized, tween 80, brij, and pvp stabilized silver nanoparticles. A stability study of silver nanoparticles revealed that SDS stabilized silver nanoparticles were more stable than others and showed better antimicrobial activity (Libor kvitek 2008). The better antimicrobial activity can be attributed not only to the higher stability but also to the disruption of the cell walls by the surfactant (SDS).

A previous study on the stability of silver nanoparticles with different coatings showed that AgNp-pvp is more stable than AgNp-cit (Huynh and Chen 2011, Stebounova, Guio and Grassian 2011). The stability might be due to the steric repulsion exhibited by the pvp coating (DLVO theory). But in the presence of chloride ions or

sulfide ions, both the AgNps show aggregation to some extent. Fungal growth medium contains different kinds of chloride, sulfide, monovalent, and divalent salts as well as nutrients (amino acids, proteins, and vitamins), which may influence their precipitation, sedimentation, aggregation, corona formation, and replacement of surface coating. Fungal cells also release enzymes like reductases and superoxide, which can reduce silver ions (from dissolution of AgNp) to AgNp and on the other hand, oxidizing agents such as H_2O_2 which, when released by the cell can oxidize AgNp to silver ion (He et al. 2012a, He, Garg and Waite 2012b, Jones et al. 2011). Our data suggests that stabilized (pvp, and citrate) silver nanoparticles interacts with the components of growth medium and forms larger aggregates/precipitates. The formation of aggregates/precipitates increases with an increase in concentration of AgNps in the growth medium and particles become unavailable for mycelial uptake. Therefore, at higher concentrations of AgNp mycelia produced higher amounts of aflatoxin.

Effect of silver nitrate on aflatoxin biosynthesis:

The antimicrobial activity of silver was found to be different in different microbial species (Ruparelia et al. 2008, Spacciapoli et al. 2001, Matsumura et al. 2003). Previous studies have reported that silver ions are more toxic than the silver nanoparticles (Morones et al. 2005). Silver ions react with the thiol group in vital enzymes containing sulfur and inactivate them or interact with DNA resulting in enhancement of pyrimidine dimerization by photodynamic reaction and might prevent DNA replication (Fox and Modak 1974). Silver ions may induce generation of reactive oxygen species, which are possibly produced during the inhibition of respiratory enzymes by silver ion interaction with the cell (Matsumura et al. 2003). It was observed that silver ion showed antifungal

activity in *Aspergillus flavus* at a concentration of 70μg/mL and aflatoxin B_1 production was also completely inhibited (Ismaiel and Tharwat 2014). The TEM image of silver ion treated (50μg/mL concentration) *A. flavus* and *P. vulpinum* showed plasma membrane detachment from the cell wall, damaged cytoplasmic organelles, and disorganized aggregated mitochondria. At lower concentrations of silver ion (8μg/mL and 12μg/mL) fungal (*A. flavus*) growth was enhanced slightly, but it could decrease aflatoxin B_1 synthesis by 27.3% and 40% respectively.

In this study it was observed that, upon exposure to $AgNO_3$, aflatoxin accumulation in the fungal growth medium increased with an increase in concentration of $AgNO_3$ as compared to the untreated control. As shown in Figure 4.5, $AgNO_3$ significantly increased aflatoxin accumulation at 50ng/mL (1.47 fold), 60ng/mL (1.52 fold), 75ng/mL (1.56 fold) and 100ng/mL (1.66 fold), unlike AgNp treatments on *A. parasiticus*. In our previous study, we have observed, $AgNO_3$ treated *A. parasiticus* produced excess amount of ROS, and also produced more aflatoxin in the growth medium as compared to AgNp-cit treated mycelia. Some studies have reported that there is a strong correlation between oxidative stress and aflatoxin production (Narasaiah, Sashidhar and Subramanyam 2006). It is possible that at very low concentrations (ng/mL) silver ions did not inhibit the fungal growth rate but induced ROS generation which enhanced aflatoxin production. We also examined the transcriptional activation of 2 superoxide dismutase genes (SOD) for different concentrations of $AgNO_3$ treated mycelia. The result suggested that transcriptional activation of cytosolic CuZnSOD and MnSOD genes increased significantly with increased $AgNO_3$ concentration (Figure 4.11), suggesting $AgNO_3$ induces ROS generation in the cytosol as well as in the mitochondria.

On the other hand, 20nm AgNp-cit treated mycelia showed significant upregulation of MnSOD for 100ng/mL and 10ng/mL concentrations but cytosolic CuZnSOD was not upregulated as compared to untreated control. Cytosolic CuZnSOD was significantly downregulated for 50ng/mL concentration. Exposure of 20nm AgNp-cit particles on *A. parasiticus* mycelia did not show any dose-response relationship in the SOD transcription accumulation. This effect might be due to unique interaction between AgNps and the growth medium. A 10ng/mL concentration was too little to produce any biological activity. At higher concentration (100ng/mL) particles formed larger aggregates and/or precipitates and became unavailable for the mycelia to uptake and therefore, no aflatoxin inhibition was observed. However, the unique interaction between silver nanoparticles and the mycelia in the growth medium and the exact cellular events triggered by the AgNps to inhibit aflatoxin biosynthesis at sublethal concentrations is yet to be elucidated.

Effect of silver nanoparticles and silver nitrate on mycelial growth rate:

Dry weight (measured as a growth rate in mg/h) of all the treated and untreated mycelia was measured to understand whether the aflatoxin inhibitory effect is growth related. The results show that there is no statistically significant difference in the growth rate (mg/h) of treated and untreated mycelia in AgNp-cit of different sizes (15nm, 20nm and 30nm), AgNp-pvp, or $AgNO_3$, treated as shown in Figure 4.6, 4.7, 4.8, 4.9 and 4.10, respectively. The results showed that the fungal growth had no effect on aflatoxin accumulation in the medium upon exposure to AgNp-cit, AgNp-pvp and $AgNO_3$. Some studies have reported that metal ions such as Zn^{2+}, Cd^{2+} can stimulate the growth of *A. parasiticus* (Failla and Niehaus 1986).

4.4 CONCLUSION

Based on the results of the current study, AgNp-cit of different sizes and AgNp-pvp can significantly inhibit aflatoxin biosynthesis in *A. parasiticus* without inhibiting the mycelial growth rate. It was found that upon $AgNO_3$ exposure, mycelial SOD gene expression upregulated significantly and upregulation was found to increase with increased $AgNO_3$ concentration in the growth medium. But we still do not know whether the uptake of AgNp-cit was size or concentration dependent. Aflatoxin biosynthesis inhibition at the cellular level in presence of different sizes of AgNps in the fungal system is yet to be understood completely. Therefore, silver nanoparticles should be subjected to further study to evaluate their exact molecular mechanisms.

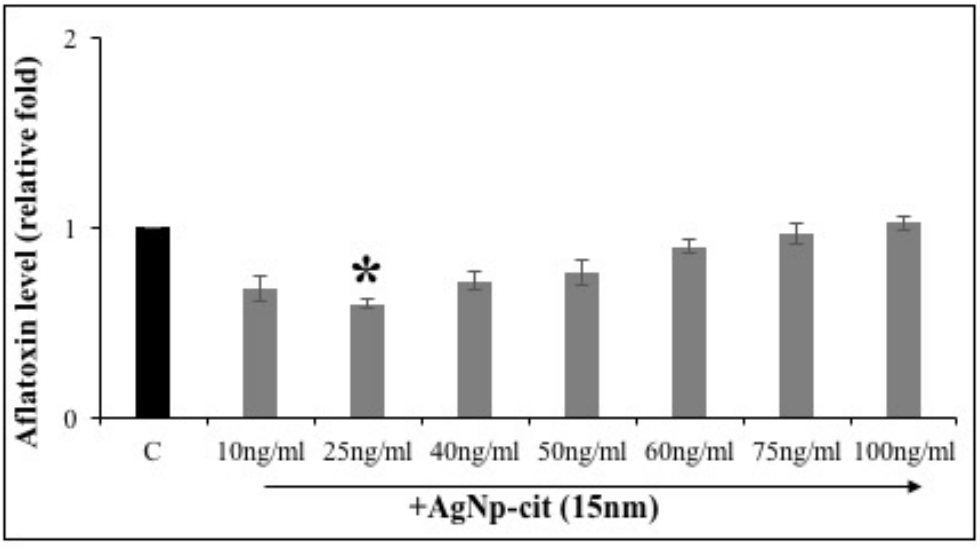

Figure 4.1: Effect of AgNp-cit (size of 15nm) on aflatoxin production by *A. parasiticus* at 40-hour time point. Aflatoxin accumulation is normalized by dry weight of the mycelia at the same time point and relative fold difference was calculated as compared to the untreated control. The black bar indicates the untreated control and the gray bars indicate the AgNp-cit treated mycelia. Statistical significance of two-tailed p-values was determined using an unpaired t-test, with n=3 and $p < 0.05$ as the significance level. '*' denotes significance.

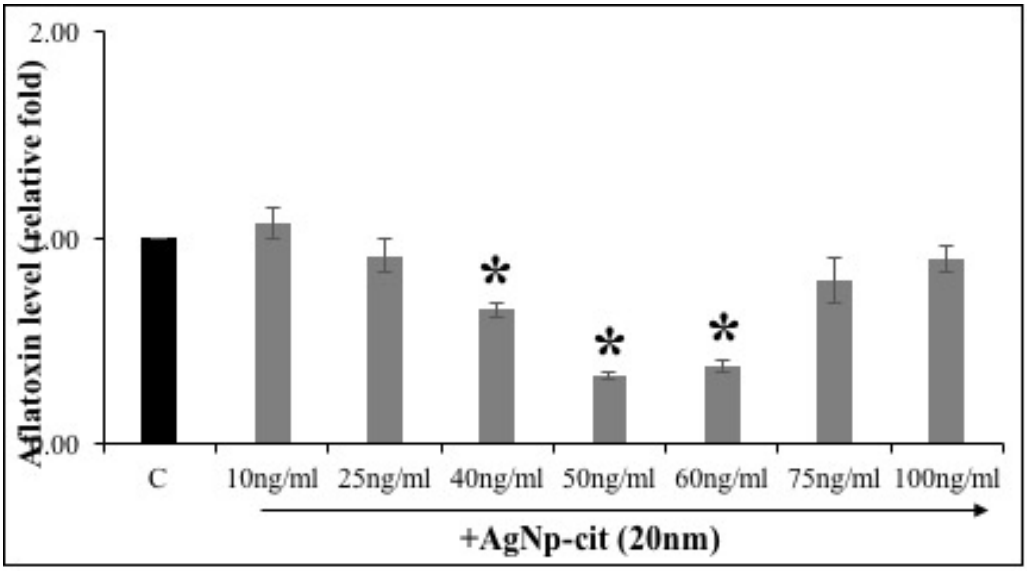

Figure 4.2: Effect of AgNp-cit (size of 20nm) on aflatoxin production by *A. parasiticus* at 40-hour time point. Aflatoxin accumulation is normalized by dry weight of the mycelia at the same time point and relative fold difference was calculated as compared to the untreated control. The black bar indicates the untreated control and the gray bars indicate the AgNp-cit treated mycelia. Statistical significance of two-tailed p-values was determined using an unpaired t-test, with n=3 and $p < 0.05$ as the significance level. '*' denotes significance.

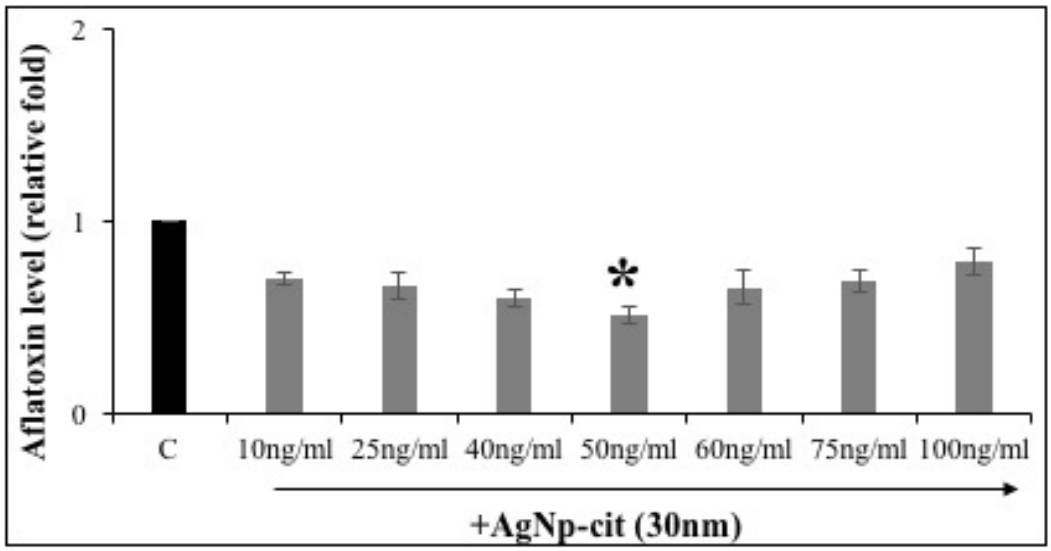

Figure 4.3: Effect of AgNp-cit (size of 30nm) on aflatoxin production by *A. parasiticus* at 40-hour time point. Aflatoxin accumulation is normalized by dry weight of the mycelia at the same time point and relative fold difference was calculated as compared to the untreated control. The black bar indicates the untreated control and the gray bars indicate the AgNp-cit treated mycelia. Statistical significance of two-tailed p-values was

determined using an unpaired t-test, with n=3 and $p < 0.05$ as the significance level. '*' denotes significance.

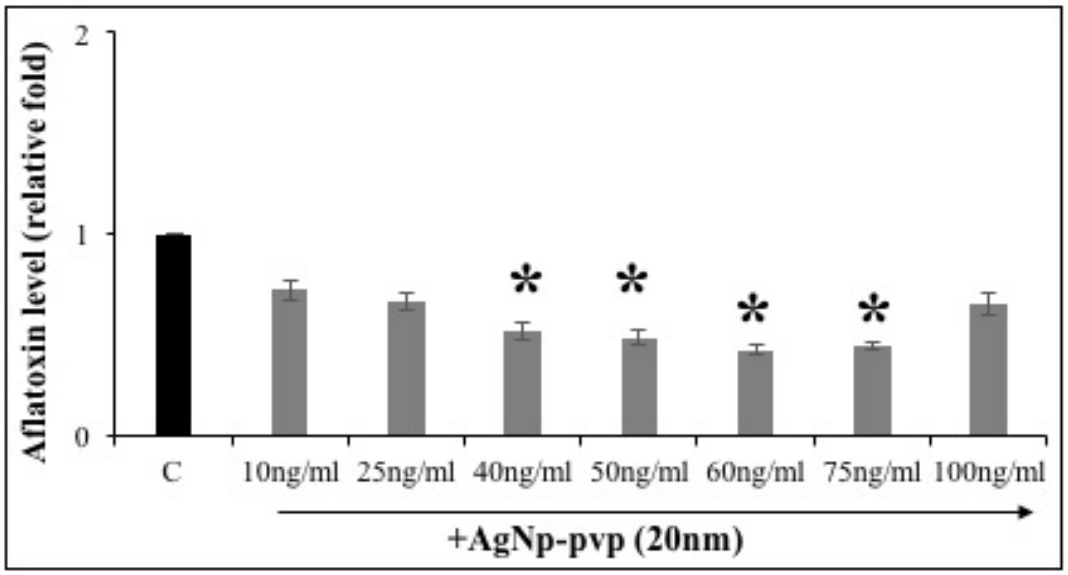

Figure 4.4: Effect of AgNp-pvp (size of 20nm) on aflatoxin production by *A. parasiticus* at 40-hour time point. Aflatoxin accumulation is normalized by dry weight of the mycelia at the same time point and relative fold difference was calculated as compared to the untreated control. The black bar indicates the untreated control and the gray bars indicate the AgNp-cit treated mycelia. Statistical significance of two-tailed p-values was determined using an unpaired t-test, with n=3 and $p < 0.05$ as the significance level. '*' denotes significance.

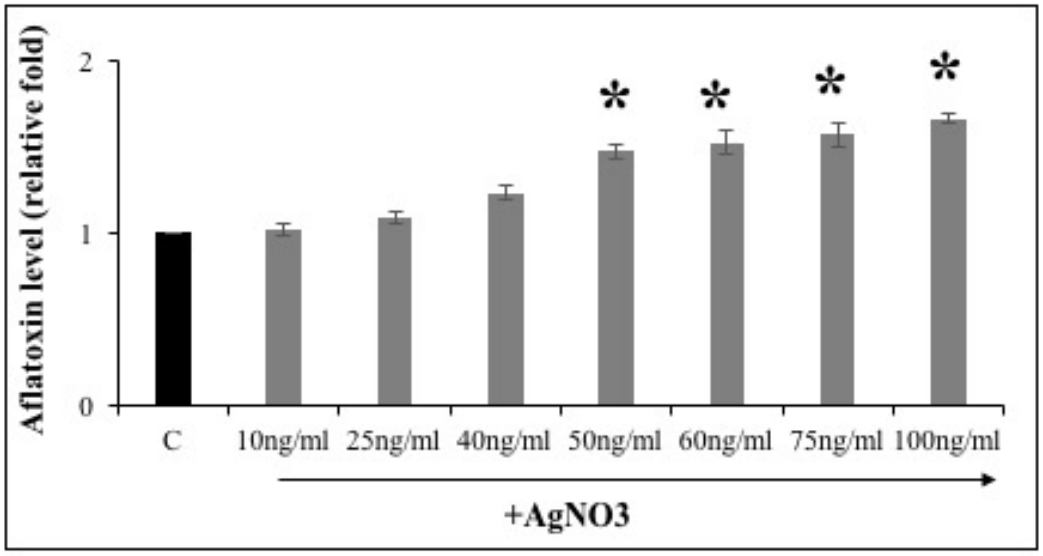

Figure 4.5: Effect of $AgNO_3$ on aflatoxin production by *A. parasiticus* at 40-hour time point. Aflatoxin accumulation is normalized by dry weight of the mycelia at the same time point and relative fold difference was calculated as compared to the untreated. The black bar indicates the untreated control and the gray bars indicate the AgNp-cit treated samples. Statistical significance of two-tailed p-values was determined using an unpaired t-test, with n=3 and $p < 0.05$ as the significance level. '*' denotes significance.

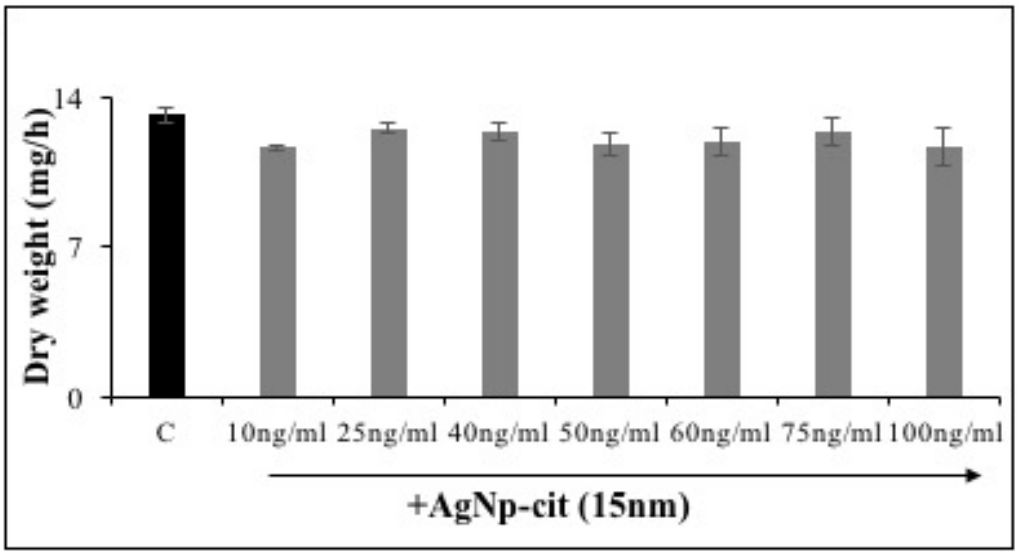

Figure 4.6: Effect of AgNp-cit (15nm size) on the growth of *A. parasiticus*. All the dry weight data was compared with the untreated set of samples. Statistical significance of two-tailed p-values was determined using an unpaired *t*-test, with n=3 and $p < 0.05$ as the significance level. The black indicates untreated and the gray bars indicate AgNp-cit treated mycelial dry weight.

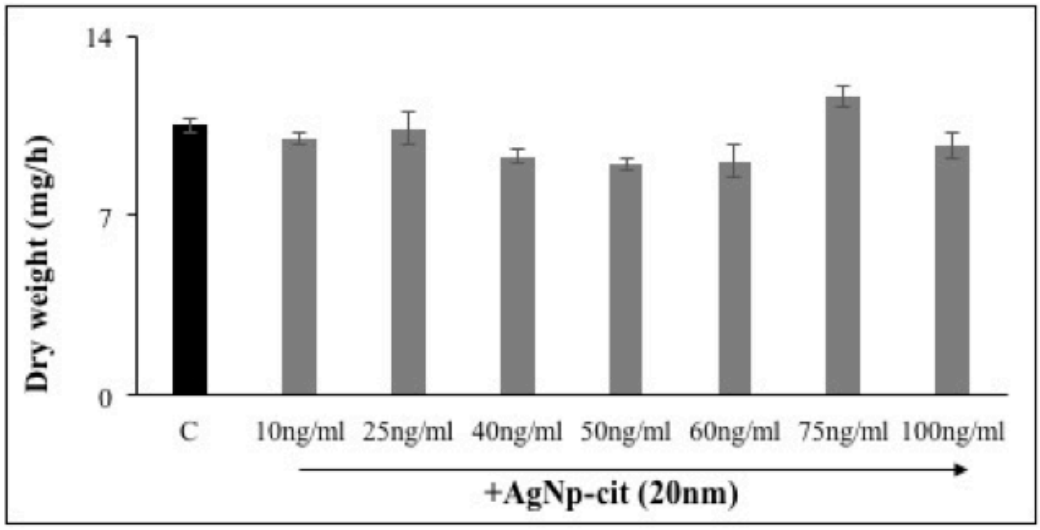

Figure 4.7: Effect of AgNp-cit (20nm size) on the growth of *A. parasiticus*. All the dry weight data was compared with the untreated set of samples. Statistical significance of two-tailed p-values was determined using an unpaired *t*-test, with n=3 and $p < 0.05$ as the significance level. The black indicates untreated and the gray bars indicate AgNp-cit treated mycelial dry weight.

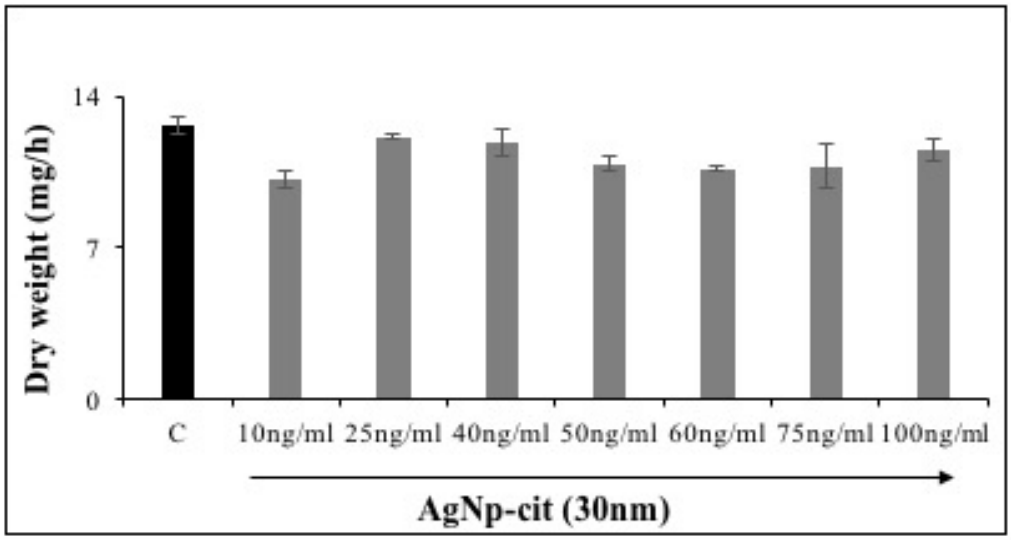

Figure 4.8: Effect of AgNp-cit (30nm size) on the growth of *A. parasiticus*. All the dry weight data was compared with the untreated set of samples. Statistical significance of two-tailed p-values was determined using an unpaired *t*-test, with n=3 and $p < 0.05$ as the significance level. The black indicates untreated and the gray bars indicate AgNp-cit treated mycelial dry weight.

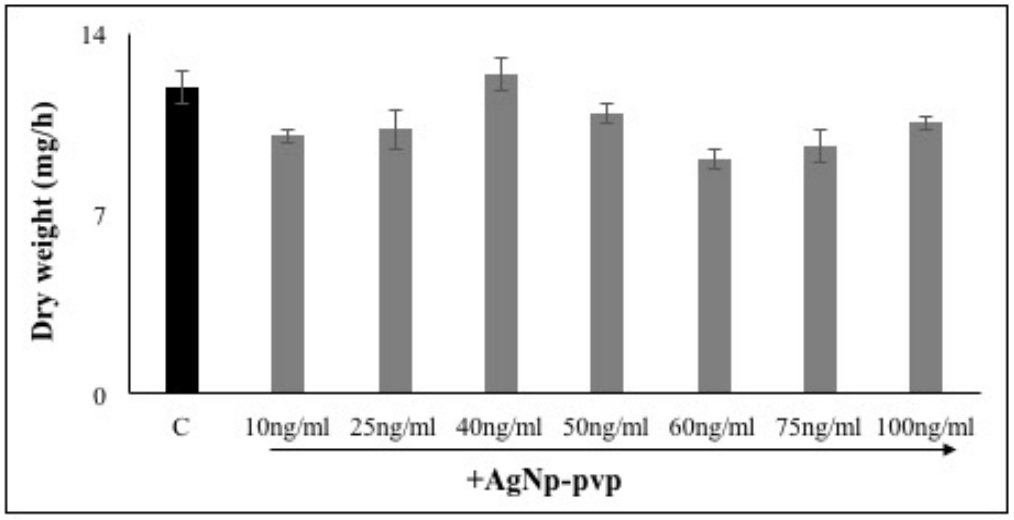

Figure 4.9: Effect of AgNp-pvp (20nm size) on the growth of *A. parasiticus*. All the dry

weight data was compared with the untreated set of samples. Statistical significance of two-tailed p-values was determined using an unpaired *t*-test, with n=3 and $p < 0.05$ as the significance level. The black indicates untreated and the gray bars indicate AgNp-cit treated mycelial dry weight.

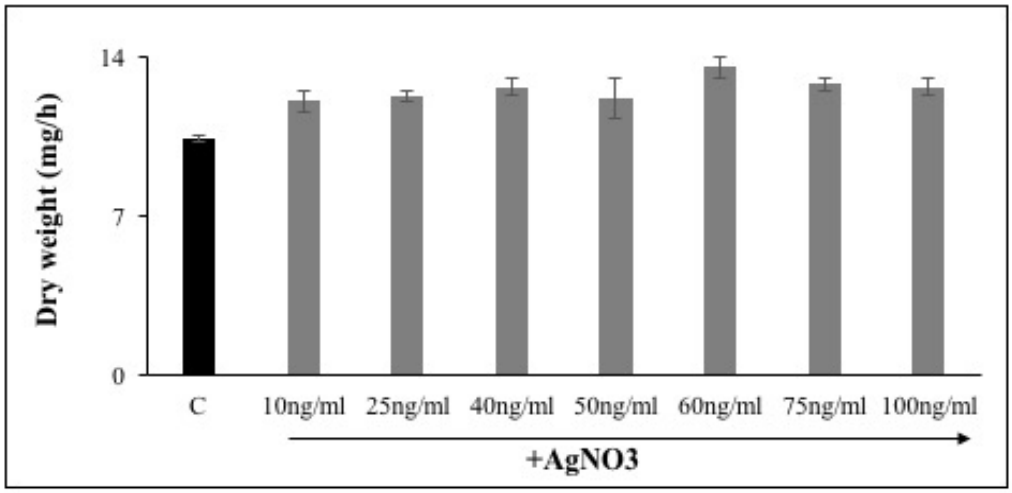

Figure 4.10: Effect of $AgNO_3$ on the growth of *A. parasiticus*. All the dry weight data was compared with the untreated set of samples. Statistical significance of two-tailed p-values was determined using an unpaired *t*-test, with n=3 and $p < 0.05$ as the significance level. The black indicates untreated and the gray bars indicate $AgNO_3$ treated mycelial dry weight.

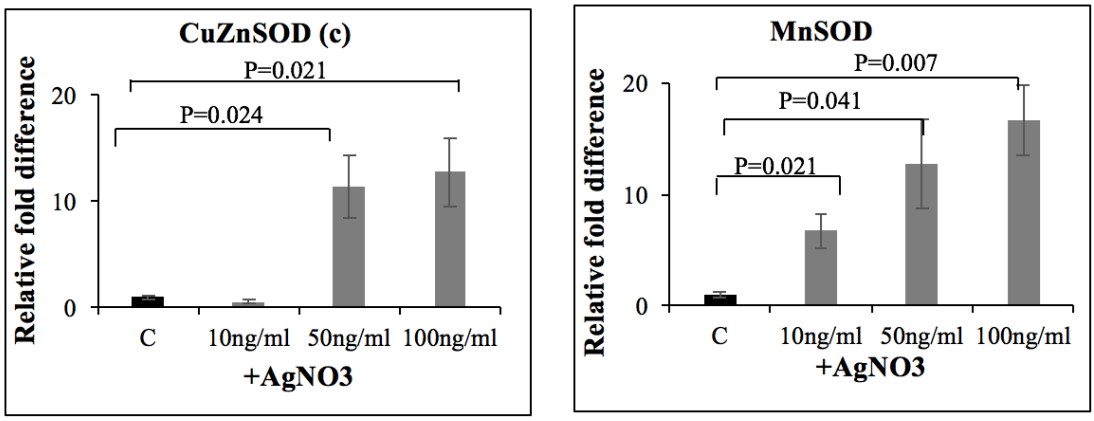

Figure 4.11: Effect of $AgNO_3$ on transcriptional accumulation of SOD genes: The cellular level of ROS is controlled by antioxidant enzymes superoxide dismutase (SODs). At 24 hours post inoculation mycelia were harvested from the growth medium and RTPCR was carried out from the RNA of the harvested mycelia to study the regulation of

SOD gene expression. The black bar indicates untreated and the gray bars indicate $AgNO_3$ treated samples indicating $AgNO_3$ enhance intracellular oxidative stress.

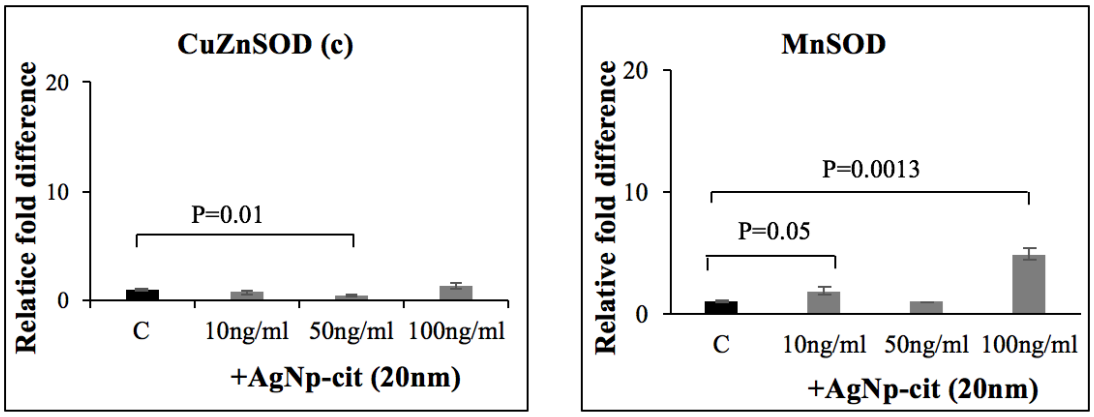

Figure 4.12: Effect of AgNp-cit on transcriptional accumulation of SOD genes: The cellular level of ROS is controlled by antioxidant enzymes superoxide dismutase (SODs). At 24 hours post inoculation mycelia were harvested from the growth medium and RTPCR was carried out from the RNA of the harvested mycelia to study the regulation of SOD gene expression. The black bar indicates untreated and the gray bar indicates AgNp-cit treated samples

CHAPTER 5

OVERALL DISCUSSION

In recent years, microbial infections have increased at an alarming rate and some microbes have developed resistance to multiple drugs which is claiming human lives (Dizaj et al. 2014). Engineered nanomaterials are showing a promising result against different persistent microbes (Yah and Simate 2015, Azam et al. 2012). Many studies have suggested that at high concentrations (μg/mL) engineered metal nanoparticles can inhibit the growth of bacteria and fungi along with their harmful metabolites (Mousavi and Pourtalebi 2015, Al-Othman et al. 2014). The release of metal nanoparticles has eminent in the environment due to enhanced use of nanoparticles in different commercial products (Aiken, Hsu-Kim and Ryan 2011), and this is a serious concern for environmental health. Although many research articles have elaborated the toxic effects of silver nanoparticles on different organisms, most of them discussed toxic effects of AgNps at high levels of exposure. It is also important to know the chronic and cumulative effects of AgNps at sublethal concentrations which is analogous to environmental concentrations (as pollutants). We still do not know a lot about the specific interactions of these engineered metal nanoparticles with microorganisms, plants, or the effect of nanoparticles on animals. No studies have reported the response of fungi exposed to nanoparticles at a concentration that does not affect the growth of the fungi

thus far. There is also very little known about the role of different coating and sizes of metal nanoparticles on mycotoxin producing fungi.

For this study citrate coated silver nanoparticles of three different sizes (15nm, 20nm, and 30nm) were synthesized by the chemical reduction method (Römer et al. 2011, Cumberland and Lead 2009) and stabilized with citrate. Monodisperse pvp coated silver nanoparticle (AgNp-pvp size of 20nm) suspension was purchased from Sigma-Aldrich. All the nanoparticles were characterized by surface plasmon UV-vis spectrophotometry using wavelengths 200nm to 800nm, dynamic light scattering spectroscopy to measure the average size of the particles, and transmission electron microscopy to evaluate the morphological characteristics of the silver nanoparticles.

In this study, we have investigated the effect of two different coatings (pvp and citrate) and three different sizes of citrate coated silver nanoparticles on the growth and aflatoxin B_1 biosynthesis in *A. parasiticus*. Aflatoxin B_1 is a secondary metabolite synthesized by a group of filamentous fungi under the genus Aspergillus and is one of the most potent naturally occurring carcinogens (Chanda et al. 2010). Aflatoxin was measured by the ELISA method and normalized by dry weight of the fungi and fungal cellular growth rate was measured by dry weight (mg/h) of the mycelia.

Our results suggest that the effect of citrate coated silver nanoparticles (AgNp-cit) on aflatoxin B_1 biosynthesis is nanoparticle size dependent. AgNp-cit size of 15 nm, showed maximum inhibition at 25ng/mL (1.7 fold). AgNp-cit size of 20nm and 30nm showed strongest aflatoxin inhibitory effect at 50ng/mL, but 20nm particles showed better inhibitory activity than 30nm particles. For pvp coated silver nanoparticles (as

AgNp-pvp, size of 20nm) the maximum aflatoxin inhibition was observed at 60ng/mL concentration (2.3 fold). On the contrary, upon exposure to $AgNO_3$ aflatoxin accumulation in the fungal growth medium increased with an increase in the concentration of $AgNO_3$ as compared to the untreated control. It was also observed that the growth rate of the mycelia was unaltered upon treatment with AgNps as compared to the untreated control. We have selected citrate coated silver nanoparticles (size of 20nm) at 50ng/ml concentration to study the molecular mechanism of aflatoxin biosynthesis inhibition by silver nanoparticles because at this concentration we have observed maximum aflatoxin inhibition. We have also observed that aflatoxin biosynthesis inhibition was mediated by transcription inhibition of the aflatoxin pathway gene cluster and at least two global regulators of secondary metabolism (*laeA* and *veA*) which can regulate the activation of the aflatoxin gene cluster.

It was also observed that AgNp-cit treated mycelia showed a significant reduction in total ROS as compared to the untreated control. It was observed that AgNp-cit mediated reduction in total ROS resulted in a significant reduction of transcriptional activation of the superoxide dismutase genes (SOD genes), a family of enzymes that scavenges superoxides (Fridovich 1995).

Our time course ICPOES data with AgNp-cit treated fungal growth media along with *A. parasiticus*, suggest that by 30-hour post inoculation total silver concentration in the growth medium decreased by 80%. Simultaneous ICPOES assessment of AgNp-cit treated mycelia showed an increase of total silver in the mycelia during 24-hour to 30-hour post inoculation.

We have evaluated the stability of AgNp-cit (size of 20nm, 50ng/mL concentration) in the fungal growth medium with surface plasmon UV-vis spectroscopy. Our results suggested that AgNp-cit in the fungal growth medium, in the presence of *A. parasiticus*, changes over time (0 to 30 hours post inoculation). The distinctive peak of AgNp-cit (20nm) at 395nm broadened and peak height also decreased by 24-hour post inoculation. At 30-hour post inoculation, the AgNp-cit peak had completely disappeared. Overall, the stability results suggest that AgNp-cit particles interact with the organic and inorganic components of the growth medium and may get aggregated/precipitated over time.

We have evaluated the effect of AgNp-cit on growth and aflatoxin biosynthesis beyond 40-hours post inoculation. It was observed that at 48-hours post inoculation, there is no significant difference in aflatoxin biosynthesis and in growth rate expressed as dry weight per unit time (mg/h) in AgNp-cit treated as compared to an untreated control. Our hypothesis is that a maximum number of nanoparticles get taken up by the mycelia at 30-hours post inoculation and we observe an aflatoxin inhibitory effect at 40-hours post inoculation. But at 48-hours post inoculation, the mycelia revert back to synthesize aflatoxin at a normal level due to lack of AgNp-cit in the growth medium. We have also observed that upon removal of AgNp-cit from the growth medium, the aflatoxin genes were expressed at levels equivalent to the untreated controls and aflatoxin synthesis was at levels similar to the untreated control. It was also observed that 40-hour post inoculation, AgNp-cit exposed mycelia resulted in ~1.3-fold increase and $AgNO_3$ exposed mycelia resulted in ~1.4-fold increase in total ROS level as compared to the untreated control.

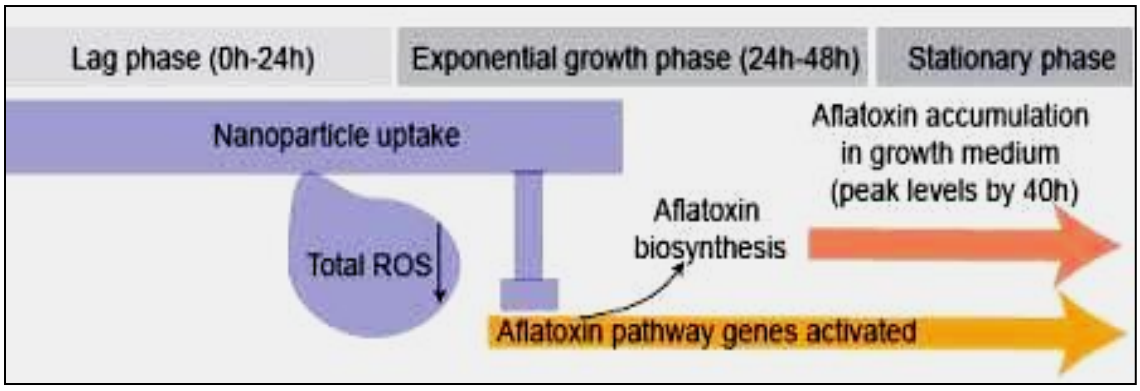

Figure 5.1: Working model to elucidate the effect of AgNp-cit on growth and aflatoxin biosynthesis in *A. parasiticus*

In summary, the possible mechanism of aflatoxin inhibition in *A. parasiticus* is described in this working model. *A. parasiticus* spores were inoculated in the fungal growth medium along with AgNp-cit. 0-hours to 24-hours post inoculation is the lag phase. During this phase, the spores adapt themselves to the growth condition. We observe AgNp-cit was taken up by the mycelia from the growth medium which resulted in significant reduction (~30%) in total ROS generation. From 24-hours to 48-hours is the log phase, or the exponential growth phase, when mycelia grow exponentially. Previous studies have shown that activation of aflatoxin biosynthesis pathway genes starts at 24 hours and aflatoxin accumulation in the growth medium reaches maxima at 40-hours post inoculation (Chanda et al. 2010). At 30-hours post inoculation, the mycelia uptake almost 80% of the total silver from the growth medium. It was observed that at 30-hours post inoculation the transcription of five aflatoxin genes and two of the global regulators of secondary metabolism were significantly reduced (~2-fold reduction in transcription level) upon exposure to AgNp-cit. The growth rate of AgNp-cit treated mycelia was similar as compared to untreated mycelia. When aflatoxin accumulation was determined

at 48-hours post inoculation, the results showed no significant difference as compared to an untreated control. It was observed that there is no effect in transcriptional activation of aflatoxin biosynthetic pathway genes upon exposure to AgNp-cit at 40-hours post inoculation and the result is comparable to the untreated control. The data demonstrates that after removal of AgNp-cit at a significant level by the mycelia from the growth medium at 30-hours post inoculation, the transcript accumulation of 5 aflatoxin biosynthetic pathway genes became equivalent to the untreated control, and aflatoxin synthesis is brought to levels similar to the untreated control at 40-hour post inoculation.

FUTURE STUDIES

In the current study, we have evaluated the effect of citrate coated silver nanoparticles (AgNp-cit), size of 20nm, on the growth and aflatoxin biosynthesis in *Aspergillus parasiticus*. We have observed AgNp-cit at concentrations that do not inhibit the growth of the mycelia as compared to the untreated control, but can significantly inhibit biosynthesis of carcinogenic mycotoxin and secondary metabolite, aflatoxin B_1 at the level of gene expression. We have also observed that upon exposure to AgNp-cit at 24-hour the total ROS generation was also significantly inhibited as compared to the untreated mycelia, which is a unique phenomenon because other studies have reported enhancement of total ROS level upon exposure to engineered metal nanoparticles. Upon mycelial uptake of AgNp-cit, the total ROS increased and the aflatoxin synthesis level becomes comparable to the untreated controls at 48-hours post inoculation. From the results, it is evident that AgNp-cit can alter secondary metabolism without altering the cellular growth.

The experimental studies that have been undertaken for this dissertation have highlighted a number of topics on which further research work would be beneficial. In particular, there is a lack of understanding on the below topics:

- How do nanoparticles interact with the biological system at different concentrations?

- How does the nanoparticle-growth medium interaction help in the inhibition of aflatoxin biosynthesis in *A. parasiticus*?
- How do different sizes and different coatings affect the molecular mechanisms of aflatoxin biosynthesis at concentrations that do not inhibit mycelial growth?
- The molecular mechanism underlying nanoparticle uptake by the mycelia
- Molecular mechanism of inhibition of mycelial total ROS upon exposure to AgNp-cit
- More detailed studies on nanoparticle mediated transient inhibition of secondary metabolism

REFERENCES

(CDC), C. f. D. C. a. P. (2004) Outbreak of aflatoxin poisoning--eastern and central provinces, Kenya, January-July 2004. MMWR Morb Mortal Wkly Rep, 53, 790-3.

Abdollahi, A. & R. L. Buchanan (1981) Regulation of aflatoxin biosynthesis: characterization of glucose as an apparent inducer of aflatoxin production. Journal of Food Science, 46, 143-146.

Afshinnia, K., I. Gibson, R. Merrifield & M. Baalousha (2016) The concentration-dependent aggregation of Ag NPs induced by cystine. Sci Total Environ, 557-558, 395-403.

Agag, B. I. (2004) Mycotoxins in foods and feeds: 1-aflatoxins. Ass. Univ. Bull. Environ. Res, 7, 173-205.

Agnihotri, S., S. Mukherji & S. Mukherji (2014) Size-controlled silver nanoparticles synthesized over the range 5–100 nm using the same protocol and their antibacterial efficacy. RSC Advances, 4, 3974-3983.

Ahamed, M., M. Karns, M. Goodson, J. Rowe, S. M. Hussain, J. J. Schlager & Y. Hong (2008) DNA damage response to different surface chemistry of silver nanoparticles in mammalian cells. Toxicol Appl Pharmacol, 233, 404-10.

Aiken, G. R., H. Hsu-Kim & J. N. Ryan (2011) Influence of dissolved organic matter on the environmental fate of metals, nanoparticles, and colloids. Environ Sci Technol, 45, 3196-201.

Al-Othman, M. R., A. E. A. ARM, M. A. Mahmoud, S. A. Fifan & M. M. El-Shikh (2014) Application of silver nanoparticles as antifungal and antiaflatoxin B1 produced by Aspergillus flavus. Dig J Nanomater Bios, 9, 151-157.

Allahverdiyev, A. M., E. S. Abamor, M. Bagirova & M. Rafailovich (2011a) Antimicrobial effects of TiO(2) and Ag(2)O nanoparticles against drug-resistant bacteria and leishmania parasites. Future Microbiol, 6, 933-40.

Allahverdiyev, A. M., E. S. Abamor, M. Bagirova, C. B. Ustundag, C. Kaya, F. Kaya & M. Rafailovich (2011b) Antileishmanial effect of silver nanoparticles and their enhanced antiparasitic activity under ultraviolet light. Int J Nanomedicine, 6, 2705-14.

Asharani, P. V., M. P. Hande & S. Valiyaveettil (2009) Anti-proliferative activity of silver nanoparticles. BMC Cell Biol, 10, 65.

Asharani, P. V., Y. Lian Wu, Z. Gong & S. Valiyaveettil (2008) Toxicity of silver nanoparticles in zebrafish models. Nanotechnology, 19, 255102.

AshaRani, P. V., G. Low Kah Mun, M. P. Hande & S. Valiyaveettil (2009) Cytotoxicity and genotoxicity of silver nanoparticles in human cells. ACS Nano, 3, 279-90.

Autrup, J. L., J. Schmidt & H. Autrup (1993) Exposure to aflatoxin B1 in animal-feed production plant workers. Environ Health Perspect, 99, 195-7.

Azam, A., A. S. Ahmed, M. Oves, M. S. Khan, S. S. Habib & A. Memic (2012) Antimicrobial activity of metal oxide nanoparticles against Gram-positive and Gram-negative bacteria: a comparative study. Int J Nanomedicine, 7, 6003-9.

Baalousha, M., Y. Nur, I. Römer, M. Tejamaya & J. R. Lead (2013) Effect of monovalent and divalent cations, anions and fulvic acid on aggregation of citrate-coated silver nanoparticles. Sci Total Environ, 454-455, 119-31.

Bayram, O., S. Krappmann, M. Ni, J. W. Bok, K. Helmstaedt, O. Valerius, S. Braus-Stromeyer, N. J. Kwon, N. P. Keller, J. H. Yu & G. H. Braus (2008) VelB/VeA/LaeA complex coordinates light signal with fungal development and secondary metabolism. Science, 320, 1504-6.

Bennett, J. W. & S. B. Christensen (1983) New perspectives on aflatoxin biosynthesis. Adv Appl Microbiol, 29, 53-92.

Besinis, A., T. De Peralta & R. D. Handy (2014) The antibacterial effects of silver, titanium dioxide and silica dioxide nanoparticles compared to the dental disinfectant chlorhexidine on Streptococcus mutans using a suite of bioassays. Nanotoxicology, 8, 1-16.

Bluma, R. V. & M. G. Etcheverry (2006) Influence of Bacillus spp. isolated from maize agroecosystem on growth and aflatoxin B(1) production by Aspergillus section Flavi. Pest Manag Sci, 62, 242-51.

Bondarenko, O., K. Juganson, A. Ivask, K. Kasemets, M. Mortimer & A. Kahru (2013) Toxicity of Ag, CuO and ZnO nanoparticles to selected environmentally relevant test organisms and mammalian cells in vitro: a critical review. Arch Toxicol, 87, 1181-200.

Bonevich, J. E. & W. K. Haller (2010) Measuring the size of nanoparticles using transmission electron microscopy (TEM). NIST-NCL Joint Assay Protocol, PCC-7 Version.

Brakhage, A. A. (2013) Regulation of fungal secondary metabolism. Nat Rev Microbiol, 11, 21-32.

Brodsky, F. M., C. Y. Chen, C. Knuehl, M. C. Towler & D. E. Wakeham (2001) Biological basket weaving: formation and function of clathrin-coated vesicles. Annu Rev Cell Dev Biol, 17, 517-68.

Bueno, D. J., J. O. Silva, G. Oliver & S. N. González (2006) Lactobacillus casei CRL 431 and Lactobacillus rhamnosus CRL 1224 as biological controls for Aspergillus flavus strains. J Food Prot, 69, 2544-8.

Burg, W. A., O. L. Shotwell & B. E. Saltzman (1981) Measurements of airborne aflatoxins during the handling of contaminated corn. Am Ind Hyg Assoc J, 42, 1-11.

Calvo, A. M., J. Bok, W. Brooks & N. P. Keller (2004) veA is required for toxin and sclerotial production in Aspergillus parasiticus. Appl Environ Microbiol, 70, 4733-9.

Camporotondia, D. E., M. L. Fogliaa, G. S. Alvareza, A. M. Meberta, L. E. Diaza, T. Coradinb & M. F. Desimonea. 2013. Antimicrobial properties of silica modified nanoparticles Spain: Formatex Research Center.

Cao, W., T. Huang, X. H. Xu & H. E. Elsayed-Ali (2011) Localized surface plasmon resonance of single silver nanoparticles studied by dark-field optical microscopy and spectroscopy. J Appl Phys, 109, 34310.

Cardwell, K. F. & S. H. Henry (2004) Risk of exposure to and mitigation of effect of aflatoxin on human health: a West African example. Journal of Toxicology: Toxin Reviews, 23, 217-247.

Carlson, C., S. M. Hussain, A. M. Schrand, L. K. Braydich-Stolle, K. L. Hess, R. L. Jones & J. J. Schlager (2008) Unique cellular interaction of silver nanoparticles: size-dependent generation of reactive oxygen species. J Phys Chem B, 112, 13608-19.

Cary, J. W., B. G. Montalbano & K. C. Ehrlich (2000) Promoter elements involved in the expression of the Aspergillus parasiticus aflatoxin biosynthesis pathway gene avnA. Biochim Biophys Acta, 1491, 7-12.

Chanda, A., L. V. Roze, S. Kang, K. A. Artymovich, G. R. Hicks, N. V. Raikhel, A. M. Calvo & J. E. Linz (2009) A key role for vesicles in fungal secondary metabolism. Proc Natl Acad Sci U S A, 106, 19533-8.

Chanda, A., L. V. Roze & J. E. Linz (2010) A possible role for exocytosis in aflatoxin export in Aspergillus parasiticus. Eukaryot Cell, 9, 1724-7.

Chang, P. K., K. C. Ehrlich, J. Yu, D. Bhatnagar & T. E. Cleveland (1995) Increased expression of Aspergillus parasiticus aflR, encoding a sequence-specific DNA-binding protein, relieves nitrate inhibition of aflatoxin biosynthesis. Appl Environ Microbiol, 61, 2372-7.

Chang, P. K., K. Matsushima, T. Takahashi, J. Yu, K. Abe, D. Bhatnagar, G. F. Yuan, Y. Koyama & T. E. Cleveland (2007) Understanding nonaflatoxigenicity of Aspergillus sojae: a windfall of aflatoxin biosynthesis research. Appl Microbiol Biotechnol, 76, 977-84.

Chang, P. K., C. D. Skory & J. E. Linz (1992) Cloning of a gene associated with aflatoxin B1 biosynthesis in Aspergillus parasiticus. Curr Genet, 21, 231-3.

Chwalibog, A., E. Sawosz, A. Hotowy, J. Szeliga, S. Mitura, K. Mitura, M. Grodzik, P. Orlowski & A. Sokolowska (2010) Visualization of interaction between inorganic nanoparticles and bacteria or fungi. Int J Nanomedicine, 5, 1085-94.

Cole, R. J. & M. A. Schweikert. 2003. Handbook of Secondary Fungal Metabolites.: Academic Press.

Cotty, P. J. (1988) Aflatoxin and Sclerotial Production by Aspergillusflavus; Influence of pH. growth, 4, 11.

--- (1997) Aflatoxin-producing potential of communities of Aspergillus section Flavi from cotton producing areas in the United States. Mycological Research., 101, 698-704.

Cotty, P. J. & R. Jaime-Garcia (2007) Influences of climate on aflatoxin producing fungi and aflatoxin contamination. Int J Food Microbiol, 119, 109-15.

Cuero, R., T. Ouellet, J. Yu & N. Mogongwa (2003) Metal ion enhancement of fungal growth, gene expression and aflatoxin synthesis in Aspergillus flavus: RT-PCR characterization. J Appl Microbiol, 94, 953-61.

Cui, Y., Y. Zhao, Y. Tian, W. Zhang, X. Lü & X. Jiang (2012) The molecular mechanism of action of bactericidal gold nanoparticles on Escherichia coli. Biomaterials, 33, 2327-33.

Cumberland, S. A. & J. R. Lead (2009) Particle size distributions of silver nanoparticles at environmentally relevant conditions. J Chromatogr A, 1216, 9099-105.

Davis, N. D., U. L. Diener & V. P. Agnihotri (1967) Production of aflatoxins B1 and G1 in chemically defined medium. Mycopathol Mycol Appl, 31, 251-6.

de Souza, W. R., E. R. Morais, N. G. Krohn, M. Savoldi, M. H. Goldman, F. Rodrigues, C. Caldana, C. T. Semelka, A. P. Tikunov, J. M. Macdonald & G. H. Goldman (2013) Identification of metabolic pathways influenced by the G-protein coupled receptors GprB and GprD in Aspergillus nidulans. PLoS One, 8, e62088.

Diaz, G. J. & H. W. Murcia. 2011. Biotransformation of aflatoxin B1 and its relationship with the differential toxicological response to aflatoxin in commercial poultry species.: InTech.

Dizaj, S. M., F. Lotfipour, M. Barzegar-Jalali, M. H. Zarrintan & K. Adibkia (2014) Antimicrobial activity of the metals and metal oxide nanoparticles. Mater Sci Eng C Mater Biol Appl, 44, 278-84.

Dobson, J. (2006) Gene therapy progress and prospects: magnetic nanoparticle-based gene delivery. Gene Ther, 13, 283-7.

Duran, R. M., J. W. Cary & A. M. Calvo (2007) Production of cyclopiazonic acid, aflatrem, and aflatoxin by Aspergillus flavus is regulated by veA, a gene necessary for sclerotial formation. Appl Microbiol Biotechnol, 73, 1158-68.

Eaton, D. L. & E. P. Gallagher (1994) Mechanisms of aflatoxin carcinogenesis. Annu Rev Pharmacol Toxicol, 34, 135-72.

Ehrlich, K. C. (2009) Predicted roles of the uncharacterized clustered genes in aflatoxin biosynthesis. Toxins (Basel), 1, 37-58.

Elechiguerra, J. L., J. L. Burt, J. R. Morones, A. Camacho-Bragado, X. Gao, H. H. Lara & M. J. Yacaman (2005) Interaction of silver nanoparticles with HIV-1. J Nanobiotechnology, 3, 6.

Emami-Karvani, Z. & P. Chehrazi (2011) Antibacterial activity of ZnO nanoparticle on gram-positive and gram-negative bacteria. Afr J Microbiol Res. , 5, 1368-1373.

Fabrega, J., S. N. Luoma, C. R. Tyler, T. S. Galloway & J. R. Lead (2011a) Silver nanoparticles: behaviour and effects in the aquatic environment. Environ Int, 37, 517-31.

Fabrega, J., R. Zhang, J. C. Renshaw, W. T. Liu & J. R. Lead (2011b) Impact of silver nanoparticles on natural marine biofilm bacteria. Chemosphere, 85, 961-6.

Failla, L. J. & W. G. Niehaus (1986) Cadmium ion stimulation of growth and versicolorin synthesis in

a mutant strain of Aspergillus parasiticus. Experimental mycology., 10, 144-149.

Fairbairn, E. A., A. A. Keller, L. Mädler, D. Zhou, S. Pokhrel & G. N. Cherr (2011) Metal oxide nanomaterials in seawater: linking physicochemical characteristics with biological response in sea urchin development. J Hazard Mater, 192, 1565-71.

Foster, H. A., I. B. Ditta, S. Varghese & A. Steele (2011) Photocatalytic disinfection using titanium dioxide: spectrum and mechanism of antimicrobial activity. Appl Microbiol Biotechnol, 90, 1847-68.

Fox, C. L. & S. M. Modak (1974) Mechanism of silver sulfadiazine action on burn wound infections. Antimicrob Agents Chemother, 5, 582-8.

Fridovich, I. (1995) Superoxide radical and superoxide dismutases. Annu Rev Biochem, 64, 97-112.

Fujishima, A. & K. Honda (1972) Electrochemical photolysis of water at a semiconductor electrode. Nature, 238, 37-8.

Galdiero, S., A. Falanga, M. Vitiello, M. Cantisani, V. Marra & M. Galdiero (2011) Silver nanoparticles as potential antiviral agents. Molecules, 16, 8894-918.

Georgianna, D. R. & G. A. Payne (2009) Genetic regulation of aflatoxin biosynthesis: from gene to genome. Fungal Genet Biol, 46, 113-25.

Ghewande, M. P. & G. Nagaraj (1987) Prevention of Aflatoxin contamination through some commercial chemical products and plant extracts in groundnut. Mycotoxin Res, 3, 19-24.

Gong, Y., A. Hounsa, S. Egal, P. C. Turner, A. E. Sutcliffe, A. J. Hall, K. Cardwell & C. P. Wild (2004) Postweaning exposure to aflatoxin results in impaired child growth: a longitudinal study in Benin, West Africa. Environ Health Perspect, 112, 1334-8.

Gqaleni, N., J. E. Smith & J. Lacey (1996) Co-production of aflatoxins and cyclopiazonic acid in isolates of Aspergillus flavus. Food Additives & Contaminants, 13, 677-685.

Groopman, J. D., P. R. Donahue, J. Q. Zhu, J. S. Chen & G. N. Wogan (1985) Aflatoxin metabolism in humans: detection of metabolites and nucleic acid adducts in urine by affinity chromatography. Proc Natl Acad Sci U S A, 82, 6492-6.

Gummadidala, P. M., Y. P. Chen, K. R. Beauchesne, K. P. Miller, C. Mitra, N. Banaszek, M. Velez-Martinez, P. D. R. Moeller, J. L. Ferry, A. W. Decho & A. Chanda

(2016) Aflatoxin-exposure of Vibrio gazogenes as a novel system for the generation of aflatoxin synthesis inhibitors. Frontiers in Microbiology, 7, 814.

Gunterus, A., L. V. Roze, R. Beaudry & J. E. Linz (2007) Ethylene inhibits aflatoxin biosynthesis in Aspergillus parasiticus grown on peanuts. Food Microbiol, 24, 658-63.

Hamid, A. S., I. G. Tesfamariam, Y. Zhang & Z. G. Zhang (2013) Aflatoxin B1-induced hepatocellular carcinoma in developing countries: Geographical distribution, mechanism of action and prevention. Oncol Lett, 5, 1087-1092.

Handy, R. D., F. von der Kammer, J. R. Lead, M. Hassellöv, R. Owen & M. Crane (2008) The ecotoxicology and chemistry of manufactured nanoparticles. Ecotoxicology, 17, 287-314.

Hassan, A. A., M. E. Howayda & H. H. Mahmoud (2013) Effect of Zinc Oxide Nanoparticles on the Growth of Mycotoxigenic Mould. SCPT, 1, 66-74.

He, D., J. J. Dorantes-Aranda & T. D. Waite (2012a) Silver nanoparticle-algae interactions: oxidative dissolution, reactive oxygen species generation and synergistic toxic effects. Environ Sci Technol, 46, 8731-8.

He, D., S. Garg & T. D. Waite (2012b) H2O2-mediated oxidation of zero-valent silver and resultant interactions among silver nanoparticles, silver ions, and reactive oxygen species. Langmuir, 28, 10266-75.

Heiligtag, F. J. & M. Niederberger (2013) The fascinating world of nanoparticle research. Materials Today, 16, 262-271.

Henglein, A. & M. Giersig (1999) Formation of colloidal silver nanoparticles: capping action of citrate. The Journal of Physical Chemistry B, 103, 9533-9539.

Henry, S. H., F. X. Bosch, T. C. Troxell & P. M. Bolger (1999) Policy forum: public health. Reducing liver cancer--global control of aflatoxin. Science, 286, 2453-4.

Hewitt, C. J., S. R. Bellara, A. Andreani, G. Nebe-von-Caron & C. M. McFarlane (2001) An evaluation of the anti-bacterial action of ceramic powder slurries using multi-parameter flow cytometry. Biotechnology Letters., 23, 667-675.

Holden, P. A., R. M. Nisbet, H. S. Lenihan, R. J. Miller, G. N. Cherr, J. P. Schimel & J. L. Gardea-Torresdey (2013) Ecological nanotoxicology: integrating nanomaterial hazard considerations across the subcellular, population, community, and ecosystems levels. Acc Chem Res, 46, 813-22.

Hough, R. M., R. R. P. Noble & M. Reich (2011) Natural gold nanoparticles. Ore Geology Reviews, 42, 55-61.

Hua, S. S., O. K. Grosjean & J. L. Baker (1999) Inhibition of aflatoxin biosynthesis by phenolic compounds. Lett Appl Microbiol, 29, 289-91.

Hug, S. J. & B. Sulzberger (1994) In situ Fourier transform infrared spectroscopic evidence for the formation of several different surface complexes of oxalate on TiO2 in the aqueous phase. Langmuir, 10, 3587-3597.

Hund-Rinke, K. & M. Simon (2006) Ecotoxic effect of photocatalytic active nanoparticles (TiO2) on algae and daphnids. Environ Sci Pollut Res Int, 13, 225-32.

Huynh, K. A. & K. L. Chen (2011) Aggregation kinetics of citrate and polyvinylpyrrolidone coated silver nanoparticles in monovalent and divalent electrolyte solutions. Environ Sci Technol, 45, 5564-71.

Huynh, V. L. & A. B. Lloyd (1984) Synthesis and degradation of aflatoxins by Aspergillus parasiticus. I. Synthesis of aflatoxin B1 by young mycelium and its subsequent degradation in aging mycelium. Aust J Biol Sci, 37, 37-43.

Iravani, S., H. Korbekandi, S. V. Mirmohammadi & B. Zolfaghari (2014) Synthesis of silver nanoparticles: chemical, physical and biological methods. Res Pharm Sci, 9, 385-406.

Ismaiel, A. A. & N. A. Tharwat (2014) Antifungal activity of silver ion on ultrastructure and production of aflatoxin B1 and patulin by two mycotoxigenic strains, Aspergillus flavus OC1 and Penicillium vulpinum CM1. J Mycol Med, 24, 193-204.

Ivask, A., I. Kurvet, K. Kasemets, I. Blinova, V. Aruoja, S. Suppi, H. Vija, A. Käkinen, T. Titma, M. Heinlaan, M. Visnapuu, D. Koller, V. Kisand & A. Kahru (2014) Size-dependent toxicity of silver nanoparticles to bacteria, yeast, algae, crustaceans and mammalian cells in vitro. PLoS One, 9, e102108.

Jain, J., S. Arora, J. M. Rajwade, P. Omray, S. Khandelwal & K. M. Paknikar (2009) Silver nanoparticles in therapeutics: development of an antimicrobial gel formulation for topical use. Mol Pharm, 6, 1388-401.

Jang, H. D., S. K. Kim & S. J. Kim (2001) Effect of particle size and phase composition of titanium dioxide nanoparticles on the photocatalytic properties. . Journal of Nanoparticle Research., 3, 141-147.

Jesline, A., N. P. John, P. M. Narayanan, C. Vani & S. Murugan (2015) Antimicrobial activity of zinc and titanium dioxide nanoparticles against biofilm-producing methicillin-resistant Staphylococcus aureus. . Applied Nanoscience. , 5, 157-162

Jia, G., H. Wang, L. Yan, X. Wang, R. Pei, T. Yan, Y. Zhao & X. Guo (2005) Cytotoxicity of carbon nanomaterials: single-wall nanotube, multi-wall nanotube, and fullerene. Environ Sci Technol, 39, 1378-83.

Jin, T. & Y. He (2011) Antibacterial activities of magnesium oxide (MgO) nanoparticles against foodborne pathogens. . Journal of Nanoparticle Research, 13, 6877-6885

Jo, Y. K., B. H. Kim & G. Jung (2009) Antifungal activity of silver ions and nanoparticles on phytopathogenic fungi. . Plant Disease. , 93, 1037-1043.

Jones, A. M., S. Garg, D. He, A. N. Pham & T. D. Waite (2011) Superoxide-mediated formation and charging of silver nanoparticles. Environ Sci Technol, 45, 1428-34.

Kachholz, T. & A. L. Demain (1983) Nitrate repression of averufin and aflatoxin biosynthesis. Journal of natural products, 46, 499-506.

Kamika, I. & L. L. Takoy (2011) Natural occurrence of Aflatoxin B1 in peanut collected from Kinshasa, Democratic Republic of Congo. Food Control., 22, 1760-1764.

Kathiravan, V., S. Ravi, S. Ashokkumar, S. Velmurugan, K. Elumalai & C. P. Khatiwada (2015) Green synthesis of silver nanoparticles using Croton sparsiflorus morong leaf extract and their antibacterial and antifungal activities. Spectrochim Acta A Mol Biomol Spectrosc, 139, 200-5.

Keller, N. P., C. Nesbitt, B. Sarr, T. D. Phillips & G. B. Burow (1997) pH Regulation of Sterigmatocystin and Aflatoxin Biosynthesis in Aspergillus spp. Phytopathology, 87, 643-8.

Khan, F. R., K. B. Paul, A. D. Dybowska, E. Valsami-Jones, J. R. Lead, V. Stone & T. F. Fernandes (2015) Accumulation dynamics and acute toxicity of silver

nanoparticles to Daphnia magna and Lumbriculus variegatus: implications for metal modeling approaches. Environ Sci Technol, 49, 4389-97.

Kim, J. S., E. Kuk, K. N. Yu, J. H. Kim, S. J. Park, H. J. Lee, S. H. Kim, Y. K. Park, Y. H. Park, C. Y. Hwang, Y. K. Kim, Y. S. Lee, D. H. Jeong & M. H. Cho (2007) Antimicrobial effects of silver nanoparticles. Nanomedicine, 3, 95-101.

Kim, K. J., W. S. Sung, S. K. Moon, J. S. Choi, J. G. Kim & D. G. Lee (2008) Antifungal effect of silver nanoparticles on dermatophytes. J Microbiol Biotechnol, 18, 1482-4.

Kim, S. & D. Y. Ryu (2013) Silver nanoparticle-induced oxidative stress, genotoxicity and apoptosis in cultured cells and animal tissues. . Journal of Applied Toxicology., 33, 78-89.

Kim, S. W., J. H. Jung, K. Lamsal, Y. S. Kim, J. S. Min & Y. S. Lee (2012a) Antifungal Effects of Silver Nanoparticles (AgNPs) against Various Plant Pathogenic Fungi. Mycobiology, 40, 53-8.

Kim, T. H., M. Kim, H. S. Park, U. S. Shin, M. S. Gong & H. W. Kim (2012b) Size-dependent cellular toxicity of silver nanoparticles. J Biomed Mater Res A, 100, 1033-43.

Kisselev, P. A., O. V. Panibrat, A. R. Sysa, M. V. Anisovich, V. N. Zhabinskii & V. A. Khripach (2016) Flow-cytometric analysis of reactive oxygen species in cancer cells under treatment with brassinosteroids. Steroids.

Klich, M. A. (2007) Environmental and developmental factors influencing aflatoxin production by Aspergillus flavus and Aspergillus parasiticus. . Mycoscience., 48, 71-80

Kondo, T., M. Sakurada, S. Okamoto, M. Ono, H. Tsukigi, A. Suzuki, H. Nagasawa & S. Sakuda (2001) Effects of aflastatin A, an inhibitor of aflatoxin production, on aflatoxin biosynthetic pathway and glucose metabolism in Aspergillus parasiticus. J Antibiot (Tokyo), 54, 650-7.

Kosman, D. J. (2003) Molecular mechanisms of iron uptake in fungi. Mol Microbiol, 47, 1185-97.

Kotzybik, K., V. Gräf, L. Kugler, D. A. Stoll, R. Greiner, R. Geisen & M. Schmidt-Heydt (2016) Influence of Different Nanomaterials on Growth and Mycotoxin Production of Penicillium verrucosum. PLoS One, 11, e0150855.

Krishnamachari, K. A., R. V. Bhat, V. Nagarajan & T. B. Tilak (1975) Hepatitis due to aflatoxicosis. An outbreak in Western India. Lancet, 1, 1061-3.

Krishnamoorthy, K., J. Y. Moon, H. B. Hyun, S. K. Cho & S. J. Kim (2012) Mechanistic investigation on the toxicity of MgO nanoparticles toward cancer cells. Journal of Materials Chemistry., 22, 24610-24617.

Kuhn, D. A., D. Vanhecke, B. Michen, F. Blank, P. Gehr, A. Petri-Fink & B. Rothen-Rutishauser (2014) Different endocytotic uptake mechanisms for nanoparticles in epithelial cells and macrophages. Beilstein J Nanotechnol, 5, 1625-36.

Lead, J. R. & K. J. Wilkinson (2006) Aquatic colloids and nanoparticles: current knowledge and future trends. Environmental Chemistry, 3, 159-171.

Lewis, L., M. Onsongo, H. Njapau, H. Schurz-Rogers, G. Luber, S. Kieszak, J. Nyamongo, L. Backer, A. M. Dahiye, A. Misore, K. DeCock, C. Rubin & K. A. I. Group (2005) Aflatoxin contamination of commercial maize products during an

outbreak of acute aflatoxicosis in eastern and central Kenya. Environ Health Perspect, 113, 1763-7.

Li, Y., W. Zhang, J. Niu & Y. Chen (2013) Surface-coating-dependent dissolution, aggregation, and reactive oxygen species (ROS) generation of silver nanoparticles under different irradiation conditions. Environ Sci Technol, 47, 10293-301.

Liang, S. H., C. D. Skory & J. E. Linz (1996) Characterization of the function of the ver-1A and ver-1B genes, involved in aflatoxin biosynthesis in Aspergillus parasiticus. Appl Environ Microbiol, 62, 4568-75.

Lima, E., R. Guerra, V. Lara & A. Guzmán (2013) Gold nanoparticles as efficient antimicrobial agents for Escherichia coli and Salmonella typhi. Chem Cent J, 7, 11.

Liu, Q., M. Zhang, Z. X. Fang & X. H. Rong (2014) Effects of ZnO nanoparticles and microwave heating on the sterilization and product quality of vacuum-packaged Caixin. Journal of the Science of Food and Agriculture. , 94, 2547-2554.

Liu, Y. & F. Wu (2010) Global burden of aflatoxin-induced hepatocellular carcinoma: a risk assessment. Environ Health Perspect, 118, 818-24.

Lowry, G. V., K. B. Gregory, S. C. Apte & J. R. Lead (2012) Transformations of nanomaterials in the environment. Environ Sci Technol, 46, 6893-9.

Lunov, O., T. Syrovets, C. Röcker, K. Tron, G. U. Nienhaus, V. Rasche, V. Mailänder, K. Landfester & T. Simmet (2010) Lysosomal degradation of the carboxydextran shell of coated superparamagnetic iron oxide nanoparticles and the fate of professional phagocytes. Biomaterials, 31, 9015-22.

Lv, M., S. Su, Y. He, Q. Huang, W. Hu, D. Li & S. T. Lee (2010) Long-Term Antimicrobial Effect of Silicon Nanowires Decorated with Silver Nanoparticles. Advanced Materials., 22, 5463-5467

Mahapatra, O., M. Bhagat, C. Gopalakrishnan & K. D. Arunachalam (2008) Ultrafine dispersed CuO nanoparticles and their antibacterial activity. Journal of Experimental Nanoscience, 3, 185-193.

Maiorano, G., S. Sabella, B. Sorce, V. Brunetti, M. A. Malvindi, R. Cingolani & P. P. Pompa (2010) Effects of cell culture media on the dynamic formation of protein-nanoparticle complexes and influence on the cellular response. ACS Nano, 4, 7481-91.

Manzo, S., A. Rocco, R. Carotenuto, F. e. L. Picione, M. L. Miglietta, G. Rametta & G. Di Francia (2011) Investigation of ZnO nanoparticles' ecotoxicological effects towards different soil organisms. Environ Sci Pollut Res Int, 18, 756-63.

Marsh, P. B., M. E. Simpson & M. W. Trucksess (1975) Effects of trace metals on the production of aflatoxins by Aspergillus parasiticus. Appl Microbiol, 30, 52-7.

Matsumura, Y., K. Yoshikata, S. Kunisaki & T. Tsuchido (2003) Mode of bactericidal action of silver zeolite and its comparison with that of silver nitrate. Appl Environ Microbiol, 69, 4278-81.

Maurer, L. L., X. Yang, A. J. Schindler, R. K. Taggart, C. Jiang, H. Hsu-Kim, D. R. Sherwood & J. N. Meyer (2016) Intracellular trafficking pathways in silver nanoparticle uptake and toxicity in Caenorhabditis elegans. Nanotoxicology, 10, 831-5.

Meghana, S., P. Kabra, S. Chakraborty & N. Padmavathy (2015) Understanding the pathway of antibacterial activity of copper oxide nanoparticles. . RSC Advances. , 5, 12293-12299.

Miao, A. J., A. Quigg, K. Schwehr, C. Xu & P. Santschi. 2007. Engineered silver nanoparticles (ESNs) in coastal marine environments: bioavailability and toxic effects to the phytoplankton Thalassiosira weissflogii. In In 2nd International Conference on the Environmental Effects of Nanoparticles and Nanomaterials: Sept 24. London, UK.

Miao, L. & D. K. St Clair (2009) Regulation of superoxide dismutase genes: implications in disease. Free Radic Biol Med, 47, 344-56.

Miclăuş, T., C. Beer, J. Chevallier, C. Scavenius, V. E. Bochenkov, J. J. Enghild & D. S. Sutherland (2016) Dynamic protein coronas revealed as a modulator of silver nanoparticle sulphidation in vitro. Nat Commun, 7, 11770.

Miller, M. J., L. V. Roze, F. Trail & J. E. Linz (2005) Role of cis-acting sites NorL, a TATA box, and AflR1 in nor-1 transcriptional activation in Aspergillus parasiticus. Appl Environ Microbiol, 71, 1539-45.

Mitchell, N. J., E. Bowers, C. Hurburgh & F. Wu (2016) Potential economic losses to the US corn industry from aflatoxin contamination. Food Addit Contam Part A Chem Anal Control Expo Risk Assess, 33, 540-50.

Moore, M. N. (2006) Do nanoparticles present ecotoxicological risks for the health of the aquatic environment? Environ Int, 32, 967-76.

Moore, T. L., L. Rodriguez-Lorenzo, V. Hirsch, S. Balog, D. Urban, C. Jud, B. Rothen-Rutishauser, M. Lattuada & A. Petri-Fink (2015) Nanoparticle colloidal stability

in cell culture media and impact on cellular interactions. Chem Soc Rev, 44, 6287-305.

Morones, J. R., J. L. Elechiguerra, A. Camacho, K. Holt, J. B. Kouri, J. T. Ramírez & M. J. Yacaman (2005) The bactericidal effect of silver nanoparticles. Nanotechnology, 16, 2346-53.

Mousavi, S. A. & S. Pourtalebi (2015) Inhibitory Effects of Silver Nanoparticles on Growth and Aflatoxin B1 Production by Aspergillus Parasiticus. Iran J Med Sci, 40, 501-6.

Murk, J. L., B. M. Humbel, U. Ziese, J. M. Griffith, G. Posthuma, J. W. Slot, A. J. Koster, A. J. Verkleij, H. J. Geuze & M. J. Kleijmeer (2003) Endosomal compartmentalization in three dimensions: implications for membrane fusion. Proc Natl Acad Sci U S A, 100, 13332-7.

Na, K., T. Bum Lee, K. H. Park, E. K. Shin, Y. B. Lee & H. K. Choi (2003) Self-assembled nanoparticles of hydrophobically-modified polysaccharide bearing vitamin H as a targeted anti-cancer drug delivery system. Eur J Pharm Sci, 18, 165-73.

Nabney, J., M. B. Burbage, R. Allcroft & G. Lewis (1967) Metabolism of aflatoxin in sheep: excretion pattern in the lactating ewe. Food Cosmet Toxicol, 5, 11-7.

Narasaiah, K. V., R. B. Sashidhar & C. Subramanyam (2006) Biochemical analysis of oxidative stress in the production of aflatoxin and its precursor intermediates. Mycopathologia, 162, 179-89.

Nasrollahi, A., K. H. Pourshamsian & P. Mansourkiaee (2011) Antifungal activity of silver nanoparticles on some of fungi. International Journal of Nano Dimension. , 1, 233-239.

Navarro, E., A. Baun, R. Behra, N. B. Hartmann, J. Filser, A. J. Miao, A. Quigg, P. H. Santschi & L. Sigg (2008) Environmental behavior and ecotoxicity of engineered nanoparticles to algae, plants, and fungi. Ecotoxicology, 17, 372-86.

Navarro, E., F. Piccapietra, B. Wagner, R. Kägi, N. Odzak, L. Sigg & R. Behra. 2007. Toxicity mechanisms of silver nanoparticles to Chlamydomonas reinhardtii. In In 2nd International conference on the environmental effects of nanoparticles and nanomaterials. London, UK.

Neal, G. E., D. L. Eaton, D. J. Judah & A. Verma (1998) Metabolism and toxicity of aflatoxins M1 and B1 in human-derived in vitro systems. Toxicol Appl Pharmacol, 151, 152-8.

Nel, A. E., L. Mädler, D. Velegol, T. Xia, E. M. Hoek, P. Somasundaran, F. Klaessig, V. Castranova & M. Thompson (2009) Understanding biophysicochemical interactions at the nano-bio interface. Nat Mater, 8, 543-57.

NESBITT, B. F., J. O'KELLY, K. SARGEANT & A. SHERIDAN (1962) Aspergillus flavus and turkey X disease. Toxic metabolites of Aspergillus flavus. Nature, 195, 1062-3.

Nesheim, S. (1971) Technical communications. Fading of aflatoxin spots on TLC plates during fluorescence densitometry. J Assoc Off Anal Chem, 54, 1444-5.

NEWBERNE, P. M., G. N. WOGAN, W. W. CARLTON & M. M. ABDELKADER (1964) HISTOPATHOLOGIC LESIONS IN DUCKLINGS CAUSED BY

ASPERGILLUS FLAVUS CULTURES, CULTURE EXTRACTS, AND CRYSTALLINE AFLATOXINS. Toxicol Appl Pharmacol, 6, 542-56.

Nowack, B. & T. D. Bucheli (2007) Occurrence, behavior and effects of nanoparticles in the environment. Environ Pollut, 150, 5-22.

Ojamäe, L., C. Aulin, H. Pedersen & P. O. Käll (2006) IR and quantum-chemical studies of carboxylic acid and glycine adsorption on rutile TiO2 nanoparticles. J Colloid Interface Sci, 296, 71-8.

Oka, H., T. Tomioka, K. Tomita, A. Nishino & S. Ueda (1994) Inactivation of enveloped viruses by a silver-thiosulfate complex. Met Based Drugs, 1, 511.

Ono, M., S. Sakuda, A. Suzuki & A. Isogai (1997) Aflastatin A, a novel inhibitor of aflatoxin production by aflatoxigenic fungi. J Antibiot (Tokyo), 50, 111-8.

Pacioni, N. L., C. D. Borsarelli, V. Rey & A. V. Veglia. 2015. Synthetic Routes for the Preparation of Silver Nanoparticles.: Springer International Publishing.

Pal, S., Y. K. Tak & J. M. Song (2007) Does the antibacterial activity of silver nanoparticles depend on the shape of the nanoparticle? A study of the Gram-negative bacterium Escherichia coli. Appl Environ Microbiol, 73, 1712-20.

Panacek, A., L. Kvítek, R. Prucek, M. Kolar, R. Vecerova, N. Pizúrova, V. K. Sharma, T. Nevecna & R. Zboril (2006) Silver colloid nanoparticles: synthesis, characterization, and their antibacterial activity. J Phys Chem B, 110, 16248-53.

Panyala, N. R., E. M. Peña-Méndez & J. Havel (2008) Silver or silver nanoparticles: a hazardous threat to the environment and human health. J Appl Biomed, 6, 117-129.

Panácek, A., M. Kolár, R. Vecerová, R. Prucek, J. Soukupová, V. Krystof, P. Hamal, R. Zboril & L. Kvítek (2009) Antifungal activity of silver nanoparticles against Candida spp. Biomaterials, 30, 6333-40.

Park, E. J., J. Yi, Y. Kim, K. Choi & K. Park (2010) Silver nanoparticles induce cytotoxicity by a Trojan-horse type mechanism. Toxicol In Vitro, 24, 872-8.

Park, J., D. H. Lim, H. J. Lim, T. Kwon, J. S. Choi, S. Jeong, I. H. Choi & J. Cheon (2011a) Size dependent macrophage responses and toxicological effects of Ag nanoparticles. Chem Commun (Camb), 47, 4382-4.

Park, K., E. J. Park, I. K. Chun, K. Choi, S. H. Lee, J. Yoon & B. C. Lee (2011b) Bioavailability and toxicokinetics of citrate-coated silver nanoparticles in rats. Arch Pharm Res, 34, 153-8.

Parkin, D. M., F. Bray, J. Ferlay & P. Pisani (2005) Global cancer statistics, 2002. CA Cancer J Clin, 55, 74-108.

Payne, G. A. & M. P. Brown (1998) Genetics and physiology of aflatoxin biosynthesis. Annu Rev Phytopathol, 36, 329-62.

Pestka, J. J. (1988) Enhanced surveillance of foodborne mycotoxins by immunochemical assay. J Assoc Off Anal Chem, 71, 1075-81.

Pitt, J. I. Mycotoxin prevention and control in foodgrains. http://www.fao.org/docrep/x5036e/x5036e04.htm (last accessed.

Pons, W. A., A. F. Cucullu & A. O. Franz (1972) Rapid quantitative TLC method for determining aflatoxins in cottonseed products. J Assoc Off Anal Chem, 55, 768-74.

Praetorius, N. P. & T. K. Mandal (2007) Engineered nanoparticles in cancer therapy. Recent Pat Drug Deliv Formul, 1, 37-51.

Prieto, R., G. L. Yousibova & C. P. Woloshuk (1996) Identification of aflatoxin biosynthesis genes by genetic complementation in an Aspergillus flavus mutant lacking the aflatoxin gene cluster. Appl Environ Microbiol, 62, 3567-71.

Pulit, J., M. Banach, R. Szczygłowska & M. Bryk (2013) Nanosilver against fungi. Silver nanoparticles as an effective biocidal factor. Acta Biochim Pol, 60, 795-8.

Rai, M., A. Yadav & A. Gade (2009) Silver nanoparticles as a new generation of antimicrobials. Biotechnol Adv, 27, 76-83.

Reverberi, M., A. A. Fabbri, S. Zjalic, A. Ricelli, F. Punelli & C. Fanelli (2005) Antioxidant enzymes stimulation in Aspergillus parasiticus by Lentinula edodes inhibits aflatoxin production. Appl Microbiol Biotechnol, 69, 207-15.

Rodriguez, S. B. & N. E. Mahoney (1994) Inhibition of aflatoxin production by surfactants. Appl Environ Microbiol, 60, 106-10.

Roduner, E. (2006) Size matters: why nanomaterials are different. Chem Soc Rev, 35, 583-92.

Roe, D., B. Karandikar, N. Bonn-Savage, B. Gibbins & J. B. Roullet (2008) Antimicrobial surface functionalization of plastic catheters by silver nanoparticles. J Antimicrob Chemother, 61, 869-76.

Roy, I., S. Mitra, A. Maitra & S. Mozumdar (2003) Calcium phosphate nanoparticles as novel non-viral vectors for targeted gene delivery. Int J Pharm, 250, 25-33.

Roze, L. V., A. E. Arthur, S. Y. Hong, A. Chanda & J. E. Linz (2007) The initiation and pattern of spread of histone H4 acetylation parallel the order of transcriptional activation of genes in the aflatoxin cluster. Mol Microbiol, 66, 713-26.

Roze, L. V., A. Chanda, J. Wee, D. Awad & J. E. Linz (2011) Stress-related transcription factor AtfB integrates secondary metabolism with oxidative stress response in aspergilli. J Biol Chem, 286, 35137-48.

Rudge, S., C. Peterson, C. Vessely, J. Koda, S. Stevens & L. Catterall (2001) Adsorption and desorption of chemotherapeutic drugs from a magnetically targeted carrier (MTC). J Control Release, 74, 335-40.

Ruparelia, J. P., A. K. Chatterjee, S. P. Duttagupta & S. Mukherji (2008) Strain specificity in antimicrobial activity of silver and copper nanoparticles. Acta Biomater, 4, 707-16.

Römer, I., T. A. White, M. Baalousha, K. Chipman, M. R. Viant & J. R. Lead (2011) Aggregation and dispersion of silver nanoparticles in exposure media for aquatic toxicity tests. J Chromatogr A, 1218, 4226-33.

Said, D. E., L. M. Elsamad & Y. M. Gohar (2012) Validity of silver, chitosan, and curcumin nanoparticles as anti-Giardia agents. Parasitology research. , 111, 545-554.

Sail, J. T. & T. J. Webster (2012) Antimicrobial applications of nanotechnology: methods and literature. . International journal of nanomedicine. , 7, 1.

Sakuda, S., M. Ono, K. Furihata, J. Nakayama, A. Suzuki & A. Isogai (1996) Aflastatin A, a novel inhibitor of aflatoxin production of Aspergillus parasiticus, from Streptomyces. . Journal of the American Chemical Society. , 118, 7855-7856.

Sakuda, S., M. Ono, H. Ikeda, T. Nakamura, Y. Inagaki, R. Kawachi, J. Nakayama, A. Suzuki, A. Isogai & H. Nagasawa (2000) Blasticidin A as an inhibitor of aflatoxin production by Aspergillus parasiticus. J Antibiot (Tokyo), 53, 1265-71.

Saptarshi, S. R., A. Duschl & A. L. Lopata (2013) Interaction of nanoparticles with proteins: relation to bio-reactivity of the nanoparticle. J Nanobiotechnology, 11, 26.

Saraf, R. (2013) Cost effective and Monodispersed Zinc Oxide Nanoparticles Synthesis and their Characterization. International Journal of Advances in Applied Sciences., 2, 85-88.

Sarikaya Bayram, O., O. Bayram, O. Valerius, H. S. Park, S. Irniger, J. Gerke, M. Ni, K. H. Han, J. H. Yu & G. H. Braus (2010) LaeA control of velvet family regulatory proteins for light-dependent development and fungal cell-type specificity. PLoS Genet, 6, e1001226.

Sarikaya-Bayram, Ö., J. M. Palmer, N. Keller, G. H. Braus & Ö. Bayram (2015) One Juliet and four Romeos: VeA and its methyltransferases. Front Microbiol, 6, 1.

Sattler, K. D. 2010. Handbook of nanophysics: nanoparticles and quantum dots.: CRC Press.

Schindler, A. F., J. G. Palmer & W. V. Eisenberg (1967) Aflatoxin Production by Aspergillus flavus as Related to Various Temperatures. Appl Microbiol, 15, 1006-9.

Schmale, D. G. & G. P. Munkvold (2009) Mycotoxins in crops: A threat to human and domestic animal health. . The plant health instructor., 3, 340-353.

Sciau, P., C. Mirguet, C. Roucau, D. Chabanne & M. Schvoerer (2009) Double nanoparticle layer in a 12th century lustreware decoration: Accident or technological mastery? Journal of Nano Research, 8, 133-139.

Seil, J. T. & T. J. Webster (2012) Antimicrobial applications of nanotechnology: methods and literature. Int J Nanomedicine, 7, 2767-81.

Semple, R. L., A. S. Frio & P. A. Hicks. 1989. Mycotoxin prevention and control in foodgrains. Bangkok: REGNET [etc.].

Shameli, K., M. B. Ahmad, M. Zargar, W. M. Yunus, A. Rustaiyan & N. A. Ibrahim (2011) Synthesis of silver nanoparticles in montmorillonite and their antibacterial behavior. Int J Nanomedicine, 6, 581-90.

Shapira, R., N. Paster, M. Menasherov, O. Eyal, A. Mett, T. Meiron, E. Kuttin & R. Salomon (1997) Development of polyclonal antibodies for detection of aflatoxigenic molds involving culture filtrate and chimeric proteins expressed in Escherichia coli. Appl Environ Microbiol, 63, 990-5.

Sharma, R. K. & R. Ghose (2015) Synthesis of zinc oxide nanoparticles by homogeneous precipitation method and its application in antifungal activity against Candida albicans. Ceramics International. , 41, 967-975.

Shimizu, K. & N. P. Keller (2001) Genetic involvement of a cAMP-dependent protein kinase in a G protein signaling pathway regulating morphological and chemical transitions in Aspergillus nidulans. Genetics, 157, 591-600.

Shirtcliffe, N., U. Nickel & S. Schneider (1999) Reproducible preparation of silver sols with small particle size using borohydride reduction: for use as nuclei for

preparation of larger particles. Journal of colloid and interface science, 211, 122-129.

Shreeve, B. J., D. S. Patterson & B. A. Roberts (1979) The 'carry-over' of aflatoxin, ochratoxin and zearalenone from naturally contaminated feed to tissues, urine and milk of dairy cows. Food Cosmet Toxicol, 17, 151-2.

Singh, R. & D. P. Hsieh (1977) Aflatoxin biosynthetic pathway: elucidation by using blocked mutants of Aspergillus parasiticus. Arch Biochem Biophys, 178, 285-92.

Spacciapoli, P., D. Buxton, D. Rothstein & P. Friden (2001) Antimicrobial activity of silver nitrate against periodontal pathogens. J Periodontal Res, 36, 108-13.

SPENSLEY, P. C. (1963) Aflatoxin, the active principle in turkey 'X' disease. Endeavour, 22, 75-9.

Stebounova, L. V., E. Guio & V. H. Grassian (2011) Silver nanoparticles in simulated biological media: a study of aggregation, sedimentation, and dissolution. Journal of Nanoparticle Research., 13, 233-244.

Stenmark, H. (2009) Rab GTPases as coordinators of vesicle traffic. Nat Rev Mol Cell Biol, 10, 513-25.

Strauss, J. & Y. Reyes-Dominguez (2011) Regulation of secondary metabolism by chromatin structure and epigenetic codes. Fungal Genet Biol, 48, 62-9.

Tang, Z. X. & B. F. Lv (2014) MgO nanoparticles as antibacterial agent: preparation and activity. Brazilian Journal of Chemical Engineering., 31, 591-601.

Tanwar, J., S. Das, Z. Fatima & S. Hameed (2014) Multidrug resistance: an emerging crisis. Interdiscip Perspect Infect Dis, 2014, 541340.

Taylor, W. J. & F. A. Draughon (2001) Nannocystis exedens: a potential biocompetitive agent against Aspergillus flavus and Aspergillus parasiticus. J Food Prot, 64, 1030-4.

Tejamaya, M., I. Römer, R. C. Merrifield & J. R. Lead (2012) Stability of citrate, PVP, and PEG coated silver nanoparticles in ecotoxicology media. Environ Sci Technol, 46, 7011-7.

Treuel, L., X. Jiang & G. U. Nienhaus (2013) New views on cellular uptake and trafficking of manufactured nanoparticles. J R Soc Interface, 10, 20120939.

Turkevich, J., P. C. Stevenson & J. Hillier (1951) A study of the nucleation and growth processes in the synthesis of colloidal gold. Discussions of the Faraday Society, 11, 55-75.

Usman, M. S., M. E. El Zowalaty, K. Shameli, N. Zainuddin, M. Salama & N. A. Ibrahim (2013) Synthesis, characterization, and antimicrobial properties of copper nanoparticles. Int J Nanomedicine, 8, 4467-79.

Vanlandingham, P. A. & B. P. Ceresa (2009) Rab7 regulates late endocytic trafficking downstream of multivesicular body biogenesis and cargo sequestration. J Biol Chem, 284, 12110-24.

Veldman, A., J. A. C. Meijs, G. J. Borggreve & J. J. Heeres-Van der Tol (1992) Carry-over of aflatoxin from cows' food to milk. . Animal Production., 55, 163-168

Wang, T., J. Bai, X. Jiang & G. U. Nienhaus (2012) Cellular uptake of nanoparticles by membrane penetration: a study combining confocal microscopy with FTIR spectroelectrochemistry. ACS Nano, 6, 1251-9.

Wang, Z., T. Xia & S. Liu (2015) Mechanisms of nanosilver-induced toxicological effects: more attention should be paid to its sublethal effects. Nanoscale, 7, 7470-81.

Weisenburger, D. D. (1993) Human health effects of agrichemical use. Hum Pathol, 24, 571-6.

Wiesner, M. R., G. V. Lowry, P. Alvarez, D. Dionysiou & P. Biswas (2006) Assessing the risks of manufactured nanomaterials. Environ Sci Technol, 40, 4336-45.

Wilkinson, J. R., J. Yu, H. K. Abbas, B. E. Scheffler, H. S. Kim, W. C. Nierman, D. Bhatnagar & T. E. Cleveland (2007) Aflatoxin formation and gene expression in response to carbon source media shift in Aspergillus parasiticus. Food Addit Contam, 24, 1051-60.

Wu, D. & P. Yotnda (2011) Production and detection of reactive oxygen species (ROS) in cancers. J Vis Exp.

Wu, F. & P. Khlangwiset (2010) Health economic impacts and cost-effectiveness of aflatoxin-reduction strategies in Africa: case studies in biocontrol and post-harvest interventions. Food Addit Contam Part A Chem Anal Control Expo Risk Assess, 27, 496-509.

Wu, F., C. Narrod, M. Tiongco & Y. Liu (2011) THE HEALTH ECONOMICS OF AFLATOXIN: GLOBAL BURDEN OF DISEASE. International Food Policy Research Institute.

Wuithschick, M., B. Paul, R. Bienert, A. Sarfraz, U. Vainio, M. Sztucki, R. Kraehnert, P. Strasser, K. Rademann, F. Emmerling & J. Polte (2013) Size-controlled synthesis

of colloidal silver nanoparticles based on mechanistic understanding. Chemistry of Materials, 25, 4679-4689.

Xia, Z. K., Q. H. Ma, S. Y. Li, D. Q. Zhang, L. Cong, Y. L. Tian & R. Y. Yang (2016) The antifungal effect of silver nanoparticles on Trichosporon asahii. J Microbiol Immunol Infect, 49, 182-8.

Xie, Y., Y. He, P. L. Irwin, T. Jin & X. Shi (2011) Antibacterial activity and mechanism of action of zinc oxide nanoparticles against Campylobacter jejuni. Appl Environ Microbiol, 77, 2325-31.

Yabe, K. & H. Nakajima (2004) Enzyme reactions and genes in aflatoxin biosynthesis. Appl Microbiol Biotechnol, 64, 745-55.

Yah, C. S. & G. S. Simate (2015) Nanoparticles as potential new generation broad spectrum antimicrobial agents. Daru, 23, 43.

Yamamoto, O., T. Ohira, K. Alvarez & M. Fukuda (2010) Antibacterial characteristics of CaCO 3–MgO composites. . Materials Science and Engineering: B, 173 208-212. .

Yamanaka, M., K. Hara & J. Kudo (2005) Bactericidal actions of a silver ion solution on Escherichia coli, studied by energy-filtering transmission electron microscopy and proteomic analysis. Appl Environ Microbiol, 71, 7589-93.

Yang, L. & D. J. Watts (2005) Particle surface characteristics may play an important role in phytotoxicity of alumina nanoparticles. Toxicol Lett, 158, 122-32.

Yeh, F. S., M. C. Yu, C. C. Mo, S. Luo, M. J. Tong & B. E. Henderson (1989) Hepatitis B virus, aflatoxins, and hepatocellular carcinoma in southern Guangxi, China. Cancer Res, 49, 2506-9.

Yin, W. & N. P. Keller (2011) Transcriptional regulatory elements in fungal secondary metabolism. J Microbiol, 49, 329-39.

Yoshinari, T., Y. Noda, K. Yoda, H. Sezaki, H. Nagasawa & S. Sakuda (2010) Inhibitory activity of blasticidin A, a strong aflatoxin production inhibitor, on protein synthesis of yeast: selective inhibition of aflatoxin production by protein synthesis inhibitors. J Antibiot (Tokyo), 63, 309-14.

Yu, J., D. Bhatnagar & K. C. Ehrlich (2002) Aflatoxin biosynthesis. Rev Iberoam Micol, 19, 191-200.

Yu, J., P. K. Chang, K. C. Ehrlich, J. W. Cary, D. Bhatnagar, T. E. Cleveland, G. A. Payne, J. E. Linz, C. P. Woloshuk & J. W. Bennett (2004) Clustered pathway genes in aflatoxin biosynthesis. Appl Environ Microbiol, 70, 1253-62.

Zhang, S., H. Gao & G. Bao (2015) Physical Principles of Nanoparticle Cellular Endocytosis. ACS Nano, 9, 8655-71.

Zook, J. M., S. E. Long, D. Cleveland, C. L. Geronimo & R. I. MacCuspie (2011) Measuring silver nanoparticle dissolution in complex biological and environmental matrices using UV-visible absorbance. Anal Bioanal Chem, 401, 1993-2002.

Šileikaitė, A., I. Prosyčevas, J. Puišo, A. Juraitis & A. Guobienė (2006) Analysis of silver nanoparticles produced by chemical reduction of silver salt solution. Mater. Sci.-Medzg, 12, 287-291.